

DELFT UNIVERSITY OF TECHNOLOGY

MASTER THESIS

TNO, THE NETHERLANDS ORGANISATION FOR APPLIED SCIENTIFIC RESEARCH

---

# Modelling for Sorbent-Based Direct Air Capture Systems

---

*Authors:*

Jamie Bender

*Supervisor TNO:*

Dr. Jasper Ros

*Supervisors TU Delft:*

Dr. Thijs Vlugt

December 20, 2022

# Contents

<b>1</b>	<b>Abstract</b>	<b>7</b>
<b>2</b>	<b>Introduction</b>	<b>8</b>
2.1	Contemporary situation	8
2.2	Commercial DAC systems	9
2.2.1	Different DAC companies	9
2.2.2	DAC plant Orca	10
2.2.3	Relating Climeworks to my model	10
<b>3</b>	<b>Literature study</b>	<b>11</b>
3.1	Carbon capture technologies	11
3.1.1	Negative emission technologies	11
3.1.2	Why DAC	11
3.1.3	DAC process explained	12
3.2	Carbon Capture and storage (CCS) technology	13
3.2.1	CCS commercially	13
3.2.2	CCS systems	13
3.2.3	CCS compared to DAC	14
3.3	DAC technology	15
3.3.1	Type of DAC system	15
3.3.2	Solvent based systems	15
3.4	Sorbent based systems	15
3.4.1	Important parameters for DAC	16
3.4.2	Physisorption	16
3.4.3	Chemisorption	17
3.5	Solid amine based sorbents	17
3.5.1	Type of amine based sorbents	18
3.5.2	Lewatit VP OC 1065	19
3.5.3	Geographical considerations	19
3.5.4	Influence of water	20
3.5.5	CO <sub>2</sub> processing	20
<b>4</b>	<b>Model Literature</b>	<b>21</b>
4.1	Process description and model considerations	21
4.2	Adsorption	21
4.2.1	Mass transfer	21
4.2.2	Equilibrium considerations (capacity)	22
4.2.3	Modelling	22
4.3	Desorption	23
4.3.1	Desorption methods	23
4.4	System to model	24
<b>5</b>	<b>Research questions</b>	<b>26</b>
<b>6</b>	<b>Introduction adsorption</b>	<b>28</b>
6.1	Adsorption	28
6.2	Adsorption model	28
<b>7</b>	<b>Setting up the mass balance</b>	<b>29</b>
7.1	Assumptions	29
7.2	Mass balance	30
7.3	Initial- & boundary conditions	31
7.3.1	LDF and k	31

<b>8</b>	<b>Modelling approach</b>	<b>32</b>
8.1	Model description . . . . .	32
8.2	Determining the system . . . . .	34
8.2.1	Governing equations . . . . .	34
8.2.2	Initial & Boundary conditions . . . . .	34
8.2.3	Equilibrium loading . . . . .	35
<b>9</b>	<b>Discretization</b>	<b>35</b>
9.1	Spatial differential $z[j]$ . . . . .	36
9.1.1	Finite difference methods . . . . .	36
9.2	Time differential - $t[j]$ . . . . .	37
9.2.1	Numerical time analysis . . . . .	38
9.2.2	Combining the equations . . . . .	38
<b>10</b>	<b>Verification and Validation</b>	<b>40</b>
10.1	Verification . . . . .	40
10.1.1	Error check analysis . . . . .	40
10.1.2	Stability check . . . . .	40
10.2	Validation . . . . .	40
10.2.1	Toth isotherm . . . . .	41
10.2.2	Experimental simulation . . . . .	42
10.3	Model results . . . . .	46
<b>11</b>	<b>Conclusions adsorption</b>	<b>46</b>
<b>12</b>	<b>Recommendations</b>	<b>46</b>
<b>13</b>	<b>Introduction desorption</b>	<b>50</b>
13.1	Desorption model . . . . .	50
13.1.1	CSTR . . . . .	50
13.1.2	Vacuum Temperature Swing Adsorption (VTSA) . . . . .	51
13.2	Desorption model . . . . .	52
13.2.1	The reactor . . . . .	52
13.2.2	The components . . . . .	53
13.3	System description . . . . .	53
13.4	Mass balances . . . . .	54
13.5	Energy Balance . . . . .	55
<b>14</b>	<b>Modelling approach desorption</b>	<b>55</b>
14.1	Modelling goal . . . . .	55
14.2	System description . . . . .	55
14.2.1	Governing equations . . . . .	56
14.2.2	Initial conditions . . . . .	57
14.2.3	The ODE solver . . . . .	57
<b>15</b>	<b>Verification and Validation</b>	<b>58</b>
15.1	Verification of the model . . . . .	58
15.1.1	Pressure . . . . .	59
15.1.2	Equilibrium loading . . . . .	60
15.1.3	Temperature . . . . .	60
15.1.4	Kinetic rate constant . . . . .	61
15.1.5	Area of heating . . . . .	62
15.1.6	Heat transfer coefficient . . . . .	63
15.2	Testing the model . . . . .	64
15.3	Case Study . . . . .	65

<b>16 Results desorption</b>	<b>68</b>
16.1 Model justification . . . . .	68
16.1.1 System . . . . .	68
16.1.2 Python script . . . . .	68
16.2 Case study results . . . . .	68
16.2.1 Productivity . . . . .	69
<b>17 Conclusion</b>	<b>70</b>
<b>18 Recommendations</b>	<b>71</b>
<b>19 Nomenclature desorption</b>	<b>72</b>
<b>20 Appendix C. [Derivations]</b>	<b>77</b>
20.1 Ordering of equations . . . . .	77
20.2 Derivation of the energy balance . . . . .	78
20.3 Molar flow rate equations . . . . .	80
<b>21 Appendix D. [Figures]</b>	<b>81</b>
<b>22 Appendix E. [Python code]</b>	<b>83</b>

## List of Figures

1	Global carbon dioxide concentration increase from the year 1960 to 2021 in ppm [1]. . . . .	8
2	An overview of the various negative emission technologies categorised. . . . .	11
3	A schematic representation of the main processes that describe a DAC system, an adsorption system where the $CO_2$ molecules adsorb to the sorbent structure while other molecules pass and a desorption system where the system is closed and the $CO_2$ stream is extracted. . . . .	12
4	Different chemical amine based mechanisms that can occur during chemisorption, depending on the amount of hydrogen atoms that are carried by the nitrogen molecule. . . . .	18
5	Chemical composition of a Lewatit VP OC 1065 molecule. . . . .	19
6	Schematic the adsorption mechanism of a $CO_2$ particle, it first passes the film layer (1), then it transports into the pores of the sorbent (2) and finally it adsorbs on to the external or internal surface of the sorbent (3). . . . .	21
7	A representation of the experimental equilibrium capacity isotherm of the Lewatit sorbent at different temperature for varying partial pressure of $CO_2$ as determined by Bos. . . . .	22
8	An adsorption and desorption cycle with the different steps in between for a DAC cycle and the in and outflow of the system for every step. . . . .	24
9	Simplified representation of the adsorption system: a PFR containing solid sorbent material through which ambient air flows from the inlet to the outlet and exits the reactor as $CO_2$ lean air. . . . .	30
10	A one-dimensional schematic of the initial state of the reactor for the concentration of $CO_2$ over the length of the reactor as determined by the initial- and boundary conditions . . . . .	31
11	Comparing the equilibrium loading values of the Toth isotherm to those of the Henry's constant, for a system at 400 ppm and 298 K as a function of the partial pressure of $CO_2$ . . . . .	33
12	A one-dimensional schematic of the spatial grid representation of the PFR that is used to describe the adsorption reaction, with an inlet velocity of air ( $u_{air}$ ) and a (n) number of grid-step ( $\Delta z$ ) from the inlet ( $z=0$ ) to the outlet ( $z=L$ ). . . . .	35
13	One dimensional grid representation of the length of the reactor for a single point in time, with grid-point from the inlet ( $i=0$ ) to the outlet ( $i=n$ ). . . . .	36
14	A schematic of the different finite difference methods that could be used to solve the spatial differential equation. . . . .	37
15	Comparing the equilibrium value of the Toth isotherm to the Henry's coefficient for adsorption at 2000 ppm at 273 K, 293 K and 313 K respectively as a function of the partial pressure of $CO_2$ . . . . .	42
16	Comparing the experimental results of a 2000 ppm system at the outlet of the reactor by Surati [2] (the black line) to the simulations done by the model for different values of $k$ and an equilibrium loading of 1.209 mol/kg for 1,400 seconds. . . . .	43
17	Comparing the fitted experimental results of a 2000 ppm system at the outlet of the reactor by Surati [2] to the simulation done by the model for $k = 0.04 \text{ s}^{-1}$ and an equilibrium loading of 1.326 mol/kg for 1,400 seconds. . . . .	44
18	Linear driving force of the final model results showing the amount of loading per second for the system with $k = 0.04 \text{ s}^{-1}$ and $q_e = 1.326 \text{ mol/kg}$ . . . . .	45
19	Reproduced representation of the experimental Toth isotherm equation as determined by Bos [3] that shows the effect of temperature and the partial pressure of $CO_2$ on the capacity of the sorbent from 0 to 1 bar . . . . .	51
20	Simplified representation of the CSTR desorption system filled with solid sorbent material. The gaseous components inside the reactor are exclusively $N_2$ and $CO_2$ as the system is heated by a heating source $Q_{in}$ . . . . .	52
21	Course of sorbent unloading for different values for initial equilibrium loading of the sorbent as a function of time. . . . .	60
22	Sorbent unloading shown as a function of time for different values of the maximum temperature in the reactor for two different initial loading values. Unloading is shown systems with an initial sorbent loading of 0.9 and 1.2 mol/kg. . . . .	61
23	Slopes of the equilibrium loading and actual loading for different values of the kinetic rate constant ( $k$ ) as a function of time. The different figures show the course of these slopes for the values of $k = 0.01$ , $k = 0.001$ and $k = 0.0005$ respectively. . . . .	62
24	Unloading of the sorbent as a function of time for different values of the heat transfer coefficient. . . . .	64
25	The case study figures showing the course of the different parameters as a function of time for the default conditions equilibrium loading, temperature, molar flow rate and number of moles respectively. . . . .	66

26	Reproduced representation of the experimental Toth isotherm equation as determined by Bos [3] that shows the effect of temperature and the partial pressure of $CO_2$ on the capacity of the sorbent from 0 to 1 bar . . . . .	81
27	Reproduced representation of the experimental Toth isotherm equation as determined by Bos [3] that shows the effect of temperature and the partial pressure of $CO_2$ on the capacity of the sorbent from 0 to 0.1 bar . . . . .	81
28	Reproduced representation of the experimental Toth isotherm equation as determined by Bos [3] that shows the effect of temperature and the partial pressure of $CO_2$ on the capacity of the sorbent from 0 to 0.01 bar . . . . .	82
29	Comparing the fitted experimental results of a 2000 ppm system at the outlet of the reactor by Surati [2] to the simulation done by the model for $k = 0.02 \text{ s}^{-1}$ and different equilibrium loading values for 1,400 seconds, solved with the Crank-Nicolson method. . . . .	82

## List of Tables

1	Terms and abbreviations . . . . .	6
2	Desorption systems default values . . . . .	58
3	Geometry of the reactor and the dimensions of the heating tubes inside the reactor as a function of the number of heating tubes for the system. . . . .	63
4	Desorption systems default values . . . . .	65
5	Resulting values from the two different situations as described for the case study, where 400 ppm $CO_2$ is assumed a loading of 0.9 mol/kg and 2000 ppm $CO_2$ is assumed a loading of 1.4 mol/kg . . . . .	70
6	Parameters used for the desorption model . . . . .	72
8	Toth isotherm parameters . . . . .	74
9	Adsorption verification table . . . . .	75
10	Experimental data Surati . . . . .	76
11	Desorption case study results . . . . .	76
12	Sequencing of adsorption equations . . . . .	77

## Nomenclature

Symbol	Meaning
$CO_2$	Carbon dioxide
$H_2O$	Water
$N_2$	Nitrogen
$RNHCOO^-$	Carbamate
CCS	Carbon Capture and Storage
CCUS	Carbon Capture, Utilization and Storage
CDR	Carbon Dioxide Reduction technologies
DAC	Direct Air Capture
GHG	GreenHouse Gas
IR	Infrared
NET	Negative Emission Technology
ppm	Parts Per Million
PGA	Purge Gas Adsorption
PSA	Pressure Swing Adsorption
PV	Photovoltaic
TSA	Temperature Swing Adsorption
VTSA	Vacuum and Temperature Swing Adsorption

*Table 1: Terms and abbreviations*

# 1 Abstract

In this thesis, the first part will be a review of the literature that includes as much of the commercially available information on carbon capture and mainly, Direct Air Capture (DAC). What are the difficulties surrounding capturing CO<sub>2</sub> from gas mixtures and what are the possible solutions that have been investigated? What type of negative emission technologies have been proposed, what are the important parameters for the design of carbon removal technologies and what are the biggest obstacles that need to be overcome? Gathering sufficient data and comparing the different findings will be of importance, given that DAC technologies are still in developing stages and information is limited. The focus of this thesis will be on chemically amine based solid sorbents, as this can be argued that this is the most promising technology for a viable DAC system.

The modelling part of the thesis will be focused on the design of and development of a DAC model in the open source software 'Python'. The amine based sorbent that is investigated and used for the creation of the model is Lewatit VP OC 1065. Using experimental data gathered from the literature together with feasible assumptions, a model will be built to recreate the whole DAC process and analyse the system. The main focus will be on acquiring a flexible model for both the adsorption and desorption parts of the DAC process to make further investigation of the system parameters possible. This model will be used after this thesis for further development and, for instance, analysing different possible sorbents.



## 2 Introduction

### 2.1 Contemporary situation

In the past decades it has become painfully clear that the temperature on earth is rising due to increasing amounts of green house gasses (GHGs) in the atmosphere. The excess amount of greenhouse gasses in the atmosphere, specifically carbon dioxide ( $\text{CO}_2$ ), is a consequence of burning of fossil fuels and the overall accumulated impact of human behaviour over the past decades. The amount of atmospheric  $\text{CO}_2$  is described in terms of parts per million (ppm) and has been increasing significantly over the last decades. In 2022, atmospheric  $\text{CO}_2$  was measured as around 420 ppm, with an annual increase of about 2.74 ppm, which is an approximately 0.65% [1]. Comparing this to the year 1970 when the amount was about 325 ppm, it can be seen that the amount of  $\text{CO}_2$  has increased with about 100 ppm within half a century.

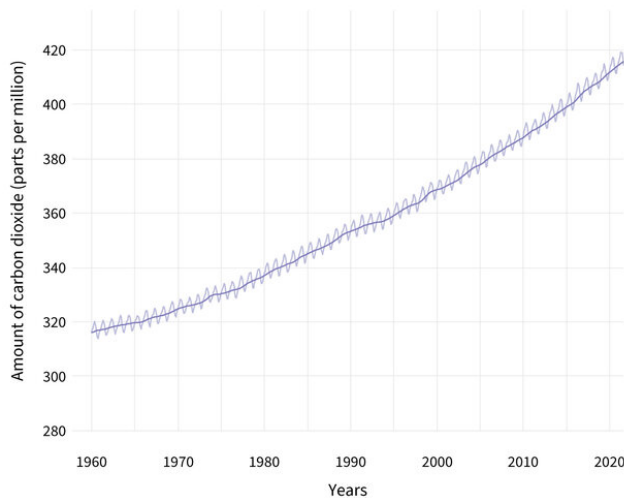


Figure 1: Global carbon dioxide concentration increase from the year 1960 to 2021 in ppm [1].

Sunlight is absorbed by the earth and heats our planet, making life on earth possible. However the accumulation of  $\text{CO}_2$  in the atmosphere traps the IR-radiation that is subsequently re-emitted from Earth's surface, driving an alarming trend of continual increase in global surface- and ocean temperatures, termed global warming [4]. Global warming in turn leads climate change, that is accompanied by more frequent and intensive droughts, heat waves and other natural disasters (such as more severe storms, wildfires and floodings). Heating of the planet affects all life forms on Earth, which must adapt to the repercussions of the direct and indirect consequences of anthropogenic greenhouse gas emissions. This includes human life but is definitely not limited to us, as it can be seen that, in order to survive, many animals are changing their way of life by, for instance, moving higher up into the mountains or migrating north to try and escape the heat, while trees and other plants are struggling to endure the dry climate of their usual niche. Forests, plants and animals are subjected to a gradual increase in the concentrations of many man-made contaminants, as well as of different environmental and industrial pollutants.

It is abundantly clear that it necessary to adapt thae way we live on earth and to reduce the amount of GHGs in the atmosphere. Awareness of these problems has fortunately been growing over the past years, as countries are changing their policies on GHG emissions, reducing dependency on fossil fuels and making the switch to renewable energy and carbon neutral fuels. 'The Paris Agreement' of 2015 stated that the goal by the year 2100 should be to limit "global temperature increase to well below 2 degrees Celsius, while pursuing efforts to limit the increase to 1.5 °C" [5]. This means that the aim is to keep the global temperature rise this century well below 2 degrees Celsius above pre-industrial levels. Countries therefore need to improve their capacity for dealing with the impacts of climate change and to strive for net zero GHG emissions and climate-resilient pathway. Two key words of the agreement are 'adaptation' and 'mitigation', and this is where new environmental technologies are fundamental for reaching the goals that are set. Climate change mitigation cannot depend solely on carbon neutral technologies and fuels: negative emission technologies (NETs) will also be essential to meeting these goals. One od these carbon removal technologies is Direct air capture (DAC), which captures the  $\text{CO}_2$  directly from ordinary air through sorbent or solvent based process plants. Ambient air blows through a DAC reactor, which separates and removes the excess  $\text{CO}_2$ . In this way, DAC technology has the potential

to extract atmospheric CO<sub>2</sub> produced by a wide variety of polluting sources, independent of where they are emitted or by the amount emitted from these sources.

Renewable energy technologies such as, wind power, solar-PV, hydro-power, etc. are increasing yearly and are well known measures for reducing our CO<sub>2</sub> production and therefore, for becoming carbon neutral in the future. Use of such technologies is also increasing rapidly each year. However these technologies are often dependent on weather and/or other variable, are not the only technologies necessary to reach the climate goals. The development of renewable energies is crucial for achieving the ambitious climate goals, but this on its own is not enough to stop the earth's temperature from rising. Technologies such as DAC require energy in order to capture and extract CO<sub>2</sub> so, in order for the whole system to be carbon negative, it is imperative that this energy be produced with renewables. This emphasises the importance of developing different technologies, none of which will be "the" solution to Global Warming on their own. Rather, it is the combination of different technologies, both existing and newly developed, that will be the key to reaching global goals.

As is to be expected with developing technologies such as DAC, there are multiple obstacles during the design and implementation process of the technology for commercial use. First of all it is good to realise what makes DAC a 'negative emission technology'. Broadly speaking, there are three important parts of the process that should be considered. The first obstacle that DAC faces is the amount of CO<sub>2</sub> that is in the atmospheric air. Although the amount of atmospheric CO<sub>2</sub> is too high at around 420 ppm, it is still a relative small proportion of the total air, presenting very real challenges for the technical process of capturing and filtering. Another complication that needs to be considered when using DAC is the amount of energy that is needed for the entire process to continuously be operated. A DAC reactor consumes considerable amounts of energy during the entire systems cycle, from capture of the air to processing of the CO<sub>2</sub>. For this reason, for a DAC plant to be have negative emissions, it needs to run almost completely on renewable energy for the process to be viable. Ultimately what is done with the pure CO<sub>2</sub> coming out of the system, determines the rate of carbon removal from the air. Whether the CO<sub>2</sub> is utilised or stored determines the overall amount of carbon removal from the air. DAC is considered a developing technology and has undergone significant technical developments in the last 2 decades.

However there are still many uncertainties and process optimisations that can be done throughout the entire process. For example, there are still many uncertainties surrounding the process steps and optimal conditions for sorbent based DAC systems. Data about different sorbents and their kinetics throughout the process are constantly being updated, and over the past few years, multiple papers have been published about various materials that could be used as part of the sorbent-based DAC process. From this experimental data, models can consequently be used to analyse the system more carefully. The development of these models is the next step in optimising sorbent based DAC, to gather more data and to accurately predict what conditions can make the different system processes operate optimally. Acquiring a model that can be used gather the necessary data to fill data gaps will help to make DAC a viable process. The model can be used to make the correct choices related to the energy and material design considerations for a DAC system.

## 2.2 Commercial DAC systems

### 2.2.1 Different DAC companies

Multiple companies globally are developing commercially viable DAC systems, with different technologies claiming to be able to achieve different carbon capture rates and commercial prices. It is important to understand the different technologies and requirements before believing some of the claims. DAC technologies have specific requirements for the capture of CO<sub>2</sub> from ambient air and therefore have larger costs. These costs can be considered the mayor bottleneck for commercial DAC implementation as it is estimated that it will cost 75 - 80 € per captured ton of CO<sub>2</sub> [6]. Costs consist of capital costs, sorbent lifetime, electricity, and heat demand. Other considerations that can influence the overall cost of a plant include CO<sub>2</sub> capacity of the sorbent and location of the DAC system.

Multiple leading companies that are developing DAC technologies use different systems for their design. A few of these companies are; Carbon Engineering, using a aqueous alkali hydroxide solution system; Carbyon, using a system containing a thin film sorbent on a porous membrane; Climeworks, using a solid amine sorbent; Global Thermostat, using a solid amine sorbent on honeycomb ceramic monoliths etc. These companies focus on different systems, depending on the type of solvent or sorbent used combined with the regeneration technique for CO<sub>2</sub> collection. All these different systems have obstacles to overcome and all of them are confronted by the

huge expense that DAC currently requires to make it a viable process. In this thesis, the focus will be on the Climeworks system and will be further investigated.

### 2.2.2 DAC plant Orca

On 8th of September 2021 project 'Orca' was launched in Iceland, which is the world's first and largest climate-positive direct air capture and storage plant, making large-scale CO<sub>2</sub> removal from atmospheric a reality. The facility consists of eight collector containers that capture air for carbon removal. These collectors have an annual capture capacity of 500 tons each, enabling a total removal of 4000 tons of CO<sub>2</sub> per year. The heat and electricity required to run the direct air capture process is supplied by the 'Hellisheidi Geothermal Power Plant', which is its main renewable energy source. After capture it mixes the CO<sub>2</sub> with water and pumps it deep underground [7]. Through natural mineralisation, the carbon dioxide reacts with the basalt rock and turns into stone within a few years. The plant is shown in the following figure ??.

Direct air capture removes an amount of CO<sub>2</sub> from the air, but could also provide a sustainable source of carbon dioxide. The carbon dioxide is captured in its pure form, meaning it can be used for several applications: the pure CO<sub>2</sub> stream can either be stored in the earth through 'mineralisation', or this CO<sub>2</sub> stream could be used as a product for functional purposes. In the latter case CO<sub>2</sub> can be produced as a useful raw material for other industrial purposes - a process known as 'utilisation' - which maintains a healthy balance of CO<sub>2</sub> in the air because no additional carbon dioxide is produced. The pure carbon dioxide can be used to produce renewable, carbon-neutral fuels and materials. In the case of utilisation, no excess CO<sub>2</sub> is produced or re-emitted to the air, however it is also not literally removed from the atmosphere thus arguably calling into question the correctness of calling it a negative emission technology. In the case of project Orca, the captured CO<sub>2</sub> is not utilised for further processing as a product but it is stored underground. Mineralisation stores the captured CO<sub>2</sub> safely underground, thus removing it from the atmosphere completely. The carbon will chemically react to form stone under the surface of the earth, therefore it avoids additional transport and processing emissions, and so it can be considered as more carbon negative than the CO<sub>2</sub> that is used for further applications.

### 2.2.3 Relating Climeworks to my model

The Climeworks DAC system is one of the first commercial DAC plants that has successfully been implemented, thus making a good case around which to build a model. It is assumed that they make use of a solid amine based sorbent that is either Lewatit VP OC 1065 or a very similar sorbent and this can be used to simulate a system similar to their DAC plant. An important characteristic of the Climeworks DAC process is that a large share (around 80%) of the energy demand can be met by low-temperature heat in the range of 80–120°C [8]. Based on the current technology, long term energy requirement projections are expected at around 2,000 kWh per ton of CO<sub>2</sub>, from which 400 kWh contributes to the electrical and 1,600 kWh to the thermal energy demand [8]. The Climeworks plant is designed such that it can be powered solely by renewable energy sources, mainly geothermal energy, and waste heat.

### 3 Literature study

#### 3.1 Carbon capture technologies

##### 3.1.1 Negative emission technologies

First of all it is good to get some perspective on negative emission technologies (NETs) and the different ways of reducing CO<sub>2</sub> from the atmosphere that are being researched. The increasing amount of CO<sub>2</sub> in the air directly highlights the growing need for these type of technologies. Consequently different types NETs have been proposed and are being developed rapidly as different solutions to the same global problem. Atmospheric CO<sub>2</sub> is naturally extracted by plants and trees however, this natural process cannot keep up with the excessive emissions, stressing the importance for NETs that can be defined as “the intentional human efforts to remove CO<sub>2</sub> emissions from the atmosphere”[9]. In spite of the increasing need for NETs and the fast pace of their development, the demand for NETs is still much higher than the amount of carbon that is captured at this point in time. Some of these technologies are already at a more developed stage, while others are still in their earlier stages of development. The different types of NETs can be classified into seven different categories, representing the different technological categories currently under research. An overview of the NETs is shown in the figure 2.

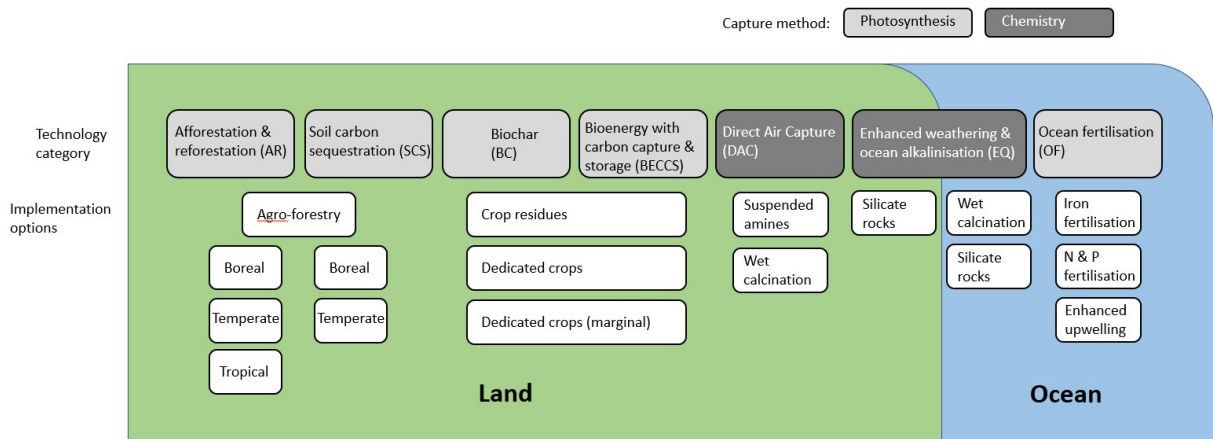


Figure 2: An overview of the various negative emission technologies categorised.

The different methods for carbon removal are either based on natural or chemical carbon capture. Natural NETs remove CO<sub>2</sub> from the air by means of photosynthesis, which is the natural way of carbon extraction that plants and trees use for growing. Chemical NETs such as DAC use synthetic or natural materials that chemically bind to the CO<sub>2</sub> for the removal process. More divisions can be made between the different technologies; however that goes beyond the scope of this thesis as the focus will be on one NET in particular, namely DAC. However when comparing technologies such as afforestation and reforestation (AR) to DAC, some clear distinctions can be made. AR is one the most studied DAC systems but is a slow process; where trees capture the CO<sub>2</sub> from the air to grow, DAC chemically binds quickly to capture the carbon for immediate carbon removal. Also when considering the amount of land that is needed for significant amounts of CO<sub>2</sub> removal, then DAC plants, either solvent or sorbent based systems, need much less area than tree plantations. These examples help underline the importance of instantaneous carbon removal systems such as DAC for shorter term solutions.

##### 3.1.2 Why DAC

This thesis will focus on a specific type of NET known as Direct Air Capture with the goal of analysing the complete DAC process in order to get a better understanding of both the system and the material properties. DAC has been getting increasing attention in the past years and is establishing itself as a promising approach to atmospheric CO<sub>2</sub> removal. Though much progress has been made for types of DAC systems in the past year, there is still much to learn about the different DAC systems. One of the major considerations of DAC implementation is to make the technology energy viable as energy, land and water usage will all be of importance for optimal siting of the plant and to minimise resource impacts. To get a better understanding of the DAC process, the key goal of this thesis will be to design a model that can simulate the DAC process. In this case a solid sorbent that absorbs CO<sub>2</sub> will be used and not rather than solvent based direct capture, that uses

absorption. More specifically, the focus will be on amine based adsorption, meaning that the solid sorbent's structure is amine based and chemically binds with the  $\text{CO}_2$  to extract this from the air. Creating a model for this type of system can be challenging due to the lack of literature and experimental data that is (publicly) known on these types of material. For that reason this model will be built around the Lewatit VP OC amine sorbent, which is a sorbent that has been investigated relatively well and on which the most public data is available.

To meet the climate goals, 10 billion tons of  $\text{CO}_2$  must be removed per year ( $= 10 \text{ GTCO}_2/\text{yr}$ ) globally by 2050 and from 2050 onwards,  $20 \text{ GTCO}_2/\text{yr}$  [10]. This emphasises the need to scale up DAC technologies rapidly, bearing in mind that the annual global  $\text{CO}_2$  capture by DAC systems in 2021 was 1000 tons a year [11]. Current DAC systems use either liquid solvents, which have been investigated more intensively, or solid sorbents. Investigation of solid sorbent DAC systems and optimizing the design parameters can be one solution to increasing the annual  $\text{CO}_2$  capture by DAC systems. While there is no one NET system that is going to scale up in time to achieve these gigatonne scale  $\text{CO}_2$  removal rates, and deployment of multiple different NET technologies will be necessary, it is important to optimise the DAC process as one of the key players for the solution to the problem. That is the main reason for this thesis: to acquire a DAC model that will help understand and optimise the process for better  $\text{CO}_2$  removal rates.

### 3.1.3 DAC process explained

A DAC plant captures  $\text{CO}_2$  from air and do it is good to give a brief description of the entire system and all the steps needed from start to finish. As mentioned, DAC systems use either liquid solvents or solid sorbents to capture  $\text{CO}_2$  using contactors: however this case will focus solely on the sorbent-based adsorption system. Initially the air need to enter the system, before it can be processed. The first step of the system uses fans that blow ambient air from the external air, through the reactor. These fans require energy to operate, which should operate completely by means of renewable energy sources. From the moment that the ambient air flows through the reactor, the actual capture of the  $\text{CO}_2$  will start. As air flows through the bed, at ambient conditions, the  $\text{CO}_2$  particles will be chemically adsorbed by the sorbent. This means that from the air mixture that flows through the system, only the  $\text{CO}_2$  molecules are bound to the sorbent material while the other gaseous compounds in the air pass through the system. After some time, most (or all) of the sites have  $\text{CO}_2$  attached to them and this is called the 'adsorption phase'. When the sorbent bed in the reactor is sufficiently saturated, the reactor is closed off from the environment and the remaining air is (mostly) extracted from the system through a vacuum. Once the system is free of air inside, the next process can start, initiating the 'desorption phase'. The goal of the desorption is to extract the bound  $\text{CO}_2$  molecules from the sorbent bed to create a pure  $\text{CO}_2$  stream. This desorption can be done in multiple ways but generally the system is heated until the  $\text{CO}_2$  releases from the sorbent. The released  $\text{CO}_2$  is then collected and led away as a pure  $\text{CO}_2$  stream for either storage or utilisation. In either case, the pure  $\text{CO}_2$  stream is an outflow that is the goal of the carbon removal technology. After the  $\text{CO}_2$  has been collected and removed from the system, the reactor is opened again to the surroundings until the temperature and pressure are back to ambient conditions. When the system is back to ambient conditions, the entire process will be repeated initiating the next carbon capture cycle. The figure 3 is a schematic representation of the adsorption and desorption steps, which are the main reactions of the process. The goal of this thesis is to simulate these process steps properly and gather missing data concerning solid sorbent DAC.

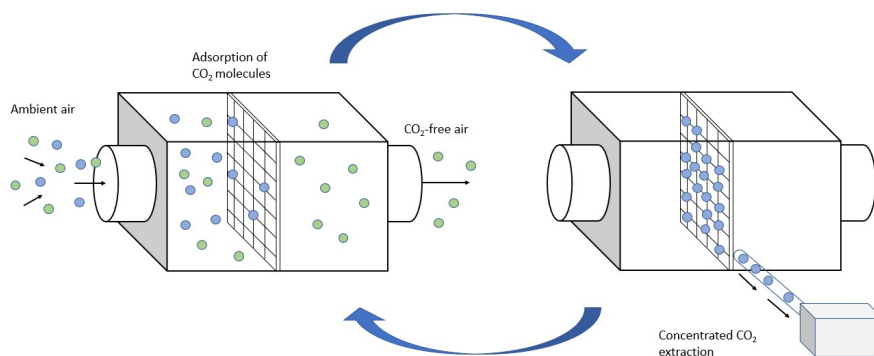


Figure 3: A schematic representation of the main processes that describe a DAC system, an adsorption system where the  $\text{CO}_2$  molecules adsorb to the sorbent structure while other molecules pass and a desorption system where the system is closed and the  $\text{CO}_2$  stream is extracted.

## 3.2 Carbon Capture and storage (CCS) technology

Capturing CO<sub>2</sub> from a large point source is in general less expensive than general carbon capture from air or other distributed sources [6]. Industrial sites are large point sources such as power plants, cement industries, oil refineries, etc. that contribute significantly to the greenhouse gas emissions that produce large amounts of carbon dioxide, however there are also smaller distributed point sources such as cars, airplanes, household or sea transport. Conventionally, recovery has been focused on large point sources, yet the CO<sub>2</sub> emission from the small distributed point sources is rising yearly and the majority of the CO<sub>2</sub> is diluted into the atmosphere: this should not be neglected. These points highlights the significance of development of both DAC and CCS technologies as future carbon reduction technologies.

### 3.2.1 CCS commercially

Another carbon capture technology that is similar to DAC is Carbon Capture and Storage, which is based on the same principle but is implemented in a different way. CO<sub>2</sub> is one of the components of air that surrounds us and that makes life on Earth possible, but as mentioned, it is only a relatively small part of the air mixture. The excessive amounts of CO<sub>2</sub> in the atmosphere is due to the fact that greenhouse gasses are emitted all over the world in large quantities and mainly from industrial sites that exhaust flue gases. At these industrial sites, the amount of CO<sub>2</sub> and other pollutants in the air is significantly higher than 'ordinary' atmospheric air. When air is polluted in such ways, it is called 'flue gas' and can consist of CO<sub>2</sub> quantities up to 30%. CCS is the carbon removal technology (CRT) that captures this polluted flue gas, rather than ambient air as in the case of DAC, and then processes it for CO<sub>2</sub> separation. Though the overall process sounds similar, the two processes are very different and run into distinct design complications. The CCS process can be divided into three basic steps: separation of CO<sub>2</sub> from flue gas streams, transportation of the CO<sub>2</sub>, and finally the permanent storage of CO<sub>2</sub>.

CCS as a system for capturing CO<sub>2</sub> from a gas mixture such as flue gas has been commercially implemented for just over a decade, since 2010 [11]. The number of operating CCS plants has been limited, with in 2017 only 17 operational CCS plants globally and 39 total CCS projects in the works [12]. A significant increase in operational CCS units between 2017 and 2021 has showed that now there are 27 fully operational CCS units and almost 200 commercial CCS facilities in the project pipelines from a diverse range of sectors including cement, steel, hydrogen, power generation and direct air capture [11]. The Global Status of CCS report determined that global storage capacity has increased 32% in the last year alone [13].

### 3.2.2 CCS systems

There are three main CCS methods for capturing CO<sub>2</sub> from large point sources, depending on how and where the CO<sub>2</sub> capture is implemented with the industrial process streams. The three CCS methods are pre-combustion, oxyfuel-combustion and post-combustion, and normally the processes by which CO<sub>2</sub> is captured involves either gas-liquid adsorption, gas-solid adsorption or separation by a membrane [14]. Deciding which is the appropriate technique for implementation depends on a variety of factors, such as what type of flue gas source and composition is in the system and which CCS method is used. One of the main concerns for all three methods is the overall energy consumption, which is significant. The energy consumption contribution is from the flue gas blowers, cooling water pumps, CO<sub>2</sub> compression and sorbent regeneration [15] and should be designed carefully to reduce energy consumption of the overall system.

**Pre-combustion** is a CCS technique where the CO<sub>2</sub> is removed from the fuel before the combustion happens. Generally steam and oxygen is added to the fuel to produce a syngas mixture. This is followed by a gas clean-up and addition of steam to convert the CO into CO<sub>2</sub> in the shift reactor. Finally the CO<sub>2</sub> is separated from the gas mixture, where the gas mixture is supplied back to the plant and the CO<sub>2</sub> is compressed.

**Oxyfuel-combustion** another point source combustion technique is oxyfuel combustion where the fuel is burned with either pure oxygen or an CO<sub>2</sub> and O<sub>2</sub> mixture. This type of combustion is not done with air thus lacks the nitrogen from the flue gas. In this case the flue gas mixture comprises of CO<sub>2</sub>, water vapor and an excess of oxygen. The exhaust gas powers the turbines followed by gas cleaning. Finally the water is removed

from the flue gas and again the pure CO<sub>2</sub> is compressed and either stored or utilised. This method has risks due to the pure oxygen and high operation costs.

**Post-combustion** is the third process and generally makes use of liquid amine absorption techniques for the separation of CO<sub>2</sub>. In the post-combustion process, the first step is the actual fuel combustion that provides energy for powering the turbines and gas-capture units followed by the flue gas clean-up. Then the treated flue-gas passes through the capture unit where generally chemical absorption takes place, followed by regeneration and CO<sub>2</sub> compression for storage or utilisation. The main disadvantages of this process is the cohesiveness of the solution and the significant energy consumption that is needed for the desorption process.

### 3.2.3 CCS compared to DAC

As mentioned before, the main difference between CCS and DAC is that CCS captures a gas mixture that has a much larger concentration of CO<sub>2</sub> in it, which is called flue gas. Flue gas is termed as: 'the mixture of gases resulting from combustion and other reactions in a furnace, passing off through the smoke flue, composed largely of nitrogen, carbon dioxide, carbon monoxide, water vapor, and often sulfur dioxide, and sometimes serving as a source from which carbon dioxide or other compounds are recovered'. The emitted flue gasses lead to higher acidity levels in the air and to increased chemically contaminated surroundings. Flue gasses are the consequence of industrial sites, where CO<sub>2</sub> emission is extremely high. The concentration of CO<sub>2</sub> in a flue gas can range from 5 to 30%, which is significantly more than that of ordinary air at 0,0042% CO<sub>2</sub>-concentration. For that reason, CCS-plants are located in areas where flue gas from can be captured from large point sources such as power plants and cement or steel industries [3]. The extreme concentrations of CO<sub>2</sub> in flue gas, makes it relatively easier for CCS to capture the CO<sub>2</sub> then when compared to DAC systems that captures the CO<sub>2</sub> from atmospheric air. The selectivity demand for the material characteristics is less high for the sorbent or solvent material chosen for CCS than that for DAC materials. In addition, CCS has other limitations, for instance it is location dependent as it must be situated at industrial sites where the carbon emission is abundantly high. DAC and CCS should not be seen as competitive technologies: CCS is restricted to point source locations while DAC is more versatile and can be considered the carbon capture technology that captures the residual CO<sub>2</sub> emissions escaping from the small distributed point sources.

### 3.3 DAC technology

#### 3.3.1 Type of DAC system

DAC technology is still in its developing phase, yet there are two main DAC technologies that have been considered to be the most promising from a technical and economic perspective. One is high temperature desorption, which is solvent based technology based on water solutions containing hydroxide solvents. The other is low temperature desorption technology, which uses mainly solid amine sorbents [6]. Sorbent material selection is crucial in either liquid or solid DAC technologies, as the material needs to have chemically specific properties for the capture of CO<sub>2</sub> at 400 ppm. For the liquid absorption system, CO<sub>2</sub> molecules diffuse into the bulk substance such as water or an alkaline medium. This is in contrast to the solid adsorption system where CO<sub>2</sub> molecules bind to the surface of the solid sorbent. Independent of which system is used, the CO<sub>2</sub> need to be subsequently released from the sorbent or the solvent by means of heat, pressure, purge or a combination of these properties.

#### 3.3.2 Solvent based systems

Flue gas carbon capture by CCS, commonly makes use of aqueous amine solvents to absorb the CO<sub>2</sub> but this technology can also be applied to DAC. The main distinction between sorbent and solvent based carbon capture is the way that the CO<sub>2</sub> particles react with the material. Sorbent based systems use solid materials that adsorb the CO<sub>2</sub> particles, while solvents are liquids which extract the CO<sub>2</sub> molecules through absorption. Aqueous amine technologies for CO<sub>2</sub> removal from gas streams has been under development since the 1930's [3]. One of the most commonly used solvent based amines is MEA (Monoethanolamine) which is used to absorb CO<sub>2</sub> from flue gas and generally combined with temperature swing absorption (TSA) to consequently desorb the CO<sub>2</sub> at elevated temperatures. This is a mature technology that uses these aqueous alkanolamines but its disadvantages are that it is energy intensive, corrosion and sorbent degradation problems [14].

Solvent based DAC systems absorb the gaseous CO<sub>2</sub> from the air, resulting in a CO<sub>2</sub>-rich liquid. Typically these type of systems are designed to have a large contact surface area between the gas and the liquid. For the liquid to absorb the CO<sub>2</sub>, a strong basic hydroxide solution is often required. This approach requires high temperatures to recover the CO<sub>2</sub> from the liquid, especially for a DAC system. The low percentage of CO<sub>2</sub> in the air demands a strong base for absorption of the CO<sub>2</sub> and drives the energy requirements higher as desorption needs to take place at 900 °C [16]. At this temperature the liquid undergoes a decomposition reaction where calcium oxide, water and carbon dioxide are formed. For solvent based DAC systems, a trade-off needs to be made between having a strong basic capture agent and the high energy demands needed for regeneration of the solvent.

Overall, the energy demands of the solid sorbent and liquid solvent systems differ due to the temperature requirements needs for regeneration of the system as is shown in the figure ???. The thermal energy requirements for the solid sorbent are around 100 °C while this is 900 °C for liquid solvents based systems. For solid sorbents this means that the thermal energy can be supplied from lower thermal energy sources like industrial waste heat or industrial heat pumps. Using heat pumps can lower the thermal energy requirements of the system due to their high performance coefficient. The high temperatures of the solvent DAC system require a different thermal energy source, which can said to be a mayor drawback for solvent based system. Furthermore the diffusion resistances and timescales become increasingly important factors as there are more significant variances in the diffusion mechanisms between the two technologies.

### 3.4 Sorbent based systems

The fact that the concentration of CO<sub>2</sub> in atmospheric air is significantly lower than its concentration in flue gas by a factor of a few hundred, leads to several big challenges within the design process. Two of these challenges are the amount of air that needs to be processed to capture significant amounts of CO<sub>2</sub> and the thermodynamic limitations, mainly during the desorption step of the system. As explained before, both solvent and sorbent based materials can be used for the DAC process; however in this thesis the choice has been made to focus solely on the chemical adsorption of solid sorbents. Compared to aqueous amines, the solid amines have some advantages like lower heat capacity, higher CO<sub>2</sub> capacity, lower energy requirement for CO<sub>2</sub> amine contacting and high selectivity for CO<sub>2</sub>. It was shown that solid amine sorbents are a good material option for CO<sub>2</sub> capture because of their high capacities at low partial pressure and relatively low regeneration temperature, approximately 100°C, thus require less energy for heating



### 3.4.1 Important parameters for DAC

Over the past years there has been a significant increase of research done on DAC technologies. For DAC technologies the important characteristics that are crucial for making CO<sub>2</sub> capture from air a feasible technology, are the selectivity, stability and regeneration characteristics of the solid sorbent.

**Selectivity:** The selectivity of a sorbent, it refers to the reaction which the sorbent prioritises when coming in contact with the air. As the concentration of CO<sub>2</sub> in air is low, the sorbent needs to be selective to the CO<sub>2</sub> for it to be able to react at such dilute levels. The sorbent needs to selectively adsorb the desired compound, CO<sub>2</sub> in this case, from all the other chemicals in the gas mixture. The reaction needs to specifically react with the CO<sub>2</sub> under ambient conditions while letting the other chemicals in the mixture pass through the reactor. So the sorbent needs to be reaction specific while the reaction rate needs to be sufficiently fast, that the desired reaction happens while the mixture propagates through the reactor and past the sorbent particles at an adequate bulk velocity. As the air flows through the system at a velocity the CO<sub>2</sub> needs to attach to the sorbent, if the reaction does not take place fast enough, then the process becomes inefficient.

Furthermore the sorbent needs to have a high loading capacity, making it possible that enough CO<sub>2</sub> molecules adsorb to the sorbent. For the system to be viable it is desirable to have sufficient quantities of CO<sub>2</sub> that can be adsorbed per cycle before the system is regenerated. This is favourable because the system becomes more efficient when the system is able to adsorb more CO<sub>2</sub> per cycle, especially given that regeneration of the reactor is an energy intensive process. The total capacity of the sorbent is determined by its equilibrium loading and depends on multiple sorbent parameters such as the pore structure, the surface area and the degree of functionalisation, which is the process of adding new functions, features, capabilities, or properties to a material by changing the surface chemistry of the material. Other external parameters that are of influence on the capacity of the sorbent are the partial pressure of the CO<sub>2</sub>, the temperature and humidity [14].

**Stability:** The stability of the sorbent is another important factor in sorbent selection for the system. The sorbent has to undergo numerous adsorption and desorption cycles during its life time. Per cycle, air flows through the reactor as the CO<sub>2</sub> molecules bind to the sorbent. This consequently followed by the desorption from the sorbent happens at an elevated temperature. Degradation of the material can be a major obstacle in the selection of valid sorbent options. During the adsorption part of the cycle the sorbent is constantly exposed to air, which contains large amount of water, oxygen and nitrogen. Oxygen can have degradation effects on materials, consequently leading to negative effects like shorter lifetime.

**Regeneration:** Whilst being selective and stable, a desired sorbent material must also meet the regeneration requirements. The speed and ease at which the sorbent can be regenerated determines whether the selected material is a viable option for DAC. As selectivity determines the rate at which the CO<sub>2</sub> is extracted from the ambient air, regeneration characteristics are determined by the efficiency at which the CO<sub>2</sub> is detached from the sorbent at the desorption stage. The rate at which this happens has to meet cycle time expectations but more importantly is that the energy requirements can be met within this time. During the desorption step, chemically bound CO<sub>2</sub> needs to be detached from the sorbent so the CO<sub>2</sub> can be extracted for its purpose of storage or utilisation. Extracting the pure CO<sub>2</sub> stream from the system is the goal of the process of capturing carbon from the air, thus being essential that the system does not exceed the energy required to capture and process it. Furthermore the CO<sub>2</sub> needs to make place for the new adsorption cycle. The adsorption sites can only be extract CO<sub>2</sub> from the air if the sites are not occupied.

A comprehensive understanding of sorbent characteristics is important for selection of plausible materials or researching optimal ways for performing these kind of processes. Especially in terms of CO<sub>2</sub> and H<sub>2</sub>O equilibrium capacity and reaction kinetics much investigation and knowledge is required.

### 3.4.2 Physisorption

Direct air capture however is a technologically based carbon capture method that uses either physical or chemical based binding to capture CO<sub>2</sub> from the atmosphere. In both cases sorbate molecules are separated selectively from a gas mixture: for physisorption molecules attach themselves to the solid by means of inter-molecular forces like van der Waals interactions and in the case of chemisorption the molecules bond together with the

sorbent chemically.

In physisorption reactions both the pore size and surface area of the sorbent are important parameters. Physical sorbent materials are preferred to have a small pore size and a large surface area like activated carbons, metal-organic frameworks (MOFs) and zeolites (which are very porous crystalline aluminosilicates). For these kind of sorbents, both van der Waals forces and electrostatic interactions play a role in capturing a particular molecule during physical adsorption. The van der Waals contribution will always be present whereas the electrostatic contributions will only be significant if the sorbent has an ionic structure [? ]. Compared to chemisorption, physisorption has much lower binding energies per molecule (10 - 1000x higher) and lower adsorption enthalpy (2 - 4x higher) [6]. However, given the characteristics of the physical sorbent systems, it can be argued that physical sorbent are less likely to be promising for DAC technologies, as CO<sub>2</sub> often binds too weakly to physical sorbent surfaces and the capacity is sensitive to the presence of moisture. In general physisorption sorbents are more dependent on the partial pressure of CO<sub>2</sub>, making them more suitable for high pressure applications, which is not the case for DAC.

### 3.4.3 Chemisorption

Chemisorption is often an exothermic process which in the case of DAC technologies, binds to CO<sub>2</sub> as air moves through the reactor and over the sorbent. The CO<sub>2</sub> molecules chemically bind to the sorbents binding sites. Only the CO<sub>2</sub> chemically reacts with the sorbent allowing the other components of air to pass through. The material chosen for this process can take the form of either a liquid solvent or a solid sorbent. Once the air is taken from the atmosphere, the CO<sub>2</sub> needs to be removed from the gas mixture. Heat is typically applied at this stage, to release the CO<sub>2</sub> from the solvent or sorbent. Doing so regenerates the solvent or sorbent for another cycle of capture. The captured CO<sub>2</sub> can be injected underground for permanent storage in certain geologic formations or used in various products and applications. Permanent storage will result in the biggest climate benefit, compared to utilisation. Using the captured carbon for products such as construction material or plastics can also provide long-term storage (decades or even centuries). However, using the carbon for products like beverages would quickly re-release carbon into the atmosphere.

## 3.5 Solid amine based sorbents

As was mentioned, a good material for sorbent selection should be able to selectively extract CO<sub>2</sub> at ambient conditions. Other important characteristics are the ease of regeneration and the stability of the material over numerous cycles. However, many physical sorbents fail to meet these criteria and are therefore not suitable for sorbent based DAC systems. Chemisorption however, is considered to have the best potential for DAC systems. Inorganic chemisorbents such as NaOH and KOH can be used, but they require high temperatures. The most promising type of sorbent is a solid amine-based sorbent, which is the type of sorbent that will be used in this thesis for the DAC model. Most of the solid amine-based sorbents can be regenerated at temperatures of about 100 °C, which is advantageous because this can be supplied by renewable energy sources or waste heat. The desired characteristics of chemical amine sorbents such as the low heat demand together high capacity, selectivity, fast uptake rate and mild regeneration conditions are reasons why they have been researched extensively recently for CO<sub>2</sub> capture [17]. They do, however also have some major drawback such as their high costs which is one of the main reasons why DAC hasn't really been commercialised yet.

For amine selection (1) the number of nitrogen atoms per amine molecule, (2) the adsorption heat and (3) the sorption kinetics contribute to the chemical reaction and efficiency of the material. The amine sorbent should be able to effectively utilise its capacity under optimal DAC process conditions. This implies that the sorbent can be regenerated while producing a high purity CO<sub>2</sub> gas, while the sorbent can be saturated with CO<sub>2</sub> within a reasonable time frame and the sorbent is suitable for application in a gas-solid contactor. Other ways to improve the sorbent capacity are to focus on finding the most suitable amine type and modifying the amine molecules to improve their reactivity.

Important for chemical adsorption is the design and development of a suitable sorbent which consist of a porous support on to which functional groups are attached using different techniques. When this functional group is an amine, then the sorbent is called as solid amine sorbent. For solid amine sorbents the chemical reaction takes place at the amine group attached to the porous support. The chemical reaction where the CO<sub>2</sub> reacts and attaches to the amine can be described by several different mechanisms, depending on the type of functional

amine that is attached to the support and the conditions under which the reaction takes place. The various amines react differently due to the number of associated hydrogen atoms. Amines can carry up to four hydrogen atoms and can therefore be classified as Primary Amines, Secondary Amines, Tertiary Amines and even Quaternary Amines.

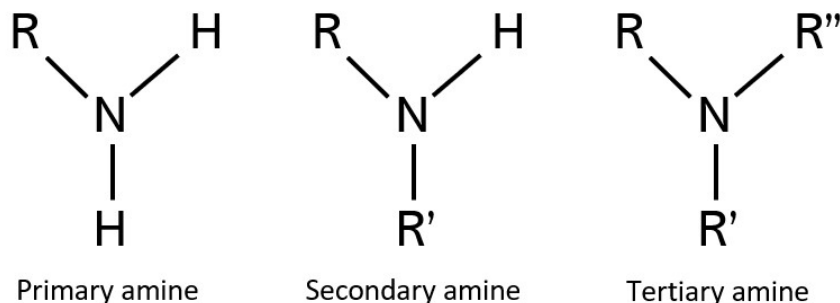
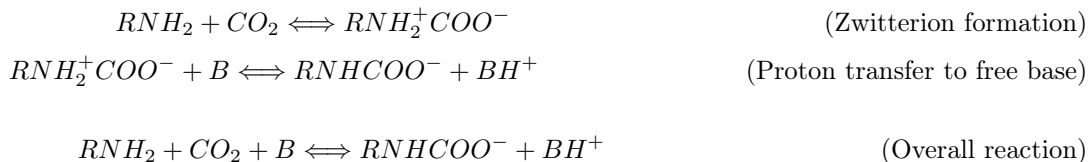


Figure 4: Different chemical amine based mechanisms that can occur during chemisorption, depending on the amount of hydrogen atoms that are carried by the nitrogen molecule.

### 3.5.1 Type of amine based sorbents

As mentioned, DAC systems can use amine based sorbents that carry between one and four hydrogen atoms. Primary and secondary amines are commonly used for DAC systems, these type of amines can react directly with  $\text{CO}_2$  molecules to produce carbamates. Tertiary amines catalyse the formation of bicarbonate which is then fixed due to electrostatic forces, so these types of amines are considered less desirable for DAC systems. As each different amine interacts with  $\text{CO}_2$  in a different way, it influences the capture speed and regenerability. In general, primary amines have a higher heat of adsorption compared to secondary and tertiary amines and they also exhibit the highest adsorption rate. The desorption rate constants may be lower for primary amines than that of tertiary amines, but the low rates of  $\text{CO}_2$  adsorption rates make tertiary amines difficult to use for gas removal. As for supported non hindered primary or secondary amines, the carbon dioxide adsorption process and mechanism depend on the amine loading and whether the feed gas is dry or humid. The Lewatit VP OC 1065 sorbent is a primary amine sorbent, so the reactions that primary amines undergo in both dry and humid conditions will be further explained.

**Dry conditions**  $\text{CO}_2$  adsorption reacts differently under dry conditions and wet conditions. Adsorption under dry conditions reacts, with a reaction that involves two steps. First an amino group and  $\text{CO}_2$  create a zwitterion molecule, followed by a reaction of a free base, which is either water or another amino group, that deprotonates the zwitterion molecule to form an ammonium carbamate [17]. Under dry conditions two amine groups are required to bind one molecule of  $\text{CO}_2$ . The reaction mechanism for primary and secondary amines under dry conditions is as follows:



**Humid conditions** In humid conditions, the zwitterion and the ammonium carbamate are formed in the same way as in dry conditions, where  $\text{CO}_2$  reacts with two amine groups. The  $\text{CO}_2$  capture by primary or secondary amines proceeds by the formation of carbamate ion according to the following equation.



### 3.5.2 Lewatit VP OC 1065

The amine sorbent that is investigated in this thesis is the 'Lewatit VP OC 1065', a commercially available supported-amine sorbent. For the Lewatit sorbent, the functional groups for CO<sub>2</sub> capture are primary benzylamine groups. The reaction mechanisms of benzylamine in aqueous solutions prefers direct carbamate formation mechanism over the zwitterion mechanism based on the experimental results by [3], showing CO<sub>2</sub> adsorption in aqueous benzylamine. The reaction takes place under ambient conditions where it extracts the CO<sub>2</sub> from atmospheric air, which contains water and is thus under humid conditions. The commercially grafted sorbent Lewatit VP OC 1065 has been found to have excellent thermal stability for desorption and good working capacity at ambient adsorption conditions. In the literature this became clear when they compare this sorbent to other potential materials [17]. However it is beyond the scope of this thesis to explain why the Lewatit sorbent reacts the way it does chemically.

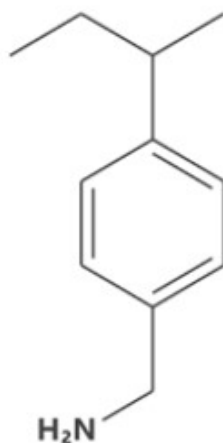


Figure 5: Chemical composition of a Lewatit VP OC 1065 molecule.

### 3.5.3 Geographical considerations

Before a DAC plant can be built and run successfully, multiple environmental considerations and constraints have to be taken into account. One of the main reasons for this is that a DAC plant needs a considerable amount of energy during the entire process to extract CO<sub>2</sub> from the air. The biggest part of the energy consumption comes from the fans that blow the air through the system and during the desorption cycle where the sorbent needs to be heated sufficiently to be able to extract the CO<sub>2</sub> from the reactor.

Firstly, the energy that is required for the process, in the form of heat and electricity, has to be generated near or at the DAC plant itself. Secondly and more importantly is that this energy has to be produced by renewable energy systems for the entire system to have a negative energy balance and therefore making the system environmentally compatible. Plainly said, the technology has to extract more carbon from the air than that it produces. Not only does the system need energy to run, also CAPEX emissions need to be taken into account. This can be described as the emissions that are generated during the production of the equipment and the building of the plant.

Though DAC is not geographically bound to industrial areas, it is still good to consider the advantages that can be gained by DAC implementation. DAC plants can be built near geologic storage sites to minimize transportation costs for storage, or near unused sources of waste heat to reduce impacts on the energy system. For DAC the system can be described as the repetitive use of a single reactor geometry, which means that the geometry of a DAC plant can be designed to be relatively small. Water usage associated with direct air capture also depends on the system type, as well as the ambient temperature and humidity. Siting DAC in cooler and humid areas could minimize water use and in some cases the systems could also produce water. Some DAC systems regenerate the sorbent using indirect heating, which allows for minimal water losses. These indirect heating systems, such as used by 'Climeworks' solid sorbent systems, are actually net water producers.

### 3.5.4 Influence of water

Because water vapour is a major component in air it is important to study the effect of humidity on solid amine sorbents. For the DAC process conditions, there is no evidence that supported amine sorbents degrade in the presence of humid vapours during adsorption. The presence of water could have positive effects for the CO<sub>2</sub> capacity, as in many cases its capacity even increases in the presence of H<sub>2</sub>O [3].

In absence of H<sub>2</sub>O during CO<sub>2</sub> adsorption on solid amine sorbent, the only available base for the proposed carbamate forming reaction is another amine group. Therefore, in order to adsorb one molecule of CO<sub>2</sub>, the two amine groups should be in close proximity. Molecular modelling of Lewatit VP OC 1065 showed that the amine groups alternate in position and this could lead to two amine groups reacting with each other despite being fixed on the surface [18]. Water has great influence on the adsorption process of amine based sorbents.

The presence of water might not lead to unwanted amine degradation, however studies show that amine sorbents degrade in an oxidising environment, where primary amines were found to be more stable than secondary and tertiary amines and the degradation rate depends on the temperature. At elevated temperatures, degradation increased and so it must be closely considered during the adsorption of the CO<sub>2</sub> as the temperature will be increased during this part of the process.

### 3.5.5 CO<sub>2</sub> processing

Separated pure CO<sub>2</sub> can be used either as a product for other industries or it can be stored. CCS makes use of suitable underground geological formations or deep ocean storage for CO<sub>2</sub> storage and in the oil recovery process, the CO<sub>2</sub> is sealed under bedrock or stored for the mineralisation process and to form carbonates underground [6]. The first pilot injection took place in Iceland in 2012 as a part of the CarbFix project, wherein 175 tons of pure CO<sub>2</sub> were dissolved in water and then injected into the basaltic subsurface at depths below 500m and at a temperature of 35 °C.

Utilisation of captured CO<sub>2</sub> can have disadvantages for the total efficiency of the DAC plant. Transport of large volumes of CO<sub>2</sub> for instance can become problematic as the vehicle transport consumes energy and creates emissions. An alternative way for transportation could be to transport the CO<sub>2</sub> in a supercritical fluid phase via a pipeline, but this also has multiple difficulties.

CO<sub>2</sub> is currently used as raw material for multiple industries like for greenhouses, food, brewing, chemicals, as well as for the production of other chemicals. Many different chemicals are produced from CO<sub>2</sub> in chemical industries, two of the most common being methanol synthesis and urea synthesis. Clearly it is desirable to recycle the captured CO<sub>2</sub> for these types of industries, yet this is impossible to do with all the captured CO<sub>2</sub>. Furthermore, it can be said that when CO<sub>2</sub> is recycled and used for other products, that it re-enters the atmosphere again and thus decreasing the efficiency of the entire DAC process. Therefore, the majority of CO<sub>2</sub> captured from DAC should be permanently stored.

## 4 Model Literature

### 4.1 Process description and model considerations

The aim of this work is to build a model that can simulate both the adsorption and desorption steps of the DAC process. This model will be built in the open source programme Python and will be based primarily on the Climeworks DAC systems. Using both experimental data and what little information there is available in the literature, a model will be built simulating the DAC process. For both models multiple assumptions will be made and explained. The goal will be to build good models that can simulate the processes accurately, by making fair assumptions that can be used to give insight into the overall DAC process.

For both models the first goal is to produce realistic values with the gathered data and general knowledge about DAC systems. A mass and/or energy balance will be set up for both processes individually. Contingent upon the outcome of these equations, the model will be built that represents both processes as well as possible taking into account the assumptions that are made. When the model gives the expected data, it then needs to be validated before actual results can be produced and analysed.

### 4.2 Adsorption

Climeworks proposed porous granulates modified with amines applied in vacuum-pressure temperature swing adsorption (VTSA) cycles [19]. In this process, unloaded sorbent material is exposed to air to capture carbon dioxide at ambient condition. Subsequently, the unit is evacuated to a pressure in the range of 20 to 400 mbar and heated to a temperature of 80 to 130 °C to desorb CO<sub>2</sub>. The combination of vacuum and temperature allows for a higher cyclic capacity, therefore limiting the amount of sorbent needed. Finally, the unit is repressurised and cooled down to ambient conditions.

#### 4.2.1 Mass transfer

The adsorption process is the rate at which the CO<sub>2</sub> is taken up by the sorbent and specifically reacts for different sorbents and reactor parameters. It is crucial to take into account the adsorption kinetics when designing the reactor optimising the process. The sorbent that will be used in this thesis for the design of the model is the solid amine sorbent Lewatit VP OC 1065. The mass transfer of the CO<sub>2</sub> on to the solid sorbent can be described in three steps. First is the external mass transfer, during which the CO<sub>2</sub> molecules diffuse from the gas mixture through the film layer resistance of the sorbent, to its outer surface. This is followed by the internal mass transfer, where the CO<sub>2</sub> particles transport into the pores through the porous surface of the sorbent. Finally the CO<sub>2</sub> molecules adsorb on to the external or internal surface of the sorbent when they react with the remaining amine groups. The adsorption step will either be stopped when the sorbent is completely loaded or when an optimum has been achieved of CO<sub>2</sub> loading for the desorption step to start.

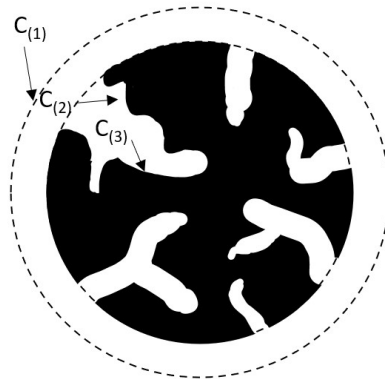


Figure 6: Schematic the adsorption mechanism of a CO<sub>2</sub> particle, it first passes the film layer (1), then it transports into the pores of the sorbent (2) and finally it adsorbs on to the external or internal surface of the sorbent (3).

A sorbent has a limited capacity to store the CO<sub>2</sub> which is dependent both on the partial pressure of the gas and its temperature. The speed of the adsorption process is determined through experimental data and simplified through a constant, in this case the linear driving force. This parameter has been obtained in other literature by doing breakthrough experiments and matching the breakthrough curve to the theoretical model [18]. In this thesis, the breakthrough curves will be used to match the model. The reactor column will initially be sorbent free as it is exposed to the ambient air and the concentration of CO<sub>2</sub> changes throughout the column as a function of time. The breakthrough curve will be matched with the concentration gradient at the outlet of the reactor until the reactor is saturated.

#### 4.2.2 Equilibrium considerations (capacity)

In an adsorption process, a dynamic phase equilibrium is established between the adsorbate in the gas phase and the solid surface of the sorbent. It is common to describe this equilibrium capacity as a function of the adsorbate concentration which is the partial pressure of the species for gas adsorption. Equilibrium capacity data is acquired through experiments, these experiments have been done in literature and the data will be used to fit the model. During such experiments [18] the amount of loading on the sorbent is measured as a function of the partial pressure of the sorbate in the gas phase: this is known as the adsorption isotherm. The isotherm shown in Figure 7 is calculated from the Langmuir equation.

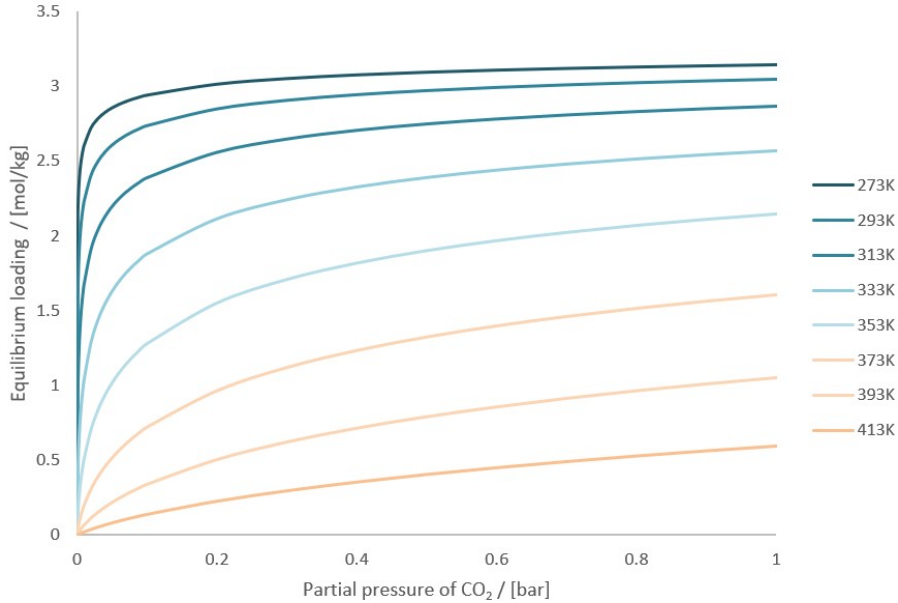


Figure 7: A representation of the experimental equilibrium capacity isotherm of the Lewatit sorbent at different temperature for varying partial pressure of CO<sub>2</sub> as determined by Bos.

#### 4.2.3 Modelling

The adsorption model should be capable of describing the adsorptive behavior of a solid sorbent in a configuration when it is exposed to the sorbate concentration, where the desired outcome are the breakthrough curves. A bed reactor with certain dimensions and void fraction, is exposed to an air stream with a certain velocity  $u$ . In order to correctly predict the breakthrough curve, the model should be able to describe the CO<sub>2</sub> concentration in both the gas phase as well as the solid phase at every instance in time for every position in the bed. To predict this behaviour, the following mass balance can be derived for the adsorption process:

$$-D_L \frac{\partial^2 c}{\partial z^2} + \frac{\partial c}{\partial t} + \frac{\partial c}{\partial z} u_{\text{air}} + \frac{\partial q}{\partial t} \rho_p \left( \frac{1 - \epsilon_b}{\epsilon_b} \right) = 0 \quad (1)$$

In the equation  $D_L$  is the dispersion term,  $c$  is the concentration of CO<sub>2</sub>,  $q$  is the sorbent loading of CO<sub>2</sub>,  $z$  is the spatial dimension,  $t$  is the time,  $u_{\text{air}}$  is the velocity of air,  $\rho_p$  is the density of the sorbent particle and  $\epsilon_b$  is the bed voidage of the sorbent. As can be seen from this mass balance, it is a partial differential equation (PDE) that is dependent on time ( $t$ ) and distance ( $z$ ). In this thesis the dispersion term, which is the higher

order term in the equation, will not be taken into account for the the mass balance. This is an assumption to initially simplify the mass balance and thus the model, as the higher order term is difficult to account for. After simplifying the mass balance by setting the dispersion term to zero, the mass balance for the adsorption will look as follows:

$$\frac{\delta c}{\delta t} + \frac{\delta c}{\delta z} u_{\text{air}} + \frac{\partial q}{\partial t} \rho_p \left( \frac{1 - \epsilon_b}{\epsilon_b} \right) = 0 \quad (2)$$

The nature of the mass transfer is determined by the isotherm whereas the complexity of the mathematical model depends on sorbate concentration in the fluid phase, the choice of the mass transfer rate equation and the choice of the flow model. The starting point for the model is the differential mass balance equations for a small control volume in the adsorption column. The solution to the mass balance equation will give the distribution of the gas composition throughout the bed.

The mass transfer rate expression for the adsorbable component into the solid phase can be represented with a linear driving force ( $k$ ). This term is commonly a set of equations containing diffusion equations to which the mass transfer term must eventually be reduced. The linear driving force has been reduced to the term ( $k$ ) and can be used in the following equation to represent the amount of sorbent that is loaded on to the sorbent as a function of time, where  $q_e$  is the equilibrium loading.

$$\frac{\partial q}{\partial t} = f(q, c) = k(q_e - q) \quad (3)$$

### Isothermal

Since adsorption is an exothermic process and temperature changes may have an effect on both the equilibrium relation as well as the adsorption rate, the internal heat generation has to be considered. However, in systems where the adsorbable component is present only at very low concentration (which is the case for DAC) the system can be classified as isothermal.

If the adsorbable component is present at low concentration, the system can be classified as a trace system. Since both the concentrations of water as well as that of carbon dioxide are very low, the DAC system can be described as a trace system. Changes in the fluid velocity across the mass transfer zone are therefore negligible.

## 4.3 Desorption

For large scale CO<sub>2</sub> capture the desorption part of the process is also crucial in the design of a viable DAC plant. Important parameters for this process are the ease of regeneration and the stability of the sorbent, and these help determine the efficiency, cost and feasibility of the DAC system. For the desorption step, the energy balance becomes of significance for the detachment of CO<sub>2</sub> from the sorbent. To begin the desorption step, after the adsorption process is finished and CO<sub>2</sub> is adsorbed to the sorbent surface, the reactor column is closed to the surrounding air and the remaining air is extracted from the system using a vacuum pump. The desorption can be initiated which is typically a combination of a vacuum and temperature swing (VTSA), where the reactor's pressure is reduced by vacuum and followed by the heating of the system. Another method for the desorption is to use a purge gas such as nitrogen, steam or oxygen. If a purge system is used, the purge flow is inserted into the system, which is either simultaneously heated or the overall pressure is reduced before the purge gas is inserted.

### 4.3.1 Desorption methods

Generally heat is used to release the captured CO<sub>2</sub> from the solid sorbent before it is regenerated for the next capture cycle. Combining a vacuum with temperature rise has been shown to be better than using either a pressure swing adsorption (PSA) or a temperature swing adsorption (TSA) method. The combined method is called a vacuum and temperature swing adsorption (VTSA) which leads to better desorption and regeneration of the sorbent. Typical regeneration temperatures for solid sorbents range between 80 °C and 120 °C, which is a relatively low temperature when compared to solvent carbon capture but is still energy intensive. Careful consideration should therefore be made as to how the column is optimally heated. The heat transfer rate of the reaction has a significant influence as the isotherm is temperature dependent. Optimising the heating step for the desorption reaction is crucial for a DAC system to be a viable carbon negative technology. The process is energy intensive and can therefore become a big obstacle in the design as the heating should be done completely



by renewable energy and latent heat. However the heating is completely necessary for the desorption to take place as both the productivity and the working capacity increase significantly. The heat transfer considerations will be the crucial for the desorption design of the system as a trade-off between the sorbent working capacity and energy consumption for sorbent heating will determine the efficiency of the system.

**VTSA** The shape of the isotherm shows that the effect of the temperature is greater than that of the pressure. The isotherm has a very steep initial curve for pressures below 0.2 bar, considering Figure 7. Though the temperature has a larger overall impact on the isotherm, more desorption could theoretically be achieved at sufficiently low pressures. The combination of decreased pressure and elevated temperatures describes a VTSA system that can achieve higher working capacities than a system that would use solely either one of the two parameters [3].

**PGA** Instead of reducing the pressure of the system, another way to regenerate the sorbent is with a purge gas that can be injected into the system to lower the CO<sub>2</sub> partial pressure. Some considerations that can be taken into account for choosing an appropriate purge gas are that the gas should preferably be inert, abundantly available, inexpensive and condensable. When using an inert, non-condensable purge gas to desorb the sorbent, the CO<sub>2</sub> in the system will be at lower concentration due to the mixture of CO<sub>2</sub> and purge gas. The gases that are commonly considered for PGA are nitrogen, air or steam. It was found that when using a purge gas flow, the desorption rate is strongly influenced by the equilibrium between the gas and adsorbed phase.

From the Lewatit isotherm, it is clear that an increase in temperature will lead to an increase in working capacity and the desorption of CO<sub>2</sub> will only happen when the equilibrium loading at the local conditions is lower than the actual loading. However, it should be realised that the isotherm lines are evaluated at the CO<sub>2</sub> outlet concentration, which is the highest CO<sub>2</sub> concentration in the column.

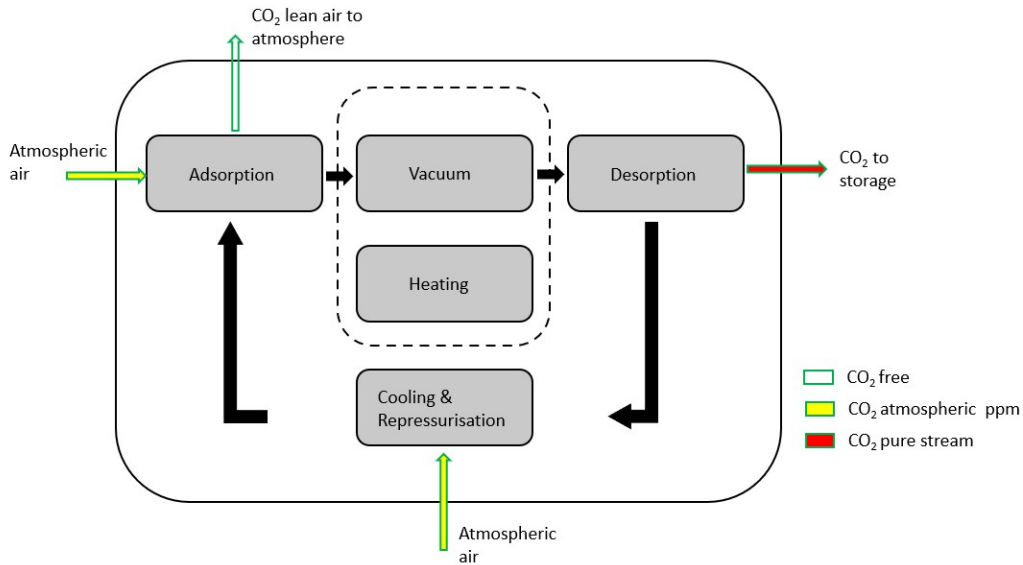


Figure 8: An adsorption and desorption cycle with the different steps in between for a DAC cycle and the in and outflow of the system for every step.

#### 4.4 System to model

A model will be built using data from the literature in combination with justified assumptions and correct reasoning. The system will be based mainly on the existing DAC system that is designed by Climeworks, in combination with available data from the literature. However there will be some differences from the existing DAC plant due to a lack of published information about the existing system. For that reason additional literature has been used to fill these knowledge gaps and to achieve a viable system that makes sense. The adsorption and desorption processes will be modelled based on the existing system of the Climeworks design. The sorbent of the system will be the a solid amine sorbent 'Lewatit VP OC 1065', that adsorbs CO<sub>2</sub> at ambient conditions and be regenerates through means of VTSA at elevated temperature and lowered pressure. Adsorption will be modelled as a Plug flow reactor (PFR) while desorption will be modeled as a continous stirred tank reactor

(CSTR): this will be further explained later in this thesis.

The first step for achieving a model is to gather correct data and use this to build the model that simulated a viable DAC process. When this is achieved, the model will be tested and verified to get a stable model that can be used to analyse the adsorption and desorption steps of the system. Having done this, a goal of this thesis is to use this model to potentially find out more about the specific reactions in the system and gather optimal parameters. The entire system will be analysed to find what optimisation is possible for the process and to test the parts of the system where design trade-offs take place and need to be investigated further. Models like this in combination with experimental data are necessary to gain knowledge about developmental systems like solid sorbent DAC.

In the work of Sabatino [19], process analysis for aqueous- and solid-based DAC technologies were done. Thermodynamic modeling was done via 'Aspen Plus' for liquid solvents and a state-of-the-art in-house code for fixed bed cycles with solid sorbents. 'Matlab' was used for mathematical algorithms to identify the optimal design. Modelling done in the thesis of Flart [18], molecular modeling was executed with 'Spartan' software and again 'Matlab' was used, but in order to extract the experimental data from a graph (a webplotdigitizer tool was used). In the case of Bos [3] 'Matlab' was used to analyse data, making use of built-in software solvers which make the model less accurate. What makes this research special is that the model is built completely from scratch, using only an open source software 'Python', which has not yet been reported in the literature. In this model, no built-in tools will be used such as automatic differential equation solvers. This was done to prevent the being 'rigid' enabling it to produce more accurate data than if solvers had been used. Furthermore this model can be used to analyse new experimental data that 'TNO' produces or to check the validity of future research papers.

## 5 Research questions

The research question of this thesis is: **"Modelling for sorbent based direct air capture systems: Will it be possible to create models that can simulate the adsorption and desorption processes of an amine based DAC system successfully and can these models be used to gather the appropriate information to help fill in knowledge-gaps surrounding the concerning system"**.

The goal of this thesis is to analyse amine based sorbent direct air capture systems. The information on sorbent based DAC is relatively limited, also due to the fact that the technology is still developing. This is one reason for the goal of this thesis, as this technology still has many unknowns such as how the processes exactly work and how they should be optimised. These "knowledge gaps" within DAC are to be investigated during this thesis, first through a thorough literature research, then by creating DAC models in Python. These model can in turn be used to analyse some of the knowledge gaps surrounding sorbent based DAC systems. Learning more about the specifics within a DAC systems and having an open source model of the system would be a very useful tool.

Two types of research questions are set-up: (1) The advantages and difficulties for creating an open source Python model (flexibility w.r.t. commercial software and solvers) (2) Giving support to researchers in the field of DAC and similar carbon capture technologies and being able to verify experimental data and to challenge claims of other papers.

### (1) Can a functional open source Python model be created for DAC technology?

- Is it possible to create a model from scratch (without solvers), that is not rigid and can be adapted for other DAC systems.
- Is it possible to recreate and validate DAC systems from experimental data, from available papers?

### (2) Can use a the created model to gather more information about the DAC system and optimize the process steps (find optimal parameters and make evaluate trade-offs)?

- Can the model be used to get a better understanding of what happens during the adsorption and desorption steps (fill data gaps e.g.)?
  1. What should the volume of a column be?
  2. What is the time needed to regenerate the system?
  3. Can we find optimal parameters for the system (such as  $T$ ,  $u$ ,  $P_{\text{CO}_2}$ )?
  4. How long does the adsorption process take for a 50% and 90% saturated loading of the sorbent?
  5. What is the best way to heat the reactor for desorption?
  6. What is the optimum desorption temperature?

# Adsorption

## 6 Introduction adsorption

DAC is a process that captures  $\text{CO}_2$  from the air in order to reduce the amount of  $\text{CO}_2$  in the atmosphere. For such systems, the primary goal of the system is a two-step process that removes the  $\text{CO}_2$  from the ambient air. The first main process is the separation of the  $\text{CO}_2$  molecules from the air, where ambient air flows into the reactor and eventually exits the reactor as  $\text{CO}_2$ -lean air. In this case the separation process is adsorption, where the goal is that the  $\text{CO}_2$  molecules bind to the sorbent in the reactor, while the other components of air pass through the reactor undisturbed. As the adsorption reaction progresses and the sorbent bed becomes saturated, it becomes harder for the  $\text{CO}_2$  molecules to find vacant adsorption sites until, eventually the reaction stops. After the sorbent bed has become saturated, the following reaction is initiated for the  $\text{CO}_2$  removal from the sorbent material. This process is the desorption reaction of a DAC system, during which the reactor becomes closed from its surroundings to make sure that no air can flow into or out of the system. Desorption can be implemented in various ways, but as will become clear, VTSA-desorption is the preferred method to describe the system. The VTSA method operates at reduced pressure, to create a vacuum, and at elevated temperatures to extract the captured  $\text{CO}_2$  from the sorbent, from which an outflow of almost pure  $\text{CO}_2$  can be processed or stored.

These two processes combined are the foundation of a DAC system and determine if DAC is possible and moreover that it is viable. Experimental data alone does not provide sufficient data and knowledge to understand and optimize the processes. Therefore it is necessary to have a model that can test experimental data, predict results and gather information about material and reactor design parameters. To build such a model that can simulate both the adsorption and desorption processes, individually and together to gather extensive data will be the main goal of this thesis. The models will be designed individually, with appropriate assumptions, to produce relevant and realistic data within viable margins.

The models will be created using the open source programme 'Python', which will be used to simulate the adsorption and desorption processes that describe a DAC system. The entire design processes will be described as complete as possible in the following parts.

### 6.1 Adsorption

The adsorption process is considered to be a 2D-process and will be designed accordingly. Adsorption of the  $\text{CO}_2$  molecules happens throughout the bed reactor as the bulk, in this case air, propagates from the inlet to the outlet of the reactor. The adsorption reaction takes place at the sorbent material's adsorption sites as  $\text{CO}_2$ -rich air flows through the bed and the  $\text{CO}_2$  molecules adsorb to the sorbent. This process occurs while the air flows in its propagation direction, which will be from here on out be described as the z-axis.

As the air flows through the reactor over the z-axis and adsorption takes place between the  $\text{CO}_2$  molecules and the sorbent, the reactor starts to become gradually more saturated and it becomes harder for the  $\text{CO}_2$  to adsorb to the remaining vacant adsorption sites. This entire process is depends both on its position in the reactor and on the time, which will be the second dimension of the adsorption process, described over the t-axis. The time it will take for a sufficient amount of  $\text{CO}_2$  to bind to the sorbent throughout the reactor, is what will be modelled with the adsorption model. Data from literature will be the source of information for the design of the model. At first, the model will be created based on the information provided by literature, which in turn will be verified and validated with known data from experimental results to check if the model produces viable results. After the model has been sufficiently validated, it can be used to analyse the adsorption parameters and predict what will happen to the system at different input variables. The model will be able to predict results and test experimental data, taking into account appropriate assumptions and the reliability of the data that has been used in the literature.

### 6.2 Adsorption model

For the adsorption process, a major challenge will be to design the model completely from scratch and create the solver system, without using other existing solver systems. This means that the adsorption model will be modelled entirely without the help of other numerical sub-systems for the design of the adsorption model. Modelling the system in this way will increase the computational power needed to run the simulations, but the main advantage is that the adsorption model will be completely flexible and will not be reliant on the work of other, which would be the case if a solver would be used. The model can be changed manually to describe any

Partial Differential Equation (PDE) system and can be designed with any desired numerical methods to achieve accurate and stable result. Furthermore this model can be used to compare its results with other similar models that make use of differential equation solvers.

During the adsorption process, ambient air flows through the reactor and the CO<sub>2</sub> molecules react with the sorbent. In this case, the sorbent that has been chosen to model the system with is an amine based sorbent, Lewatit VP 1065, which chemically reacts with the CO<sub>2</sub> molecules that flow through the pores of the sorbent material. From the literature it is understood that water adsorption also takes place during the adsorption process, which cannot be neglected for an actual DAC system. However, for the first design of this model water co-adsorption will not be taken into account, which will simplify the initial design. Eventually the model can be expanded by adding other reaction mechanisms to the system like water co-adsorption. However, this will not be done within the time-span of this thesis.

## 7 Setting up the mass balance

The first step in designing any model is to consider what happens within the system, considering the system's control volume and consequently setting-up the mass- and energy balances that describe the system. The assumptions that are made for any process help determine the mass and energy balances that describe the overall reaction in the system. All assumptions made during the design of the models will be explained, why the assumptions are made and what the possible consequences could be on the results.

### 7.1 Assumptions

The adsorption system will be designed as an 1D-axial system that will be evaluated over its spatial z-axis and over time. The other assumptions that are made for the design of the adsorption model are summed up below and will be explained subsequently.

- Ambient conditions (1 bar, 298 K)
- Isothermal process (constant temperature)
- Pressure change is negligible
- Purely CO<sub>2</sub> adsorption
- Henry's coefficient
- No dispersion term
- 1<sup>st</sup>-order linear driving force (LDF)
- Kinetic rate constant is assumed to be constant
- Plug flow reactor (PFR)
- Bed is completely free of CO<sub>2</sub> as reaction starts
- Explicit Forward Euler (first estimation)
- Implicit Backwards Euler (determining solution)

The adsorption reaction will start at ambient conditions, this means that the initial temperature of the system is at 298 K and the pressure is at 1 bar. As the adsorption reaction takes place, the system is considered to be isotherm: the temperature stays constant for the entire adsorption process. This is also the case for the pressure inside the reactor. For the initial model design, the system ignores any water co-adsorption effects and the sorbent adsorbs purely the CO<sub>2</sub> molecules. The adsorption reaction will initially be modelled using a Henry's coefficient, which will represent a linear simplification of the Toth isotherm. The adsorption mass balance will not take into account any dispersion effects, the mass balance of the system will be a 1<sup>st</sup>-order PDE. The adsorption reaction of the CO<sub>2</sub> molecules on to the sorbent will be represented by a first order linear driving force and the kinetic rate term that is used in the LDF equation is assumed to be a constant. The adsorption system will be considered as a PFR that flows from its inlet at ( $z=0$ ) to its outlet at ( $z=L$ ) and the reactor will be completely free of CO<sub>2</sub> molecules as the reaction starts: the initial concentration of CO<sub>2</sub> in the reactor is zero. The last two assumptions describe how the reactor will be solved numerically. First, the Forward Euler method will be used to make a first rough estimation, which will in turn be used for the Backwards Euler method to iterate the value until a desirable solution has been achieved. All of these assumptions will be explained more elaborately in the following chapters.

## 7.2 Mass balance

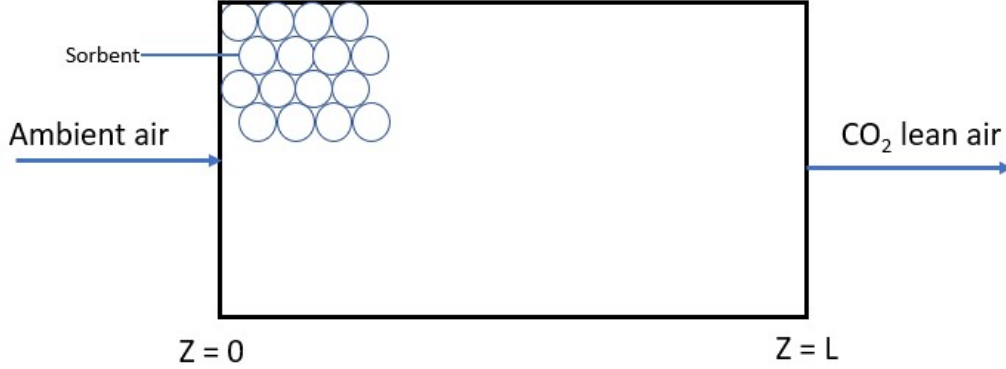


Figure 9: Simplified representation of the adsorption system: a PFR containing solid sorbent material through which ambient air flows from the inlet to the outlet and exits the reactor as CO<sub>2</sub> lean air.

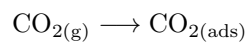
The mass balance that will describe the adsorption reaction can be described by a single mass balance. The reaction is considered to be isothermal thus no energy balance will be needed to describe the system. The adsorption mass balance can be derived from a general mass balance to describe the adsorption system that will be modelled in this paper and can be written as the equation below:

$$\frac{\delta c}{\delta t} = -u_{\text{air}} \frac{\delta c}{\delta z} - \rho_p \cdot \left( \frac{1 - \epsilon_b}{\epsilon_b} \right) \cdot \frac{\delta q}{\delta t} \quad (4)$$

This equation is a first order partial differential equation (PDE) which changes over time ( $t$ ) and distance ( $z$ ). Where the total concentration change of CO<sub>2</sub> over time depends on the change of its concentration over distance and its sorbent loading over time. The sorbent loading will be described as a function of the linear driving force (LDF) which can be described by the following equation:

$$\frac{\delta q}{\delta t} = k(qe - q) \quad (5)$$

The parameters of the mass balance are:  $u_{\text{air}}$ , which is the propagation velocity of the bulk fluid (air),  $\rho_p$  is the particle density,  $\epsilon_b$  is the sorbent bed void fraction,  $c$  is the concentration of gaseous CO<sub>2</sub> in the air and  $q$  is the amount of CO<sub>2</sub> that is adsorbed on to the sorbent. The adsorption mass balance is a first order PDE containing three separate differential equations. With two differential equations for the concentration of CO<sub>2</sub> in the air, one changes over time ( $t$ ) and the other changes over distance ( $z$ ). The concentration of CO<sub>2</sub> in the air, at 400 ppm and 298 K, is 0.0163 mol/m<sup>3</sup>, this will be the initial condition for the concentration of the ambient air that flows into the system. Initially, the concentration of CO<sub>2</sub> in the bulk air will reduce as it propagates through the reactor and the CO<sub>2</sub> molecules react with the sorbent. As time passes, the sorbent material becomes more and more saturated until no vacant adsorption sites remain for the CO<sub>2</sub> molecules to adsorb on to. As sorbent saturation is reached, the concentration level of CO<sub>2</sub> in the bulk reaches 0.0163 mol/m<sup>3</sup> and the sorbent has reached its maximum loading capacity. The sorbent loading ( $q$ ) is assumed to be initially at zero as no CO<sub>2(g)</sub> has interacted with the sorbent. As the air flows through the reactor, the CO<sub>2</sub> molecules adsorb on to the sorbent, this reaction only occurs if there is a substantial driving force for this reaction. Equation [5] represents the driving force behind the adsorption reaction, which is in this case represented by a linear driving force equation. The sorbent loading differential equation can be described by the kinetic rate constant ( $k$ ) multiplied by difference between actual sorbent loading ( $q$ ) and the loading equilibrium ( $qe$ ).



The equations above is the chemical reaction of the CO<sub>2</sub> between its gas- and adsorbed phase. The equilibrium loading is a function of the partial pressure of CO<sub>2</sub> in the gas phase as it adsorbs on to the sorbent and can be described by the adsorption isotherm of the sorbent material. As the CO<sub>2</sub> adsorbs to the sorbent, the actual loading  $q$  increases and the difference between the equilibrium loading and the actual loading becomes smaller as a function of time. When the difference between  $qe$  and  $q$  system reaches zero, there is no longer a driving force between the gaseous and adsorbed CO<sub>2</sub> molecules and the adsorption reaction stops. The linear driving force

is the mass transfer rate from the (adsorbable) gas phase into the (adsorbed) solid phase, as the CO<sub>2</sub> is adsorbed.

### 7.3 Initial- & boundary conditions

The initial- and boundary conditions should be chosen appropriately to properly solve the mass balance of the system. When selecting suitable conditions to describe the system, the initial state of the reactor should be considered. Initially, there are CO<sub>2</sub> molecules in the reactor, this means that as the adsorption reaction starts the concentration of CO<sub>2</sub> is zero over the length of the reactor. At this point in time, no CO<sub>2</sub> has been adsorbed on to the sorbent and the actual loading is also initially zero. This can be described by the following initial conditions (ICs):

**Initial conditions:**

- $c(z, 0) = 0$
- $q(z, 0) = 0$

The initial condition for the concentration is valid for all the grid-point inside the reactor. However this is not true for the concentration at the inlet of the reactor, here the concentration is equal to that of the ambient air. At the boundary of the reactor, the concentration of the CO<sub>2</sub> in air is dependent on the concentration of CO<sub>2</sub> in the ambient air that will flow through the reactor when the adsorption reaction commences. The boundary condition (BC) at the inlet of the reactor can be described as follows:

**Boundary condition:**

- $c(0, t) = c_{in}$

These initial- and boundary conditions are necessary to solve the mass balance equation. To use these equations inside the model, they first need to be discretized. This means that the equation needs to be rewritten in numerical form, such that the program, in this case Python, can use the equation and solve it numerically to get to the predicted solutions. This will be further explained in the following part.

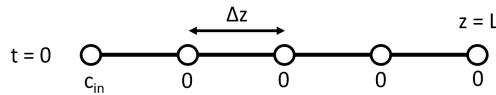


Figure 10: A one-dimensional schematic of the initial state of the reactor for the concentration of CO<sub>2</sub> over the length of the reactor as determined by the initial- and boundary conditions

#### 7.3.1 LDF and k

As is mentioned earlier, the adsorption reaction is described by a first-order linear driving force equation, where the driving force is the difference between the equilibrium loading and the actual loading of the CO<sub>2</sub>. The rate at which the reaction occurs is dependent on the kinetic rate constant ( $k$ ). The kinetic rate constant is a simplification of a set of equations that generally describe the diffusion reaction and all resistances that occur during adsorption mechanism. In this case  $k$  is assumed to be a constant that can be changed for the model to match the results as determined by the experiments. In reality, the system of equations that describe  $k$ , should be determined based on the experimental data. If the system of equations would be determined successfully, it should be able to take into account all the resistances that occur during the adsorption reaction as CO<sub>2</sub> diffuses on to the various sites of the sorbent. However this is out of the scope of this thesis and  $k$  is assumed to be a constant

$$\frac{\partial q}{\partial t} = f(q, c) = k(qe - q)$$

The LDF equation describes a simplification of the gas-phase mass balance where the CO<sub>2</sub> transports from the gas phase to the adsorbed phase, where the mass transfer resistance is described by a (lumped) mass transfer coefficient ( $k$ ). This parameters in this equation are ( $k$ ) which is the kinetic rate constant, ( $qe$ ) is the equilibrium loading of CO<sub>2</sub> and  $q$  is the actual loading of CO<sub>2</sub> on the sorbent. The difference between the equilibrium loading and the actual loading is the driving force for the adsorption reaction to take place, where the LDF is a frequently used approximation for these type of dispersed plug flow models that describe adsorption processes.



The LDF is a lumped mass transfer coefficient that contains all the transfer resistances during the adsorption reaction [20]. These resistances occur during adsorbate transport when CO<sub>2</sub> adsorbs on to a sorbent particle. First, surface diffusion occurs when the CO<sub>2</sub> passes the film layer of the sorbent particle, then CO<sub>2</sub> molecules encounter the micro- and macro-pore resistances as they diffuse into the pores of the sorbent particles and react with the free amines on the solid surface of the sorbent.

Implementing the LDF to lump these resistances assumes that only one of these mass transfer resistances is dominant for the adsorption reaction, for it to be valid. The lumped mass transfer coefficient  $k$  can be experimentally determined to fit the isotherms. This value determines the rate of the adsorption reaction by approximating the all the resistances into one coefficient that fits the experimental results. One of the goals of this model will be to evaluate different values of  $k$  and to determine which of the values gives the best representation of the experimentally determined results.

## 8 Modelling approach

The adsorption model will be constructed based on the mass balance and subsequently validated by using experimental data to compare if the model is able to simulate the experimental data realistically. First the model is modelled with Python based on the general governing equations and assumptions of the system. The equations need to be discretized for the system to be solved numerically with the model. If this is done correctly, the model will be able to predict the concentration and loading of CO<sub>2</sub> in the reactor for any place and time. The solutions will be determined by means of an implicit numerical method that finds the solutions iteratively. Consequently the model will be tested by using the results presented by breakthrough experiments to determine the validity of the model: the model will use experimental data to check if the results of the model are in accordance to the experimental results. This will determine if the model is capable of describing the behaviour between the sorbent and the CO<sub>2</sub> properly.

The rate of adsorption is one of the key parameters in the adsorption reaction and is determined by breakthrough experiments. For this model the concentration and loading values are measured at the outlet of the reactor and these values will be compared to the breakthrough results. The adsorption rate determines the rate at which the concentration of CO<sub>2</sub> inside the reactor is back to ambient conditions and breakthrough has occurred. Once the system has been successfully validated, the model can be used to analyse the adsorption reaction in detail for the different parameters and different conditions.

### 8.1 Model description

#### No dispersion

The starting point for the design of the model is to set-up the correct conservation equations that describe the adsorption system. From the control volume (CV) of the PFR, the correct mass balance can be derived. The ambient air flows through the CV from the inlet to the outlet of the system, which are the boundaries of the CV. Adsorption of the CO<sub>2</sub> molecules occurs as the air flows through the reactor bed and the CO<sub>2</sub> reacts with the sorbent material. For amine based adsorption systems as described in this thesis, the overall mass balance equation is generally written as the following equation 6, like has been described by [18], [20].

$$-D_L \frac{\partial^2 c}{\partial z^2} + \frac{\partial c}{\partial t} + u_{air} \frac{\partial c}{\partial z} + \rho_p \cdot \left( \frac{1 - \epsilon_b}{\epsilon_b} \right) \cdot \frac{\partial q}{\partial t} = 0 \quad (6)$$

In this equation,  $D_L$  describes the dispersion effects during adsorption. Equation 6 describes the adsorption reaction with a second-order partial differential equation that is typically hard to solve. As 2<sup>nd</sup>-order PDEs are hard to solve, the dispersion term has been neglected in this thesis in order to simplify the system. The dispersion term is the 2<sup>nd</sup>-order differential equation inside Equation 6 and if this term is assumed to be zero, then the mass balance equation becomes a 1<sup>st</sup>-order PDE and the system becomes easier to solve. Ignoring the dispersion effects during the adsorption process will influence the results produced by the model, but can still give a good insight to the system. In order to obtain a good first adsorption model, the dispersion is ignored for simplicity but should be considered for further investigation of a realistic adsorption system. Creating a model, that can describe the adsorption based on the aforementioned 2<sup>nd</sup> order PDE would be a good follow-up to this thesis. The goal of this thesis however, is to create a model that can solve the PDE independently of existing differential equation solvers. Thus ignoring the dispersion effects during adsorption, the mass balance equation can be reduced to the following equation:

$$\frac{\partial c}{\partial t} + u_{air} \frac{\partial c}{\partial z} + \rho_p \cdot \left( \frac{1 - \epsilon_b}{\epsilon_b} \right) \cdot \frac{\partial q}{\partial t} = 0 \quad (7)$$

### Henry's coefficient

The equilibrium loading inside the LDF of the mass balance, can be determined with a Toth isotherm. The isotherm values (Table 8) and equations (Equation 17) have been experimentally determined in other works like that of Bos [3]. From these equations, the equilibrium loading is calculated based on the partial pressure of CO<sub>2</sub> and the temperature of the system. For this model however, the temperature is constant and the Toth isotherm equations have been substituted by the Henry's constant for simplicity. The Henry's coefficient is a linear constant that gives deviating results compared to that of the Toth isotherm, this can be seen in Figure 11. However The Henry's constant can be used in the model as a good first attempt at simulating the adsorption process with viable results.

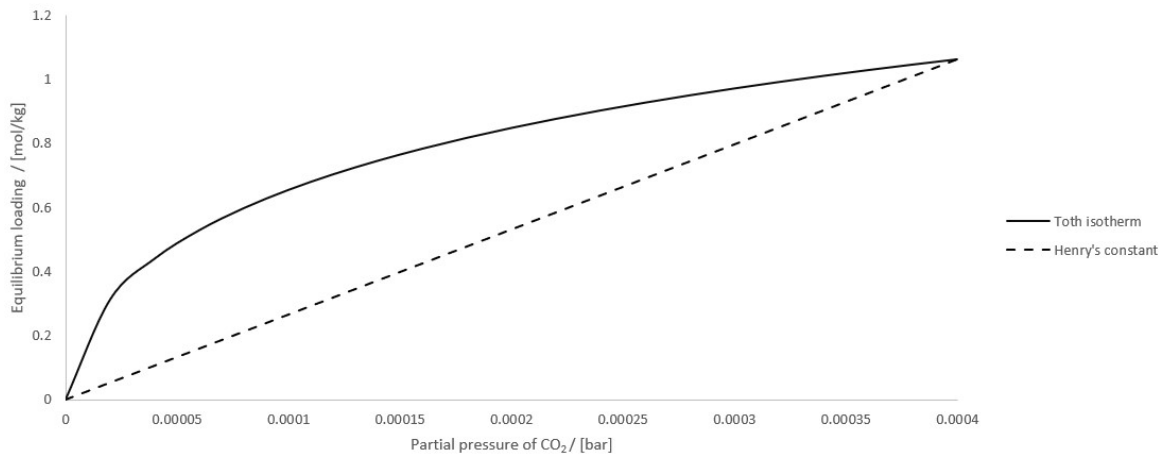


Figure 11: Comparing the equilibrium loading values of the Toth isotherm to those of the Henry's constant, for a system at 400 ppm and 298 K as a function of the partial pressure of CO<sub>2</sub>.

### Isothermal

The adsorption reaction of the CO<sub>2</sub> reacting with the sorbent is an exothermic reaction, thus it is expected that the temperature would increase due to the internal heat generation. The concentration of CO<sub>2</sub> in air, that reacts with the sorbent, is so low that the change in temperature can be considered to be negligible.

### Constant velocity

The temperature of the bulk fluid and the solid sorbent are constant throughout the adsorption process, thus the velocity does not change due to temperature changes. Furthermore, the length of the reactor for the adsorption process is evaluated at relatively short lengths. If the adsorption reactor would be designed to be longer, then the velocity would decrease significantly over the distance and the pressure drop would become a challenge for the system.

### No pressure drop

The velocity and temperature are considered to be constant throughout the system and they will no affect the pressure inside the system, while the bulk flows through the reactor. Because the reactor has a relatively short length and the pressure of the environment is the same as the pressure inside the reactor, the pressure drop can be ignored. However if the inlet velocity of the system would be increased, such that the fans suck the air in at a higher inlet velocity, the pressure would drop significantly at the inlet and increase the effect of the pressure drop on the system.

## Pure CO<sub>2</sub> adsorption

The assumption in this model is that the water co-adsorption can be neglected, even though this is not the case for an actual DAC system. From literature it is known that water has a big influence on the adsorption process due to that water molecules also get adsorbed to the sorbent during the adsorbing step. For simplicity, the model is designed to neglect water molecules being adsorbed. Though it has been acknowledged that the presence of water also has positive effects on a DAC system like is investigated by Young [21], the model will ignore co-adsorption effects.

## 8.2 Determining the system

### 8.2.1 Governing equations

The mass balance of the system, containing the LDF, is the PDE that needs to be solved in order to be able to simulate the adsorption process. The equations below show the mass balance and the loading differential equation as described by the LDF.

$$\frac{\partial c}{\partial t} + u_{\text{air}} \frac{\partial c}{\partial z} + \rho_p \cdot \left( \frac{1 - \epsilon_b}{\epsilon_b} \right) \cdot \frac{\partial q}{\partial t} = 0 \quad (\text{MB})$$

$$\frac{\partial q}{\partial t} = k(q_e - q_{CO_2}) \quad (\text{LDF})$$

Rewriting the mass balance, with the loading differential in terms of the LDF, the mass balance can be written in its final form shown in Equation 8, which is a 1<sup>st</sup>-order PDE that changes with respect to time and distance.

$$\frac{\partial c}{\partial t} = -u_{\text{air}} \frac{\partial c}{\partial z} - \rho_p \cdot \left( \frac{1 - \epsilon_b}{\epsilon_b} \right) \cdot k(q_e - q_{CO_2}) \quad (8)$$

Due to the fact that the system behaves isothermally, no energy balance needs to be solved for this system. The temperature remains constant and therefore the mass balance can be solved with the three initial- and boundary conditions for this system.

### 8.2.2 Initial & Boundary conditions

The initial conditions describe the system at its initial state, before the process has started. Initially the reactor is assumed to be free of air, there is no CO<sub>2</sub> in the reactor until air starts to flow through the system. Consequently, no CO<sub>2</sub> has yet been adsorbed. This could be different after an entire DAC cycle would have taken place, depending on the efficiency of the desorption process. After desorption has taken place, it is not likely that all the CO<sub>2</sub> molecules have been desorbed from the sorbent, this would mean that the initial condition of the loading non-zero after the first complete DAC cycle. However, the initial conditions will both be initially considered to be zero.

$$\text{Domain for } c(z,0) = 0 \quad \in [0 < z \leq L] \quad c(z,0) = 0 \quad (\text{IC 1 @ } t = 0)$$

$$\text{Domain for } q(z,0) = 0 \quad \in [0 \leq z \leq L] \quad q(z,0) = 0 \quad (\text{IC 2 @ } t = 0)$$

The mass balance system needs to be solved for three different variables, this means that there are at least three conditions needed to be able to solve the mass balance. The first two conditions are initial conditions and are valid only at the start of the process for (t=0). The boundary condition states that the concentration of CO<sub>2</sub> at the inlet of the reactor is always the equal to the CO<sub>2</sub> concentration in the ambient air. This conditions is an inlet boundary condition and is true for (z=0) at any point in time. The concentration of CO<sub>2</sub> in the air surrounding the reactor is 400 ppm, and this is assumed to also be true for concentration of CO<sub>2</sub> at the inlet of the reactor.

$$\text{Domain for } c(0,t) = c_{\text{in}} \quad \in [t \geq 0] \quad c(0,t) = c_{\text{in}} \quad (\text{BC 1 @ } z = 0)$$

### 8.2.3 Equilibrium loading

Generally the equilibrium loading is described by an isotherm, often the Toth isotherm as is done with the desorption model. This isotherm is determined by a set of equations and parameters that are found experimentally from literature. The isotherm has in this case been replaced by a linear Henry's coefficient for simplicity of the initial model.

$$qe = H \cdot c_{\text{CO}_2} \quad (9)$$

In this case the equilibrium loading  $qe$  has been described by the Henry's coefficient and the concentration of  $\text{CO}_2$  in the reactor. The Henry's coefficient is taken to be a value that linearises the estimation for the equilibrium loading. During validation of the model, this equation can be rearranged to find the correct value for the Henry's constant that describes the experimental results from the determined initial  $\text{CO}_2$  concentration and the final loading.

## 9 Discretization

During the discretization of the adsorption system, the letters A and B are used to represent the constant values in the mass balance as follows:

$$A = u_{\text{air}}$$

$$B = \rho_p \cdot \left( \frac{1 - \epsilon_b}{\epsilon_b} \right)$$

The goal of the adsorption system is to model the PDE system without implementation of existing solvers: the model will be independent of other ODE solver systems existing in Python. To do this, it is necessary to discretize the mass balance that describes the system. Discretization of the system means that the mass balance equation will be written rewritten so it can be solved numerically by the model. This means that the differential equations should be described by grid-point in terms of distance, denoted by subscript [i], and time, denoted by subscript [j]. Equation 10 shows the discretization of the adsorption mass balance.

$$\frac{\partial c_{i,j}}{\partial t} = -A \cdot \frac{\partial c_{i,j}}{\partial z} - B \cdot k(qe_{i,j} - q_{\text{CO}_2,i,j}) \quad (10)$$

Discretization of the system, means that the reactor can be thought of as a string of one dimensional grid-point that divide the length of the reactor into intervals of  $\Delta z$ . The number of steps ( $\Delta z$ ) that is chosen, determines the number of grid-points that will be calculated for every time-step. The grid-point representation of a single time interval is shown in Figure 12.

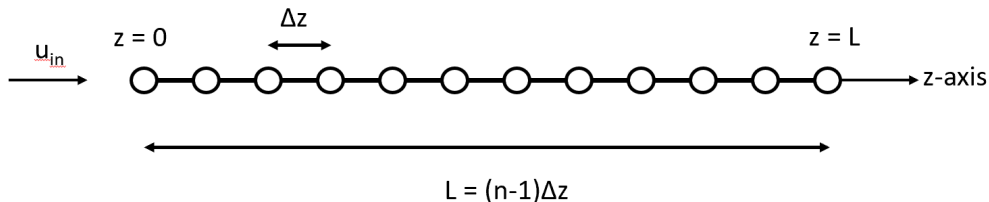


Figure 12: A one-dimensional schematic of the spatial grid representation of the PFR that is used to describe the adsorption reaction, with an inlet velocity of air ( $u_{\text{air}}$ ) and a ( $n$ ) number of grid-step ( $\Delta z$ ) from the inlet ( $z=0$ ) to the outlet ( $z=L$ ).

The mass balance equation for the adsorption process is a partial differential equation that consists of three ODEs, two with respect to time and one with respect to space. The spatial differential can be written numerically with the finite difference method, leaving only the time differentials.

## 9.1 Spatial differential $z[i]$

The length of the reactor is now considered as a 1D-axis consisting of grid-points that represent the length of the reactor, at which the concentration and loading can be determined as air flow through the reactor. Each individual grid-point is a numerical representation of a single point over the length of the reactor. The different grid-point are assigned to the number that coincides with their position in the reactor, from the inlet  $[i=0]$  to the outlet  $[i=n]$  with intervals of  $\Delta z$  as is shown in Figure [13]:

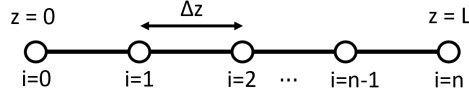


Figure 13: One dimensional grid representation of the length of the reactor for a single point in time, with grid-point from the inlet ( $i=0$ ) to the outlet ( $i=n$ ).

The mass balance contains one spatial differential equation:  $\frac{\partial c_{i,j}}{\partial z}$ . This ODE can be written numerically as a function of the grid-points. Discretization of the spatial differential can be done for the one-dimensional grid by means of the Euler method. A distinction can be made between the three different situations on the grid: the inlet  $[i=0]$ , the outlet  $[i=n]$  and all the points in between the boundaries  $[0 < i < n]$ . For the inlet of the reactor a Euler Forward method is used to calculate the next value.

$$\frac{\delta c_i}{\delta z} \approx \frac{c_{i+1} - c_i}{\Delta z} \quad (\text{Inlet})$$

For all the other grid-point over the length of the reactor, including the grid at the outlet of the reactor, are determined with the Backward Euler method. The Backward Euler method uses the corresponding and the following grid-point to calculate the next value.

$$\frac{\delta c_i}{\delta z} \approx \frac{c_i - c_{i-1}}{\Delta z} \quad (11)$$

Implementing the discretized Euler methods into the actual mass balance for the spatial differential presents two different equations. Implementing these in the model for the two different situations makes it possible to solve the system for any point of the  $z$ -axis if necessary:

$$\frac{\partial c_{i,j}}{\partial t} = -A \frac{(c_{i,j} - c_{i+1,j})}{\Delta z} - B \frac{\partial q_{i,j}}{\partial t} \quad (i=0)$$

$$\frac{\partial c_{i,j}}{\partial t} = -A \frac{(c_{i-1,j} - c_{i,j})}{\Delta z} - B \frac{\partial q_{i,j}}{\partial t} \quad (i \neq n)$$

### 9.1.1 Finite difference methods

The equations shown before show how the spatial discretization can be applied for the different points on the axis. However these equations will not all be needed as the boundary condition states that the 0<sup>th</sup> grid point will always be the constant independent of time. For all the other point on the  $z$ -axis, this is not the case and these need to be calculated for every other point for every time step. This will be done with the finite difference method which is shown in the figure 14:

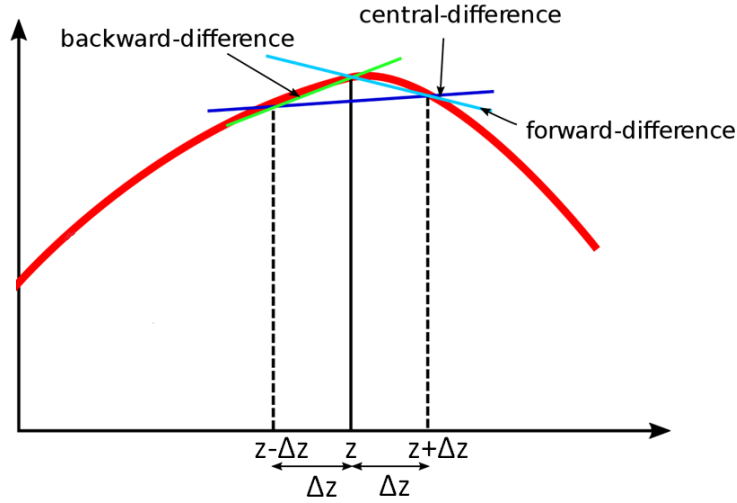


Figure 14: A schematic of the different finite difference methods that could be used to solve the spatial differential equation.

A way of solving an ODE boundary value problem is through the finite difference method, at evenly spaced grid points the finite difference method can be used to approximate the differential equations. This way, the differential equation can be changed into a system of algebraic equations to solve as the derivatives in the differential equation are approximated. The axis of the reactor can be divided into [n] equally spaced intervals of length [j]. Figure 14 shows the different finite difference methods for estimating the values, for the adsorption process the boundary and initial conditions should be considered.

As mentioned, the inlet concentration at grid zero is always the same, due to the boundary condition. For all other grid-points, backward difference method can be used to estimate the value for the following grid-point. This process will repeat itself for all the entire length of the reactor. Implementing the appropriate discretization method into the mass balance and solving it as an Euler Upwind system, the mass balance can be written as the following equation.

#### Backward difference

$$\frac{\partial c_{i,j}}{\partial t} = -A \frac{c(z, t) - c(z - \Delta z, t)}{\Delta z} - B \frac{\partial q_{i,j}}{\partial t} \quad (12)$$

## 9.2 Time differential - t[j]

The mass balance of the adsorption system is a PDE that has been discretized over distance [z] (Equation 12) and has been written as a function of only the time differentials. The mass balance can be solved as an ODE with respect to time as can be seen in the following equation:

$$\frac{\partial c_{i,j}}{\partial t} = -A \frac{(c_{i-1,j} - c_{i+1,j})}{2\Delta z} - B \frac{\partial q_{i,j}}{\partial t} \quad (13)$$

Solving the mass balance for its the time derivatives, it can be rewritten with time-stepping schemes. Two possible discretization methods for the mass balance are the Euler-Backward or the Crank-Nicolson methods. As with the spatial discretization, the time domain can be written in terms of grid-point, with time intervals of  $\Delta t$  for the temporal domain. Time grids are denoted with the subscript [j], that span from zero to time is  $t_{\max} = T$ . The sequences below show how the numeric notation should be interpreted for the time-steps ranging from time is zero to its final time step (T).

$$\begin{aligned} 0 &= t_0, t_1, t_2, \dots, t_{\max} = T \\ 0 &= [j = 0], [j = 1], \dots, [j = M - 1], [j = M] = T \end{aligned}$$

Time discretization considers short time intervals  $(t_j, t_{j+1})$  where  $t_{j+1} = (t_j + \Delta t)$ , alternatively this can be written as  $u_j \approx u(t_j)$  and  $u_{j+1} \approx u(t_{j+1})$  for any variable  $u$ . The following equations show different methods to

solve the time differentials numerically for the Forward Euler, the Backward Euler (also known as the Upwind method) and the Crank-Nicolson method respectively.

$$u_{j+1} = u_j + f(t_j, u_j)\Delta t(+O(\Delta t)^2) \quad (\text{Explicit Euler})$$

$$u_{j+1} = u_j + f(t_{j+1}, u_{j+1})\Delta t(+O(\Delta t)^2) \quad (\text{Implicit Euler})$$

$$u_{j+1} = u_j + \frac{1}{2}[f(t_{j+1}, u_{j+1}) + f(t_j, u_j)]\Delta t(+O(\Delta t)^3) \quad (\text{Crank-Nicolson})$$

The higher order terms can be ignored in for this adsorption mass balance and in the following part, it will become clear which of these methods will be used and how they will be applied in the model.

### 9.2.1 Numerical time analysis

Time stepping methods use advanced transient step-by-step solutions or compute stationary solutions. In order to solve the the time-dependent differentials, explicit- and implicit methods can be used as numerical approaches for obtaining numerical approximations for the solutions of time-dependent ODEs and PDEs. The main difference between explicit- and implicit methods is that explicit methods calculate the state of a system at a later time from the current state of the system. While implicit methods find a solution by solving an equation involving both the current state of the system and the later one. These equations can be used to numerically estimate the time-dependent differential equations in order to achieve non-exact solutions for new time-steps. Explicit methods, such as Forward Euler are less accurate but are easy to implement and can be used to obtain a rough initial estimation for the next time step, which can in turn be used as the input for the implicit method. The implicit methods such as Backwards Euler and Crank-Nicolson can use the initial explicitly estimated value to calculated the value implicitly. Subsequently, the implicit solution can be used as the new input to get a new solution and this iteration-loop continuously produces better solutions. Once the implicit iteration-loop has achieved a sufficiently accurate solution for the time-step, the switches back to the explicit method and repeats the process for the following time-step. Every new value is calculated for all grid-point over the length of the reactor before the next estimation or iteration is executed. The explicit method is used only as a first estimate, if an explicit method would be used to get the final solutions it would need an impractically small time-step compared to implicit methods that can use larger time-steps: requiring less computational power. The combination of the initial explicit estimation and the implicit iteration-loop can provide a model that can predict accurate solution. For this adsorption model, the Forward Euler will be the explicit method and the Backward Euler is the preferred implicit method for solving the system.

$$\frac{u_{j+1} - u_j}{\Delta t} = f(t_j, u_j) \quad (\text{Explicit Euler})$$

$$\frac{u_{j+1} - u_j}{\Delta t} = f(t_{j+1}, u_{j+1}) \quad (\text{Implicit Euler})$$

The Crank-Nicolson was also considered for the implicit method, however it was found that this method showed undesirable instabilities.

$$\frac{u_{j+1} - u_j}{\Delta t} = \frac{1}{2}[f(t_{j+1}, u_{j+1}) + f(t_j, u_j)] \quad (\text{Crank-Nicolson})$$

### 9.2.2 Combining the equations

The Euler equations will be used to accurately predict the values for every grid on the z-axis at every point in time except for inlet of the reactor, as this value is always equal to its BC. So at the first grid-point [i=0], the concentration is known but the loading is not, and needs to be calculated.

**For i in range [0]**

$$c_{i,j} = c_{in} \quad (\text{Boundary Condition})$$

$$\frac{\partial q_{i,j}}{\partial t} = k(qe_{i,j} - q_{i,j})$$

For all the other grid-points of the z-axis, the discretized adsorption mass balance equation is used to predict the concentration and loading inside the reactor during the adsorption process at any given time. The following equations show the two explicit and the two implicit equations that will be used to calculate the concentration and loading of CO<sub>2</sub> for every point in the reactor at any time.

**For i in range [i=1:i=N]**

$$\frac{\partial c_{i,j}}{\partial t} = -A \frac{c_{i,j} - c_{i-1,j}}{\Delta z} - B \frac{\partial q_{i,j}}{\partial t}$$

$$\frac{\partial q_{i,j}}{\partial t} = k(qe_{i,j} - q_{i,j})$$

$$\frac{\partial c_{i,j+1}}{\partial t} = -A \frac{c_{i,j+1} - c_{i-1,j+1}}{\Delta z} - B \frac{\partial q_{i,j+1}}{\partial t}$$

$$\frac{\partial q_{i,j+1}}{\partial t} = k(qe_{i,j+1} - q_{i,j+1})$$

The differentials for the mass mass balance and the LDF equations can be rewritten numerically, this is how the equations will be solved in the model. Rewriting the differentials numerically can be done in as follows:

**Explicit Euler - first estimation**

$$\frac{C_{i,j+1}^{\text{exp}} - C_{i,j}}{\Delta t} = F(C_{i,j}, q_{i,j}) \quad \& \quad \frac{q_{i,j+1}^{\text{exp}} - q_{i,j}}{\Delta t} = G(C_{i,j}, q_{i,j})$$

**Implicit Euler - first solution**

$$\frac{C_{i,j+1}^{\text{imp}} - C_{i,j}}{\Delta t} = F(C_{i,j+1}^{\text{exp}}, q_{i,j+1}^{\text{exp}}) \quad \& \quad \frac{q_{i,j+1}^{\text{imp}} - q_{i,j}}{\Delta t} = G(C_{i,j+1}^{\text{exp}}, q_{i,j+1}^{\text{exp}})$$

**Implicit iteration loop**

$$\frac{C_{i,j+1}^{\text{imp}} - C_{i,j}}{\Delta t} = F(C_{i,j+1}^{\text{imp}}, q_{i,j+1}^{\text{imp}}) \quad \& \quad \frac{q_{i,j+1}^{\text{imp}} - q_{i,j}}{\Delta t} = G(C_{i,j+1}^{\text{imp}}, q_{i,j+1}^{\text{imp}})$$



## 10 Verification and Validation

One of the main challenges during the design of the adsorption model is to construct it without additional existing solver systems. Discretization of the mass balance was done so the system can be solved numerically with in Python. The next step is to implement the discretized equations into the Python code in a way, such that it solves the adsorption system and the results can be simulated. As the model is constructed, it should be tested and evaluated to check whether it works properly and produces viable results. The modelled results can be checked by comparing them with experimental data results to determine the model's validity. Comparing the model results to the experimental results should eventually give similar results and any differences between the results should be explainable. It is critical to understand the effects of the assumptions and simplifications have been made, to understand any differences between experimental and modelled results.

### 10.1 Verification

Once a working model has thought to have been achieved, it needs to be extensively tested. The model should be able to produce both accurate and stable results for any set of inputs. The complete step-by-step grid representation of the adsorption model can be found in Appendix C 12. Initially, generally accepted adsorption values from literature have been used to determine if the model produced plausible results and the stability of the model was determined by varying the  $\Delta t$  and  $\Delta z$  of the model.

#### 10.1.1 Error check analysis

An error analysis has been built into the model to be able to check what number of implicit iterations is needed to obtain solutions within the margin of machine precision. After every iteration, the solution changes and becomes more accurate. When the difference between two consecutive iterations is the order of  $10^{-7}$ , then the solution is believed to be accurate. This error analysis can be turned on or off with a built-in switch inside the model. The reason for this on-off switch is that the error check does not need to be done for every simulation and it increases the computational power needed for a simulation. Once the error check determines what the number of iterations should be to achieve the desired accuracy, this value can be used and the error analysis check can be switched off for further simulations.

One of the drawbacks of this model is the amount of time-steps that is needed to simulate an the adsorption system. Even after simplifications of the Python code, to try to reduce the amount of memory capacity that is needed to simulate the system, copious amounts of time-steps are needed to simulate the entire process. Nested dictionaries have been used in the Python model to calculate all the numerical grid-points system and one draw-back of the nested dictionaries is that they increase the computational power and the time needed to run a simulation.

#### 10.1.2 Stability check

It is important for this type of system to determine the appropriate stability region for the system to work. The model will be stable for appropriate time-stepping ( $\Delta t$ ) and spatial-stepping ( $\Delta z$ ) values. The stability conditions also depend on the geometry of the reactor because enough steps must be taken over the length of the reactor to properly simulate a stable and accurate adsorption system. When the boundaries have been determined for the system, validation of the model can start: experimental data will be used to examine the accuracy of the model and validate if the model produces the expected data.

### 10.2 Validation

Validation of the model is done by using experimental data to see if the experimental results can be reproduced. The experimental data that has been used by Surati [2] will be used to validate this model. All variables and results will be carefully analysed and implemented into the model to check if it can accurately reproduce the experimental data as presented by Surati [2] and to determine which corresponding value for  $k$  shows the best resembling results. The dimensions and values that have been used for the experimental set-up can be found in Appendix B 19. These values are used as the inputs for the model to determine if the experimental results can be replicated. The concentration inside the reactor is used to compare the results, more specifically the concentration at the outlet of the reactor. Using the same values and dimensions in the model as was used for the experiments, the results should be similar.

### 10.2.1 Toth isotherm

During the design of the model, the Toth isotherm has been disregarded and replaced with a Henry's coefficient for simplicity. Constructing the model to be able to solve the PDE mass balance has proved to be challenging. Using a Henry's coefficient, instead of the Toth isotherm, has made the development and problem analysis of the model easier. Eventually the Henry's coefficient should be replaced with the isotherm as this will give a better representation of the reality. The Henry's coefficient has been calculated from the concentration of CO<sub>2</sub> in air, in this case at 2000 ppm, and the final equilibrium loading value that was achieved with the experimental set-up. Dividing the loading by the concentration gives an value that could be used for the Henry's approximation of the adsorption system in m<sup>3</sup>/kg.

$$H = \frac{qe}{c_{in}}$$

The Toth isotherm is a set of experimentally determined equations that determines the equilibrium loading of the Lewatit sorbent during the DAC process. The isotherm parameters have been determined by Bos [19](#) and the resulting equilibrium loading is sensitive to temperature and partial pressure variations inside the system. The adsorption reaction occurs at constant temperature, which makes it possible to simplify the system by substituting it with a Henry's coefficient. The Henry's coefficient is a linear approximation of the isotherm and notable differences can be seen from [Figure 15](#).

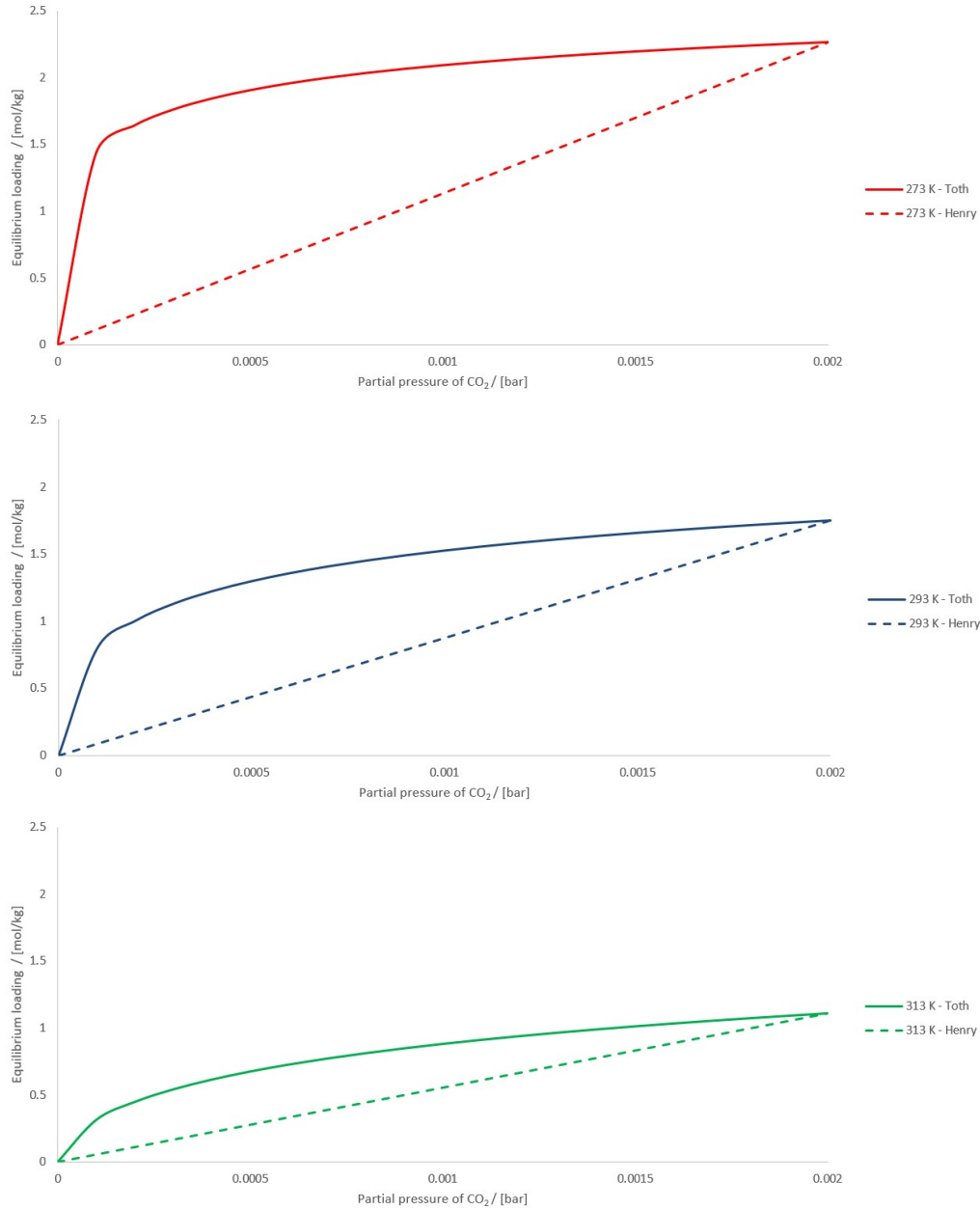


Figure 15: Comparing the equilibrium value of the Toth isotherm to the Henry's coefficient for adsorption at 2000 ppm at 273 K, 293 K and 313 K respectively as a function of the partial pressure of CO<sub>2</sub>.

In Figure 15 it can be seen that the differences between the Henry's coefficient and Toth isotherm become smaller at elevated temperature. In appendix D, the figures can be found for varying temperatures at 400 ppm 21. The Henry's coefficient, as an approximation for the Toth isotherm, gives slightly better values for the equilibrium loading for a system that processes air at lower concentrations of CO<sub>2</sub> and at increased temperatures. At elevated temperatures, the isotherm graph becomes flatter and the difference becomes smaller. Increased CO<sub>2</sub> concentrations lead to higher equilibrium loading values for the isotherm and this also shows bigger deviations between the results.

### 10.2.2 Experimental simulation

The experimental data from the paper by Surati [2] was obtained and used to plot the experimental results of the adsorption reaction at 2000 ppm. The graph, representing the experimental data, can be used to make a comparison with the results of the model with the same input parameters. The geometry of the experimental set-up and the other experimental parameters that have been implemented into the mode. The variables have

been rewritten if necessary: for instance, the paper by Surati uses the molar flow rate of 4000 ml/min and this corresponds to a velocity of 0.248 m/s taking into account the geometry of the reactor and any other experimental parameters. Some characteristics, such as the void fractions of Lewatit, have not been defined for the experiment. For these undetermined value, a reasonable value from literature has been used. Combining all the information, Figure 16 has been produced for a system that has a sorbent loading of 1.209 mol/kg.

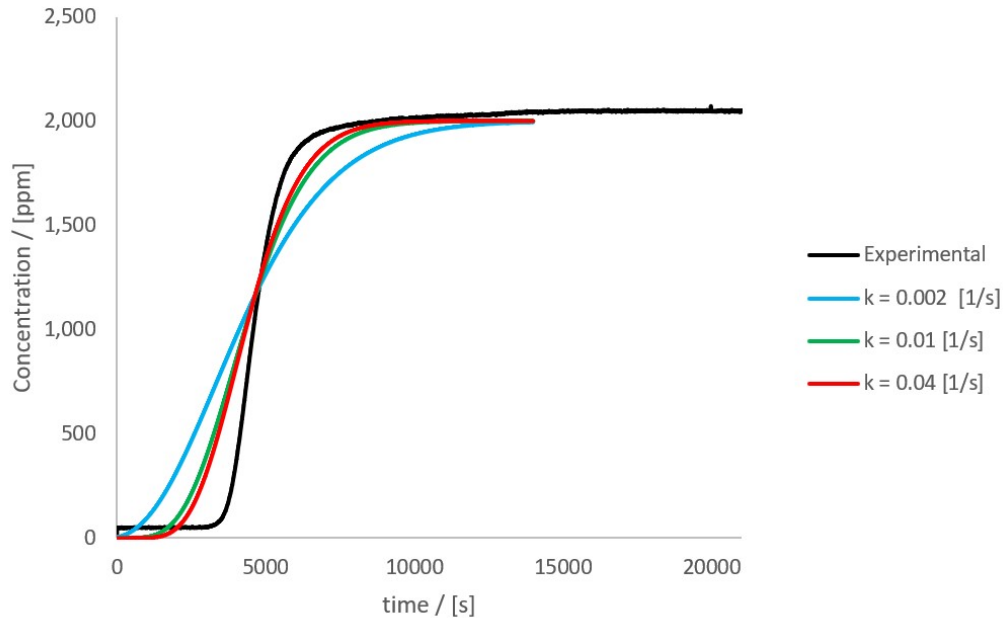


Figure 16: Comparing the experimental results of a 2000 ppm system at the outlet of the reactor by Surati [2] (the black line) to the simulations done by the model for different values of  $k$  and an equilibrium loading of 1.209 mol/kg for 1,400 seconds.

Comparing the graphs for the different values of  $k$ , some observations can be done. For instance that for higher  $k$  values, the graph is steeper and it starts to rise later in time. Higher values for  $k$  indicate faster reaction kinetics between the sorbent and the  $\text{CO}_2$  in the air that passes through the reactor. Figure 16 represents the concentration of the  $\text{CO}_2$  at the outlet of the reactor. At elevated  $k$  values, more complete adsorption reaction occurs within the reactor and it takes longer for  $\text{CO}_2$  rich air to reach the outlet. For increased  $k$ , it takes longer for  $\text{CO}_2$  rich air to reach the outlet of the reactor, the  $\text{CO}_2$  molecules react faster with the sorbent and more  $\text{CO}_2$  is extracted as the bulk it propagates through the reactor. Consequently the  $\text{CO}_2$  reaches the outlet later, but the curve is steeper due to the increased kinetics.

Another observation, when considering Figure 16, is that the experimental results start above zero and never reach 2000 ppm. In reality, results start at 0 and reach exactly 2000 ppm, therefore it can be concluded that there was a deviation in the experimental data. This could for instance be due to wrong calibration of the equipment or that the data boundaries were not correctly aligned, resulting in deviating values. The experimental data was subsequently multiplied with a factor of approximately 1.047 to fit the curve of the experimental results from 0 to 2000 ppm. The equilibrium loading of the new experimental data has consequently increased to 1.326 mol/kg and is shown in Figure 29.

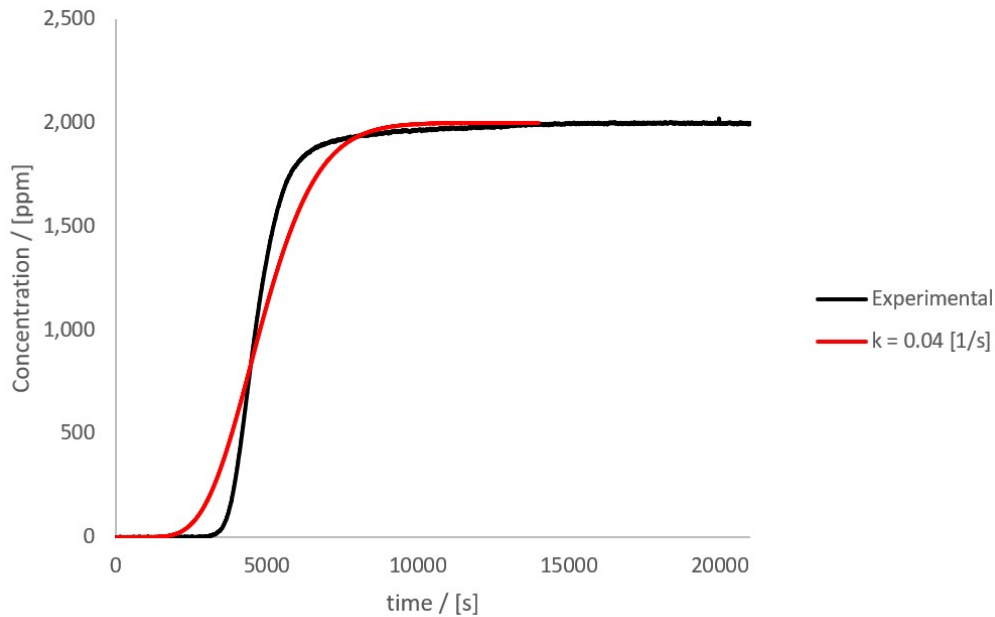


Figure 17: Comparing the fitted experimental results of a 2000 ppm system at the outlet of the reactor by Surati [2] to the simulation done by the model for  $k = 0.04 \text{ s}^{-1}$  and an equilibrium loading of 1.326 mol/kg for 1,400 seconds.

The graphs in Figure 29 show that the model simulation is similar to the experimental results. The shape of the graphs are similar, yet there are some clear differences which are most likely not due to errors in the Python code, but due to the assumptions and simplifications that have been made. One of these assumptions is the use of the Henry's coefficient instead of the Toth isotherm. Figure 15 clearly shows the difference between the two methods and it can be observed that the equilibrium loading of the Henry's coefficient is lower for the entire system compared to that of the Toth isotherm. An effect of having a lower equilibrium loading value is that the driving force of the system will be lower throughout the entire process, which results in a slower adsorption reaction. This could be one of the main reasons as to why the experimental results show a steeper curve than the model simulation.

Another assumption that has been made is that  $k$  has been considered as a constant. In reality this parameter describes the reaction rate as a function of all the diffusive resistances that occur during the adsorption reaction. As the sorbent becomes increasingly saturated, it becomes harder for the  $\text{CO}_2$  molecules to adsorb to the sorbent to the remaining adsorption sites. The kinetic rate constant does not take these effects into account and could explain the differences between the top slopes of the graphs.

Other assumptions that could have a significant effect on the reaction and help explain some of the differences are the dispersion term that has been ignored for this adsorption system. The sorbent material has been pre-treated to extract all moisture from it, variations between the density of the actual sorbent and the density used in the model could remain. Inaccuracies due to the numerical methods could cause some deviations.

### Crank-Nicolson

Both the Backward Euler and the Crank-Nicolson method have been used to produce the model results. The Crank-Nicolson method, however, provided results that showed undesirable instabilities and the Backward Euler method was decided to provide better results. The Crank-Nicolson results can be found in Appendix D 21.

### Linear driving force

To check what happens between the equilibrium loading and the actual loading, the linear driving force has been plotted for the different simulations. Figure 18 shows the course of the adsorption reaction at the outlet as a function of time for the various situations.

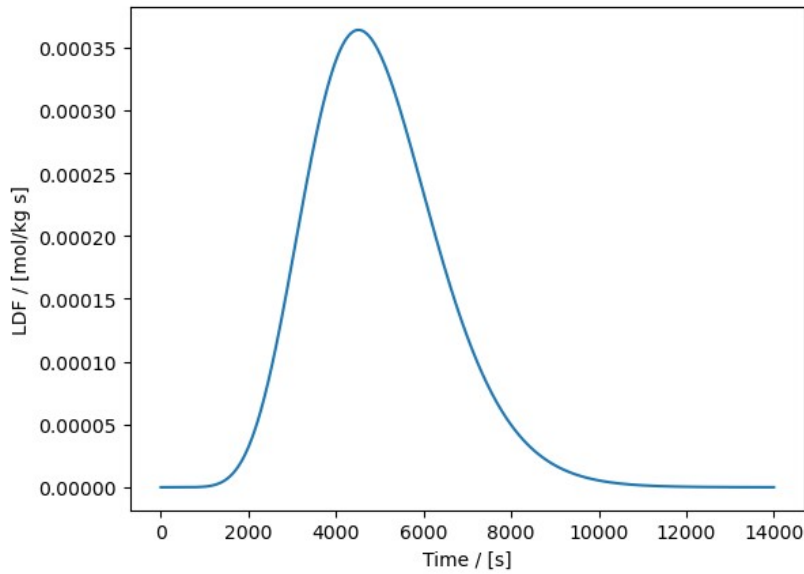


Figure 18: Linear driving force of the final model results showing the amount of loading per second for the system with  $k = 0.04 \text{ s}^{-1}$  and  $q_e = 1.326 \text{ mol/kg}$

As expected, the LDF is initially zero and increases rapidly once  $\text{CO}_2$  arrives at the outlet for the first time. The adsorption reaction at the outlet of the reactor starts this moment in time and subsequently decreases again when the reaction slows down and goes to zero.

### Sorbent loading check

The model simulations were constantly checked by calculating the area above the graph to find out what the actual loading was for the corresponding simulation. The area above the graph gives the units of concentration times seconds and can be used to calculate the actual amount of loading approximately. This calculated value for the sorbent loading should be (almost) the same as the input value for the equilibrium loading from which the Henry's coefficient has been calculated.

### Sorbent density

Another notable correction was to determine the correct density of the Lewatit sorbent that was used during the experiment. This specific sorbent was pre-treated to extract all the moisture from the sorbent, which consequently reduced the total mass of the sorbent by 48% of its original "wet" mass. Correcting this value to match that of the experimental results, a density was calculated of  $562.414 \text{ kg/m}^3$  instead of  $880 \text{ kg/m}^3$  which was determined in literature. The density correction had a huge influence on the final results and the productivity of the system.

### Productivity of the system

The final productivity of the model is determined by the total mass of the amount of loaded  $\text{CO}_2$  during the adsorption reaction, the time it takes for the sorbent to be loaded and the total volume of the reactor. The productivity of a system is often determined at 50 or 90% of its total capacity.

$$Prod_{90} = \frac{m_{\text{CO}_2, \text{loaded}}}{t_{90} \cdot V_R}$$

The equation represents the model's adsorption productivity at 90% of the total adsorption loading:  $m_{\text{CO}_2, \text{loaded}}$  is mass of all the  $\text{CO}_2$  that has adsorbed at 90% capacity of the reaction in kg,  $t_{90}$  is the time it takes for 90% sorbent capacity to become saturated in hours and  $V_R$  is the total reactor volume. The productivity of the final adsorption model at 90% of the sorbent capacity is  $9.489 \text{ kg} \cdot \text{hrs}^{-1} \cdot \text{m}^3$ .

Comparing this value to the productivity that has been determined by [2], it shows a substantial difference as the value in the paper had been determined to be approximately  $24 \text{ kg} \cdot \text{hrs}^{-1} \cdot \text{m}^3$ . This has been investigated and it showed that the wrong productivity was calculated by [2]. The reasons being that the wrong mass was

used during the productivity calculation and the wrong equilibrium loading was used. The sorbent loading that was determined for the reaction, did not correlate to the data that was measured during the experiments. The equilibrium loading that for this experiment as determine by Surati was 1.494 mol/kg or 1.406 mol/kg at 90% capacity of the reaction. The experimental data of the measurements during the process could be accessed to determine what the actual equilibrium loading of the reaction should be. The experimental data was used in Python to determine the area above the graph of the concentration in the outlet of the reactor as a function of time. The total area above the plot, which was in ppm · s, was rewritten to determine what the total amount of loading was during the process. From this calculation an equilibrium loading of 1.209 mol/kg was determined for the data that was acquired during the experiment. This value was ultimately fitted to create a figure that started at 0 ppm and ended at 2000 ppm, which lead to a equilibrium loading of 1.326 mol/kg

## 10.3 Model results

### Nested dictionaries

Initially the adsorption model was designed with nested dictionaries, a nested dictionary is a dictionary within a dictionary. The reason for choosing this method was that it made it possible to develop a system that was able to solve the PDE that describes the mass balance. Nested dictionaries can be used to determine any specific grid-point in the system for space or time. Looking at the adsorption equation it can be seen that the grids [i-1] and [i+1] are needed, furthermore predictions are done for following time-steps, based on previous time-steps, thus [j-1] is needed. These functions can be directly used in dictionaries and this was the for most reason of programming it this way. An other advantages of a using dictionaries is that it is a smart dictionary, meaning that it remembers every grid-point for the chosen dictionary and it can easily be found what the values are for specific points in time for the z-grids.

The problem however with using multiple of these (nested) dictionaries for the adsorption model is that adsorption reactions need to run for long periods of time. In the case that very large amounts of time-steps are needed for a model to achieve the desired values, dictionaries can cause problems as the needed memory capacity becomes extremely large and the model becomes too large to simulate as all the values are remembered. For this reason, most of the dictionaries were removed to make the adsorption model simpler and easier to run. Most of the values that are not of interest have been changed to lists and are overwritten for every value, instead of making a new value and remembering both the new and old values.

## 11 Conclusions adsorption

The adsorption model has successfully been modelled with the open source programme Python, without implementation of existing solver systems. Experimental data has been used to validate the model and it was possible to simulate the experimental system, despite there being differences. Differences between the numerical model simulation and the experimental results are most likely due to the assumptions and simplifications that have been applied to the model. The assumption that probably has the biggest impact on the system is the use of the Henry's coefficient, which will affect the equilibrium loading of the system and thus the driving force of the adsorption reaction. A value of  $k = 0.04 \text{ s}^{-1}$  has been found to give the most similar result to that found with the experimental set-up, though it will not be likely be the actual value for k that describes this system.

The adsorption reaction has been modelled with the use of nested dictionaries, which provided to be an excellent solution for designing a system that should solve the mass balance numerically. The dictionaries can be used to obtain information for any point in space or time during the reaction, the disadvantage however is that they requires much computational power and time to simulate systems that require copious time-steps.

## 12 Recommendations

### Model recommendations

- This first order partial differential equation is designed in Python as a nested dictionary that can be used to refer to any point in space and in time because the dictionary saves all the values within the dictionary. For the equations used to solve this system, it is necessary to be able to use the other grid-point in time in space to

solve the equation and find the next estimation. Nested dictionaries have that capability and made it possible to design the code that can solve the system for any position in time and space. However this showed the mayor draw-back for designing the model in this way for this type system that are dependent on many time- and spatial-steps. Dictionaries save all the values that calculated during the process and require enormous amounts of memory space to be able to simulate a system that requires operating for long time intervals. In this case the adsorption system needs to be simulated for at least 9000 seconds with a time-step of 0.001 which means that there are 9,000,000 data-points calculated and remembered for every dictionary. This means that the simulations become very computer intensive and require at least an hour to complete the results. The advantage of the dictionaries is the fact that they remember every data-point and can be used to examine what happens at any place and at any time throughout the entire process. For systems that require less steps in time and space, dictionaries are very useful but in this case memory capacity problems have occurred and it might be desirable to design the model in a different way. The memory capacity problems that occurred during the adsorption model simulation might be the consequence of an inefficient way of programming due to the numerous loops. During the expansion of the model, this should be considered to achieve more efficient and less computer intensive simulations.

- Another possible way to make the code more efficient could be to use different numerical solving methods for the design of the code. For this system implicit methods are used to describe the system which need to be solved by iterating the values and explicit methods often have stability problems that would occur. Alternative methods could prove to be better for such a system and should be considered for solving this type of system in further research.
- Building an adsorption model that solves the PDE with with the use of an existing solvers could provide a useful comparison. Comparing the differences and similarities could show the advantages of solving the system this way and what inaccuracies occur when using a pre-built solver. On the contrary it could also prove that the the advantages are negligible and that solvers work good enough for these type of systems.

## General adsorption recommendations

- The reaction rate of the adsorption system have been simplified by describing this function by the kinetic rate constant  $k$ . In actuality this constant is a set of equation that is determined by the different resistances that occur during the adsorption process. In most literature and during the construction of this system, it has been represented by a single constant that has been fitted to match the speed for overall reaction. However it would be incredibly interesting to get a better understanding of what happens during the adsorption reaction and which parts influence the system the most.
- This model does not take into account the influence of water on the system. In actuality, not all the vacant sorbent sites would be occupied by  $\text{CO}_2$  molecules but  $\text{H}_2\text{O}$  would also adsorb to the sorbent during this process. Water co-adsorption will have a significant influence on the overall performance of the system, though these effects are not believed to be purely negative for the adsorption process.
- Degradation effect on the overall process can be considered and analysed how these would influence the productivity of the system and when sorbent should be replaced before the system would become inefficient.
- The adsorption reaction itself consumes/produces heat for the reaction to take place which has not been taken into account. This could be analysed to determine if this can be neglected as has been done or should be accounted for.
- An interesting improvement of the overall system would be to implement the dispersion term into the mass balance, which would influence the system significantly. As the dispersion term is would make the mass balance a 2<sup>nd</sup>-order PDE system the discretization of the system should be re-evaluated to be able to numerically solve such a system.
- Finding a way to correctly implement the Toth isotherm into the model would be a good first step for improving the model. As explained in the previous sections, the Henry's coefficient is a linear constant that does not accurately represent the course of the equilibrium loading during the adsorption process. Integrating



the actual Toth isotherm as provided by Bos [3] could provide the model with continuously better estimations throughout the simulations.

- Continuing on the Toth isotherm, it could be investigated how accurate this isotherm represents an actual system for the low-pressure region. For which pressure is this isotherm actually fitted and would the system change if this part of the isotherm would be improved.

## Desorption

## 13 Introduction desorption

The second main process of a DAC system is the desorption of the systems adsorbed material. During the adsorption step,  $\text{CO}_2$  has been collected from the air and is adsorbed on to the sorbent material while the rest of the bulk components flow through the system. In this case the bulk material is air, which is comprised mainly of nitrogen, oxygen, argon and carbon dioxide. After enough adsorbate has been captured, in this case the adsorbate is  $\text{CO}_2$ , and the sorbent is sufficiently saturated, the reactor is closed off from the environment and no more air flows through the system. Then the goal is to collect the  $\text{CO}_2$  molecules from the sorbent and extract the adsorbate as a (almost) pure  $\text{CO}_2$  stream for storage or utilization. There are different methods to regenerate the system, in this case the model will simulate desorption based on a VTSA system where the reactor is vacuumed to a lower pressure and heated to achieve  $\text{CO}_2$  unloading. In the literature it has been shown that the combination of vacuum and heating is much more effective than either PSA or TSA alone. This offers a major advantage when designing a desorption system because heating the system sufficiently to be able to extract enough  $\text{CO}_2$  from the solid sorbent demands a lot of energy.

### 13.1 Desorption model

The desorption reaction of a DAC system is the part of the process where the most uncertainty lies, due to lack of experimental data and public information. In contrast to the adsorption process which is done under constant temperature, the desorption system needs to be heated and is a non-isothermal process. For the design of the desorption, the system will be dependent on its mass and energy balances, which will be the foundation for creating a realistic simulation of the system. In this chapter it will be explained how these equations are derived and why certain assumptions have been made. Unlike with the adsorption system, the desorption process will be modelled as a function of time only and will be independent of the spatial domain. The system of equations are set-up from the assumptions that are made to describe the desorption process and from here the goal is to create a good desorption model for a DAC system, with its code written in Python.

The desorption model will be modelled in a different way than was done with the adsorption system. For this part of the DAC system the goal is not to build the model completely independent of pre-coded solvers, but to create a code that can simulate the desorption process appropriately. The desorption process has other main challenges compared to the adsorption process and will be modelled accordingly. As with any system it will be important to describe the control volume properly by determining the correct mass and energy balances that describe the system and to implement these properly in the Python code. For the desorption system it will be important to correctly define the energy balance that describes the heating of the entire system as the temperature influences the overall system significantly. This will all be clarified later on in this chapter.

For this desorption system, some important assumptions have been made that influence the overall design of the model and are important to mention. First of all the assumption has been made that during the adsorption process, only  $\text{CO}_2$  has been adsorbed and nothing else is attached to the sorbent. Secondly, the reactor is assumed to initially be completely filled with gaseous  $\text{N}_2$  before the desorption reaction has started. Furthermore the reactor is assumed to have a constant volume and pressure, and is also considered to be an adiabatic system, with no heat loss to the surroundings.

#### 13.1.1 CSTR

This desorption system can be completely described by three mass balances and an energy balance that are all dependent on each other. This system will be described as a CSTR with only time dependent differentials, and the entire system will independent of direction. The fact that all the equations are ODEs makes it considerably less complex to solve then for a system described by PDEs. Because the system is modelled as a CSTR, some assumptions are made in order to describe the system which, had the system been modelled as a PFR, would have been different.

An important assumption to be made with a CSTR system is that perfect mixing occurs. The gasses inside the reactor interact to form an ideal gas-mixture. The solution exhibits thermodynamic properties that correspond to the mixture of the ideal gases. This means that the volume change of mixing and the enthalpy of mixing are zero. Furthermore, there is no spatial gradient in the system and the properties such as the temperature, the concentration, etc are independent of this spatial gradient. This assumptions simplifies the model because no

spatial gradient influences the systems properties and the they are the equally divided throughout this system as a consequence. The ideal gas-mixture inside the system is described to contain only ideal gasses that are heated according to ideal heat transfer.

The conservation equations that describe the mass and energy balances are influenced by the decision to model the system as a CSTR. The two continuous reactor systems that are generally considered for these types of processes are the PFR (Plug Flow Reactor) and the CSTR (Continuous Stirred Tank Reactor). The adsorption system is described by a PFR, but for the desorption model the reaction will be described as a CSTR system that is independent of position. For a CSTR, ideal mixing occurs within the reactor and properties like the concentration and temperature are equal throughout the reactor. The composition of the stream flowing out of the reactor is identical to that of the bulk inside the reactor.

### 13.1.2 Vacuum Temperature Swing Adsorption (VTSA)

The desorption method that is chosen for this model is the VTSA method, which uses a combination of reduced pressure (vacuum) and increased temperature to unload the  $\text{CO}_2$  from the sorbent. Other methods that could be used like TSA and PSA, but have been determined not to be as effective as VTSA for this type of system. Purge by injection techniques can also be considered for the model, as the assumption will be made that the gas inside the system consists purely of  $\text{N}_2$  which can be considered to be due to stripping by nitrogen. For this system the isotherm shown in the figure, which is reproduced from the paper by Bos [3], should be considered as it shows the effect of pressure and temperature variations on the equilibrium loading (capacity) of the system, see Figure 26. From this data, it can be seen that pressure has a small region of significant influence on the capacity and that the temperature at which the process operates mainly determines the amount of desorption that can be achieved for the system.

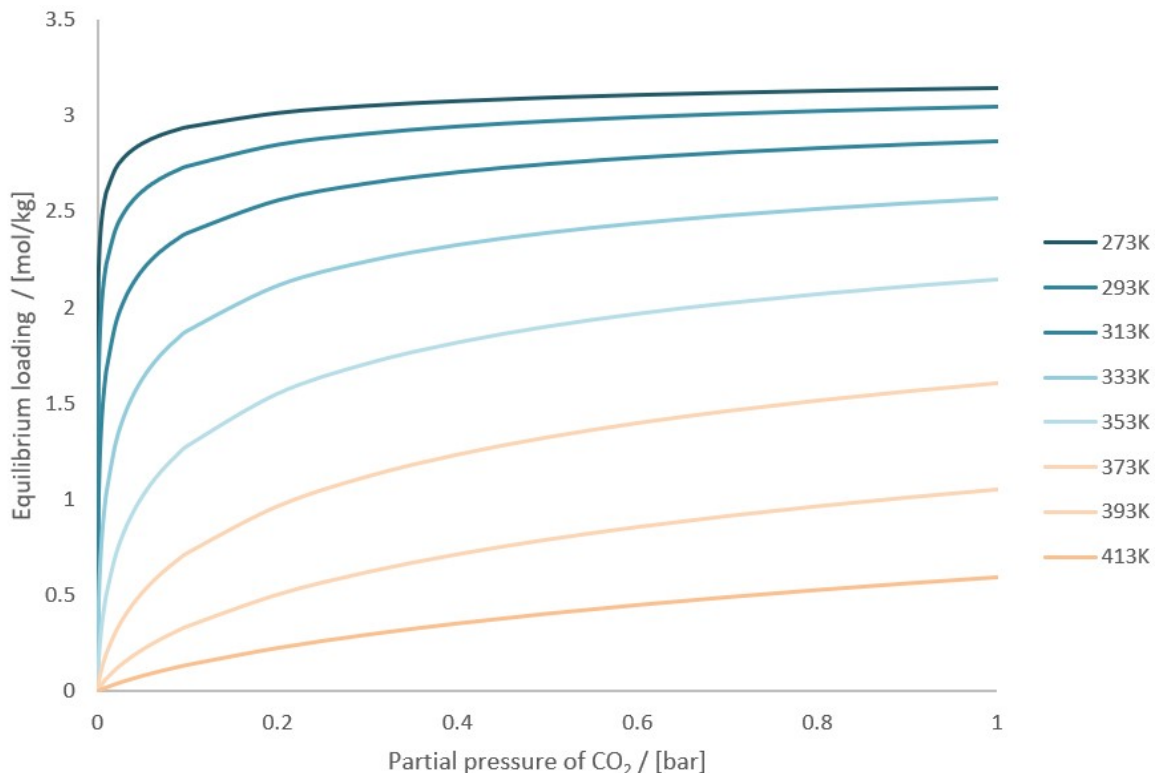


Figure 19: Reproduced representation of the experimental Toth isotherm equation as determined by Bos [3] that shows the effect of temperature and the partial pressure of  $\text{CO}_2$  on the capacity of the sorbent from 0 to 1 bar

## 13.2 Desorption model

As mentioned, the desorption system described in this thesis is modelled as a CSTR and VTSA is the desorption method used to unload the  $\text{CO}_2$  from the sorbent. Multiple assumptions have been made to describe this system in Python and these assumptions are the following:

### Reactor system:

- Constant Pressure
- Constant Volume
- Ideal gas mixture
- Reactor initially filled with nitrogen
- Loses no heat to environment
- Vacuum is reached before the start of the model (pre-desorption)
- No inflow into the system
- Desorption purely due to VTSA
- Heating done directly from heating element inside the system
- Reaction heat of the desorption reaction is equal to that of the adsorption reaction
- LDF can be used for  $r_A$  for  $\text{CO}_2$  releasing from the sorbent
- Solved with LSODA method

These assumptions are combined with the control volume to describe the complete desorption system. The reactor is shown schematically in Figure 20:

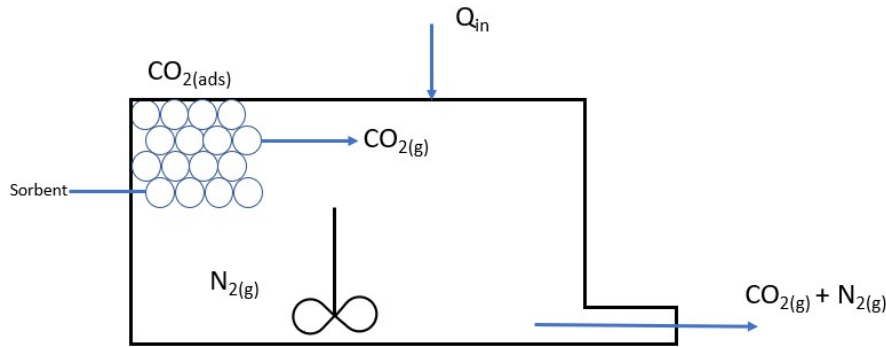


Figure 20: Simplified representation of the CSTR desorption system filled with solid sorbent material. The gaseous components inside the reactor are exclusively  $\text{N}_2$  and  $\text{CO}_2$  as the system is heated by a heating source  $Q_{in}$

### 13.2.1 The reactor

Before the desorption process starts, the adsorption reaction needs to be concluded and the reactor sealed off from its environment. Now the reactor is a closed system and can be vacuumed to reduce pressure from 1 bar to the desired operating pressure for the system. Vacuuming of the system happens before the desorption reaction starts and for the model it is assumed that no  $\text{CO}_2$  unloading occurs when the vacuum takes place. When the desired reactor pressure is reached, it will stay constant throughout the entire desorption process. Though constant pressure is assumed during the process, the partial pressures of the components can change while the overall pressure inside the reactor stays constant. Not only should the pressure be constant, but the volume of the reactor should also remain constant throughout the entire process. The volume of the reactor will never change for the entire DAC system during both the adsorption and desorption reaction, but the advantage of the model is that it can be used to evaluate what would happen to the system for different dimensions for the volume of the system.

The flow through the control volume determines the systems equations, and in this case there is no inflow into the reactor only outflow. The  $\text{CO}_2$  that was loaded on to the sorbent during the adsorption, creates the outflow of the desorption reaction when it unloads, which in turn, drives the gas-mixture out of the reactor. For the unloading reaction of the  $\text{CO}_2$ , which creates the outflow out of the system, no purge gas is used and the reaction occurs simply due to the decreased pressure and increasing temperature of the VTSA method. The reactor is heated by a heating element in order for desorption to occur, while it is assumed that the system loses

no heat to its environment. No heat is lost from the system and no heat is added externally to the reactor; it is assumed that the entire system is heated internally by heating element and the entire reactor, with all the components inside it, are heated evenly.

### 13.2.2 The components

The gas inside the reactor is described as an ideal gas mixture, where all the gaseous components inside the reactor can be described by the ideal gas law. For DAC system the bulk inside the reactor is air, which can be treated as an ideal gas. For simplicity the desorption reaction is modelled with a reactor that is initially filled with only nitrogen instead of air and the sorbent is fully loaded with CO<sub>2</sub>. Air is comprised largely of nitrogen (78%) and so it is easier to describe the system as if the reactor is filled only with N<sub>2</sub> instead of including all the components that air is out of. Therefore it is assumed that when the desorption reaction commences, there is only N<sub>2</sub> in the reactor when the CO<sub>2</sub> molecules start to unload from the sorbent. In this system, the components CO<sub>2</sub> and N<sub>2</sub> are denoted with the subscript A and B for respectively. For the desorption, like with the adsorption, the reaction can be described with the LDF, and the reaction enthalpy ( $\Delta H$ ) that occurs is also the same as for the adsorption reaction.

## 13.3 System description

The system that is chosen to describe the desorption process will be describes as a one dimensional CSTR model with appropriate mass and energy balances, describing what is happening to the system. First of all, this system must be considered as a reactor with no inflow into the reactor. The desorption column has been closed from the environment and then a vacuum is created within the sytem, lowering the pressure in the reactor. In an actual desorption system, during the pre-desorption, the vacuum could extract some the remaining gaseous elements from the reactor. Although this will not be taken into account for this model, that would be an advantage because the goal is to extract pure CO<sub>2</sub> and before that can happen, the resulting bulk inside the reactor needs to be removed. The gaseous bulk that lingers inside the reactor would be air, which is composed out of multiple different molecules. However in this model, this bulk is simplified by considering the air as consisting only of nitrogen, its largest component. This makes modeling easier, but it must be remembered that this will have effect on the overall result.

Two other important components of air, O<sub>2</sub> and H<sub>2</sub>O, which would normally have a significant effect on the desorption process, will not be taken into account for this model. Oxygen mainly affects the reaction through the oxygen degradation that occurs on the sorbent. For water, the effects are different; in this case the assumption has been made that no water co-adsorption has occurred during the adsorption reaction and only CO<sub>2</sub> has been adsorbed on to the sorbent. The other effect that water would have on the desorption are the effects on the partial pressures, which would lead to a faster unloading of the sorbent.

### Definitions

- $A = \text{CO}_2$
- $B = \text{N}_2$
- $n_{A,g} = n_A$
- $n_{B,g} = n_B$
- $n_{A,ads} = q_A \cdot m_s$
- $\frac{dn_{A,ads}}{dt} = \frac{dq_A}{dt} \cdot m_s$
- $c_{v,A,ads} = c_{v,A,g}$
- $M_t = \text{Total molar flow rate (mol/s)}$

The definitions show the simplifications that have been made and some definitions of terms that have been used during calculations and derivations.

### Assumptions

1.  $n_B = n_t + n_A$
2.  $\frac{dV}{dt} = 0$
3.  $\frac{dP}{dt} = 0$
4.  $\frac{dn_t}{dt} \neq 0$
5.  $\frac{dT}{dt} \neq 0$

The assumptions show that it has been assumed that the amount of gaseous moles of N<sub>2</sub> in the reactor is dependent on the total amount of gaseous moles of CO<sub>2</sub> in the reactor. The amount of CO<sub>2</sub> that occurs in

the reactor drives the  $N_2$  out as this amount increases during desorption. The other assumptions that have been made are that the volume and the total pressure inside the reactor are constant, while the total number of gaseous moles in the reactor and the temperature of the entire system are not constant during desorption.

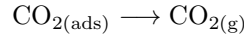
### 13.4 Mass balances

As with any engineering system, the starting point is to set up the appropriate mass and energy balances that describe the specific system. These governing equations can directly be simplified due to the fact that there is no inflow for the desorption system. Outflow, generation and consumption can occur for the system as is shown by the following general mass balance where  $\dot{n}$  represents the molar flow:

$$\frac{\partial \dot{n}}{\partial t} = -\dot{n}_{\text{out}} + \dot{n}_{\text{gen}} - \dot{n}_{\text{cons}}$$

For this specific desorption system, where only  $CO_2$  is adsorbed on to the sorbent and the reactor is filled with only  $N_2$ , the overall mass balance can be written in terms of three different mass balances that describe the subsystems inside the reactor. This is different from the adsorption process where the system is described by a single mass balance. This desorption system will be described by three different mass balances and an energy balance. The three different mass balances describe the unloading reaction where the  $CO_{2(\text{ads})}$  desorbs from the sorbent into the gas phase, the total gaseous  $CO_2$  mass balance and the total gaseous mass balance that describes the combined mass balance of all the gaseous particles through the system.

The first mass balance is the unloading reaction, where the adsorbed  $CO_2$  molecules are released by the sorbent and go from the adsorbed phase to the gaseous phase:



$$\frac{\partial q_{CO_2}}{\partial t} = -k \cdot (qe_{CO_2} - q_{CO_2}) \quad (1)$$

This reaction represents the generation term of the overall mass balance and is described by the LDF. As mentioned there is no inflow into the system, but there is a generation of  $CO_{2(\text{g})}$  molecules into the reactor as the adsorbed  $CO_2$  unloads from the sorbent. This accumulation is the driving force behind the outflow of the system, as the pressure and volume of the reactor stay constant. The unloading  $CO_2$  molecules mix ideally with the  $N_{2(\text{g})}$  in the reactor before the accumulating gaseous molecules flow out of the reactor due to the increasing partial pressure of the gas mixture. This is what happens in the second mass balance, which can be considered as the total  $CO_2$  mass balance:

$$\frac{dn_{CO_2}}{dt} = -M_t \cdot \frac{n_{CO_2}}{(n_{CO_2} + n_{N_2})} - m_s \cdot k \cdot (qe_{CO_2} - q_{CO_2}) \quad (2)$$

In this equation the first term describes the molar flow rate out of the reactor of the  $CO_{2(\text{g})}$  part in the ideal gas mixture. Where  $M_t$  is the total molar flow rate out of the system which is multiplied by the molar fraction of  $CO_{2(\text{g})}$ . The second term is the amount of  $CO_{2(\text{g})}$  that accumulates in the system due to the unloading reaction of the  $CO_2$  from the adsorbed-phase to the gas-phase. This part of the equation is calculated by multiplying the sorbent mass ( $m_s$ ) by LDF, which is represented by multiplying the kinetic rate constant ( $k$ ) by the driving force of the adsorption reaction.

The last mass balance is the complete gas-phase mass balance of the bulk inside the system. This mass balance is similar to the second mass balance, only the outflow is now the combination of all the gaseous components in the reactor. In this system, these are just the  $CO_{2(\text{g})}$  and the  $N_{2(\text{g})}$  molecules that comprise the total gas bulk inside the reactor:

$$\frac{dn_t}{dt} = -M_t - k \cdot m_s \cdot (qe_{CO_2} - q_{CO_2}) \quad (3)$$

The last mass balance is the total mass balance of all the gaseous components and from these last two mass balances, the total amount of  $N_{2(\text{g})}$  in the system can be derived. Initially the system will contain only  $N_{2(\text{g})}$  and no  $CO_{2(\text{g})}$ , but as time progresses more  $CO_{2(\text{g})}$  enters the system until no nitrogen remains in the reactor. At this point, a pure  $CO_{2(\text{g})}$  stream can be extracted from the system and this is the total amount of  $CO_{2(\text{g})}$  that is removed from the air for one simulated DAC cycle.

## 13.5 Energy Balance

The three mass balances together describe the overall mass balance of the system. The desorption process is a non-isothermal system that requires the addition of an energy balance to describe the complete system. Starting from a general energy balance, the equation can be rewritten for this specific system to the following equation and its derivation can be found in appendix D:

$$\frac{dT}{dt} = \frac{1}{n_A c_{v,A} + n_B c_{v,B} + m_s c_s} \left( -m_s T M_t \left( \frac{n_A}{n_t} c_{p,A} + \frac{n_B}{n_t} c_{p,B} \right) - \Delta H_{\text{rxn}} m_s k (q_e - q_A) + UA(T_H - T) \right) \quad (4)$$

The four balance equations combined are the governing equations that describe the desorption system and can together be used to solve the differential equations for any time-step. With the assumptions made for this desorption system, the general energy balance could be rewritten as the equation above. The energy balance that has been derived has been written in terms of its temperature differential and combining it with the mass balance equations, the derivative can be solved and the temperature of the system can be calculated for any point in time. The right hand side of the equation shows three different terms in the large squared brackets. The first term inside these squared brackets is the total energy outflow of the system, the second term is the heating of the system done by the heating elements inside the reactor and the last term is the reaction heat that is needed for the unloading reaction. All three of these terms are multiplied by a term that contains the specific heat capacity for all the components inside the reactor. For the calculation of the energy balance equation the specific heat capacities of CO<sub>2</sub>, N<sub>2</sub> and the solid sorbent are used ( $c_A$ ,  $c_B$  and  $c_s$  respectively),  $\Delta H_{\text{rxn}}$  is the reaction heat of the desorption reaction,  $U$  is the overall heat transfer coefficient of the system,  $A$  is the area of heating of the heating element and  $T_H$  is the temperature of the heating element used to heat the system.

$$\begin{aligned} \text{Flow out of the reactor} &= -m_s T M_t \left( \frac{n_A}{n_t} c_{p,A} + \frac{n_B}{n_t} c_{p,B} \right) \\ \text{Heat of the desorption reaction} &= \Delta H_{\text{rxn}} m_s k (q_e - q_A) \\ \text{Heat added to the system} &= UA(T_H - T) \end{aligned}$$

## 14 Modelling approach desorption

### 14.1 Modelling goal

There is very little available data about the desorption reaction of DAC systems, as there is limited published experimental data. For adsorption, though also limited, there is more publicly known than for the desorption reaction. This is one of the main reasons why it is important to build a desorption model that can simulate this process for DAC systems: to have a model that is able to provide information about the systems mechanics and that can predict how the different characteristics affect the overall productivity. Using Python, the main goal to build a model that can realistically simulate the desorption process of a DAC system, based on assumptions made for the system. The desorption reaction is described by four different relatively simply solvable ODEs, which is in contrast to the adsorption system where the systems mass balance equation is based on a complex PDE. It is not the goal to build the solver for this system as in the case of the adsorption model, but to create a working desorption model. In this way, a built-in ODE solver can be used to help create a model that can be used to investigate the desorption system and the evaluate the different parameters. One paper from literature provides some experimental desorption data, in the paper by Young et al. [21]. This paper along with a case study will be used to investigate the desorption reactor and its characteristics.

### 14.2 System description

For the desorption model, the choice was made to implement the 'SciPy' solver system, which can use an ODE solving method that can simultaneously solve the four governing equations. With the data provided by the literature, the three different mass balances and the energy balances can be solved to calculate the desired



values and provide results for the different system designs. From the mass balances and the energy balance the values for  $q_A$  (the sorbent loading of  $\text{CO}_2$ ),  $n_A$  (the amount of gaseous  $\text{CO}_2$  moles in the reactor),  $n_t$  (the total amount of moles of the gas mixture in the reactor) and  $T$  (the reactor temperature) are calculated respectively for every time-step. The equilibrium loading is determined by the Toth isotherm, which can be found with all the requisite equations in Appendix A. The latter equation is a function of the partial pressure of  $\text{CO}_2$  and is a function of both the  $n_A$  and  $T$  as is shown below:

$$qe_A(n_A, T) = \frac{q_s \cdot b \cdot P_A}{((1 + (b \cdot P_A)^{t_h})^{t_h^{-1}})} \quad (14)$$

In this equation there are four different variables,  $q_s$  (the maximum  $\text{CO}_2$  capacity),  $b$  (Toth isotherm equilibrium parameter),  $t_h$  (Toth isotherm heterogeneity parameter) and  $P_A$  (the partial pressure of  $\text{CO}_2$ ). The first three parameters are experimentally determined Toth isotherm variables provided by the paper by Bos [3] and are calculated using the equations in Appendix B 19. All three of these parameters are dependent on the temperature and can be calculated from the other equations in Appendix A. The partial pressure of the  $\text{CO}_2$  in this equation depends on the amount of  $\text{CO}_{2(g)}$  in the reactor and changes as the sorbent unloads. The partial pressure in this equation is calculated with the ideal gas law and is dependent on  $n_A$  and  $T$  as is shown below:

$$P_A = \frac{n_A \cdot R \cdot T}{V}$$

The other important algebraic equation in the model are the equations to calculate the amount of gaseous moles of  $\text{N}_2$  in the system and the molar flow rate equation which is determined by rewriting the governing equations so it can be solved for  $M_t$  as can be seen in the appendix C.

$$n_B = n_t - n_A \quad (15)$$

$$M_t = m_s \cdot k(q_A - qe) + \frac{n_t}{T} \cdot \frac{1}{c_{p,A} \cdot n_A + c_{p,B} \cdot (n_t - n_A) + c_{v,A,g} \cdot q_A \cdot m_s + c_s \cdot m_s} \cdot \left[ T \cdot m_s \cdot k(q_A - qe) \cdot \left( \frac{n_A}{n_t} (c_{v,A,g} - c_{v,B,g} - c_{p,A} + c_{p,B}) - c_{p,B} \right) + UA(T_H - T) + \Delta H \cdot m_s \cdot k(q_A - qe) \right] \quad (16)$$

#### 14.2.1 Governing equations

The four ODEs that describe the desorption system are all time dependent variables that change for every instance in time and are denoted with the subscript [j]. The variables that change as a function of time can be recognised by this subscript [j], which indicates the specific moment in time. The ODEs are solved simultaneously to calculate all the different time dependent variables at any given moment. The equations are discretized and listed below:

$$\frac{dq_{A,j}}{dt} = k \cdot (qe_{A,j} - q_{A,j}) \quad (1)$$

$$\frac{dn_{A,j}}{dt} = -M_{t,j} \cdot \frac{n_{A,j}}{(n_{A,j} + n_{B,j})} - m_s \cdot k \cdot (qe_{A,j} - q_{A,j}) \quad (2)$$

$$\frac{dn_{t,j}}{dt} = -M_{t,j} - m_s \cdot k \cdot (qe_{A,j} - q_{A,j}) \quad (3)$$

$$\frac{dT_j}{dt} = \frac{1}{n_{A,j}c_{v,A,j} + n_{B,j}c_{v,B,j} + m_s c_s} \cdot \left( -m_s T_j M_{t,j} \left( \frac{n_{A,j}}{n_{t,j}} c_{p,A,j} + \frac{n_{B,j}}{n_{t,j}} c_{p,B,j} \right) - \Delta H_{\text{rxn}} m_s k (qe_{A,j} - q_{A,j}) + UA(T_H - T_j) \right) \quad (4)$$

### 14.2.2 Initial conditions

The desorption system is modelled as a CSTR that is completely independent of position, therefore there are no boundary conditions. The system can be solved when the initial conditions are determined for the individual ODEs. These initial conditions are variables that can be set to the desired input values to evaluate a given system. The default initial conditions used during the desorption model verification and simulations are the following:

1.  $q_{A,0} = q_{\text{ads}}$
2.  $n_{A,0} = \frac{P_{A,0} \cdot V_g}{R \cdot T_0}$
3.  $n_{t,0} = \frac{P_{\text{vac}} \cdot V_g}{R \cdot T_0}$
4.  $T_0 = T_{\text{amb}}$

These are the initial conditions that are used to solve the ODEs that describe the desorption system. The first is the initial condition for the sorbent loading,  $q_{\text{ads}}$ , which in reality will be the amount of sorbent that has loaded on to the sorbent during the adsorption reaction. However the two models can be evaluated individually and the desorption value can analysed independently by changing this initial value manually. The initial temperature will be the temperature at which the adsorption reaction took place which in this case is taken to be ambient temperature ( $T_{\text{amb}} = 25^\circ\text{C}$ ), but could in reality be higher or lower dependent on where the DAC plant would be situated. The initial value  $n_{t,0}$  is calculated with the ideal gas law and depends on the initial values for  $P_{\text{vac}}$  (the pressure of the reactor after vacuum has occurred),  $V_g$  (the gas volume of the reactor),  $R$  (the universal gas constant) and  $T_0$  (the initial temperature of the system).

The second initial condition for the  $n_{A,0}$  is calculated with the ideal gas equation, however it is a little more complex. The value for  $n_{A,0}$  has been determined by rewriting the Toth isotherm equation, where the partial pressure of  $\text{CO}_2$  inside the isotherm equation has substituted by the ideal gas law equation. Consequently the equation was rewritten to a form from which the starting value for the molar  $\text{CO}_2$  value can be calculated. This process has been done in Maple to determine this equation and implemented in the model.

$$P_{A,0} = \frac{n_{A,0} \cdot R \cdot T_0}{V_g}$$

$$qe_{A,0} = \frac{q_s b \frac{n_{A,0} \cdot R \cdot T_0}{V_g}}{\left(1 + \left(b \frac{n_{A,0} \cdot R \cdot T_0}{V_g}\right)^{t_h}\right)^{\frac{1}{t_h}}}$$

The initial values for the equilibrium loading ( $qe_{A,0}$ ), the molar flow rate  $M_t$  and the moles of gaseous  $\text{CO}_2$  ( $n_{A,0}$ ) are dependent on each other. For different values in the model, these initial values can vary and a jump irregularity can occur at this initial system if an incorrect value for  $n_{A,0}$  is taken. To stabilize the graphs of the model for any taken values in the system, the initial condition  $n_{A,0}$  is matched to the input values of  $qe_A$  and  $M_t$ , as has just been explained.

### 14.2.3 The ODE solver

The method that was first considered to solve the differential equations of this model is the Runge-Kutta 4<sup>th</sup> order method. The RK4 method uses a weighted average of four different slopes to estimate the next value: this is a forward prediction method. The RK4 method is the classical Runge-Kutta method and is widely used for solving initial-value problems of differential equations. The "RK45" method, however showed large instabilities as the desorption system was modelled. This method was substituted with a method called "LSODA", which is an integration scheme that uses automatic time-stepping that uses either forward or backwards solver method depending on its numerical stability. After implementing the "LSODA" method, the model simulations are mostly stable and show reasonable predictions for the system. For the Python model, the ODE integrator "SciPy" has been used to solve the ODE solver methods. Inserting the mass and energy balance differential equations with the initial conditions solves the ODEs for the desired values.

## 15 Verification and Validation

### 15.1 Verification of the model

The foundation for this model has been determined by the parameters found from literature and the assumptions that are made for designing a reactor that should represent the desorption process of a DAC system. The default values that are used for the parameters during the models design, can be found in Table 2. The Toth isotherm can be used to predict the value for the equilibrium loading  $qe_A$  where A represents the CO<sub>2</sub> and the values for the isotherm are based on the data as determined by Bos [3]. For the desorption reaction the isotherm is dependent on two variables, the temperature of the reactor and the partial pressure of the CO<sub>2</sub>, which is a function of the number of moles of CO<sub>2</sub> in the gas phase. All the other Toth parameters are constants and are assumed to be correctly fitted by Bos [3].

Table 2: Desorption systems default values

Variables			
Parameter	Default value	Unit	Equation
$L_R$	0.081954	m	Reactor length [2]
$D_R$	0.5	m	Diameter
$A_R$	0.1963	m	Reactor cross-sectional area
$V_R$	0.0161	m <sup>3</sup>	Volume reactor
$V_g$	$6.115 \cdot 10^{-3}$	m <sup>3</sup>	Volume gaseous part of reactor
$V_s$	0.01	m <sup>3</sup>	Volume sorbent bed reactor
$m_s$	8.78	kg	Mass of sorbent
$n_{A,0}$	$6 \cdot 10^{-5}$	mol	Initial amount of gaseous moles CO <sub>2</sub>
$n_{t,0}$	0.0617	mol	Initial total amount of gaseous moles
$q_{A,0}$	0.9	mol · kg <sup>-1</sup>	Initial sorbent loading
$qe_0$	0.9	mol · kg <sup>-1</sup>	Initial equilibrium loading
$T_{des}$	393	K	Max heating temperature
$P_{vac}$	0.25	bar	Desorption vacuum pressure
$k$	0.001	s <sup>-1</sup>	Kinetic rate constant
$A_{tube}$	0.0129	m <sup>2</sup>	Total contact area of single heating tube
$A$	0.129	m <sup>2</sup>	Total contact area
$V_{tube}$	$0.161 \cdot 10^{-3}$	m <sup>3</sup>	Total volume of a single heating tube
$L_{tube}$	0.081954	m	Length of heating tubes
$R_{tube}$	0.025	m	Radius of heating tubes
$n_{tube}$	10	-	Number of heating tubes
$X_{tubes}$	10	%	Percent volume of heating tubes
$U$	750	W · m <sup>-2</sup> · K <sup>-1</sup>	Overall heat transfer coefficient

The desorption reaction is represented by multiple reactions that describe the system and all these equations are ODES, making it easier to find a stability conditions for the model. There is no spatial differential because this system only depends on time; this means that the duration and  $\Delta t$  for this model can be changed easily to find the systems stable conditions. Once this is done, the model can be used to analyse the values of the various parameters of the system for the verification and validation of the model. The most important parameters of this system that will be investigated for the desorption system are the following:

- $P_{vac}$  = The regeneration pressure [bar]
- $T_{des}$  = The maximum heating temperature of desorption [K]
- $k$  = The kinetic rate constant of the desorption reaction [s<sup>-1</sup>]
- $V_R$  = The reactor volume [m<sup>3</sup>]
- $U$  = Overall heat transfer coefficient [W · m<sup>-2</sup> · K]
- $A$  = Area of heating [m<sup>2</sup>]
- $q_{A,0}$  = Initial sorbent loading [mol · kg<sup>-1</sup>]

- $n_t$  = Total number of gaseous moles in the reactor [mol]
- $n_A$  = Total number of  $\text{CO}_{2(g)}$  moles in the reactor [mol]
- $n_B$  = Total number of  $\text{N}_{2(g)}$  moles in the reactor [mol]
- $M_t$  = Molar flow rate of ideally mixed bulk out of the reactor [ $\text{mol} \cdot \text{s}^{-1}$ ]
- $Prod$  = Productivity of the reactor [ $\text{kg} \cdot \text{hr}^{-1} \text{m}^{-3}$ ]

The default values that are used for the desorption model are shown in the appendix B 2 and are chosen values based on literature and logical reasoning. These values will be the standard conditions for the evaluation of the desorption system and are used to determine what happens to the system when these values are varied. In the following sections, an analysis will be made of what happens when all the values are kept constant while changing one variable. This will help determine how the different parameters influence the desorption process and this can be used to help check if the model does what is expected. For instance, logically a reactor heats faster when the heat transfer coefficient is increased while all the other values are the same. The model predictions should be in line with what logic and data dictate, so this process verifies the model's validity. To help explain what happens during the process, various graphs present the different loading values for various parameters when they are changed for the system.

### 15.1.1 Pressure

The desorption model is based on the VTSA system, where the capacity is mostly dependent on the pressure and the temperature, as can be seen from the isotherms in Figure ???. These are the two main parameters that determine the equilibrium loading of the system and therefore the amount of desorption that is possible within the system. It can be argued that the temperature has the most significant influence on the desorption process, when considering the isotherm. Increasing the temperature lowers the equilibrium loading and this determines the overall capacity that can be achieved. The pressure of the system has significant influence in the low pressure region where the graph shows the steepest slope. So the temperature has the largest influence on the systems capacity, though it is still important to decrease the systems pressure adequately.

At pressures approaching zero, the curve of the isotherms is incredibly steep and for this region the experimental data is limited. The model could be used to get a more accurate interpretation of this steep slope at the low pressure region. It is also good to realise that the lower the value of the vacuum pressure, the more energy intensive the process can become. Depending on what vacuum pressure is required, it may be necessary to use more vacuum pumps to bring the system down to the desired low pressure value. Vacuum pump systems that are generally used for these type of applications can usually decrease the pressure inside the reactor by a factor of four. This means that by implementing one vacuum pump in this system, a pressure of 0.25 bar could be achieved. If a second pump is implemented, a pressure of 0.0625 bar could theoretically be achieved. From the isotherm it becomes clear that lower pressure values are desired because at lower pressure, lower values for the equilibrium loading can be achieved. For the repressurisation of the reactor, no equipment is necessary as the reactor in- and outlet can be opened and atmospheric air will flow into the system until 1 bar is reached. However, this is not the case for the repressurisation of the  $\text{CO}_2$  stream and it will cost a significant of energy to bring the  $\text{CO}_2$  back up to 1 bar. If the energy requirements for the system would be implemented into the model, a trade-off should be made to calculate what the optimal pressure will be for the system that does not result in extreme energy demands for the system. For decreased pressure, the capacity increases and the productivity of a reactor increases by a factor 3 between 0.5 and 0.25 bars and by a more than a factor 2 from 0.25 to 0.0625 bars. In theory, this sound like lower pressures will provide better desorption system, yet the energy demand will increase significantly nothing can be said conclusively for an actual DAC desorption system.

The cyclic capacity of the process becomes considerably better for lower pressure values, as the minima for the equilibrium and the actual loading become lower while the initial loading remains the same. This leads to a larger driving force and a more complete unloading reaction. The capacity of the desorption is the difference between the initial value of the loading and the minimum value for the equilibrium loading. When this difference becomes smaller, the driving force and the total capacity become smaller, leading to less  $\text{CO}_2$  unloading. Increasing the pressure decreases the total capacity of the reaction and the reaction becomes less efficient. This is in line with the expectations illustrated in the isotherms and it can be concluded that a lower pressure is desirable for the desorption stage.

In the lower pressure regime, it takes slightly less time for the reactor to reach 50% and 90% of its desorption capacity and for all the  $N_2$  to leave the reactor than for higher pressure values. The fact that the molar flow rate is higher while the decreased pressure permits less moles of gaseous particles to occur in the reactor could explain the faster evacuation of the nitrogen particles. Bearing in mind the ideal gas law it is understandable that a larger reactor pressure leads to a higher value for the number of moles in the reactor. In turn this leads to a smaller molar flow rate because the partial pressure of the gas components is less effective and the driving force for the flow becomes less significant.

### 15.1.2 Equilibrium loading

The initial value for the equilibrium loading is set to be the same as for the initial actual loading in this model. The actual loading represents the amount of  $CO_2$  that is loaded on to the sorbent at the start of the desorption; in other words it is the total amount of adsorbed  $CO_2$  after the adsorption process. Increasing this value will increase the cyclic capacity of the reactor because the lowest achievable loading values stay the same but the initial values, the maxima, are increased. This is logical because a higher initial loading means that there is more  $CO_2$  attached to the sorbent that can be unloaded for the desorption cycle. This can be seen in Figure 21:

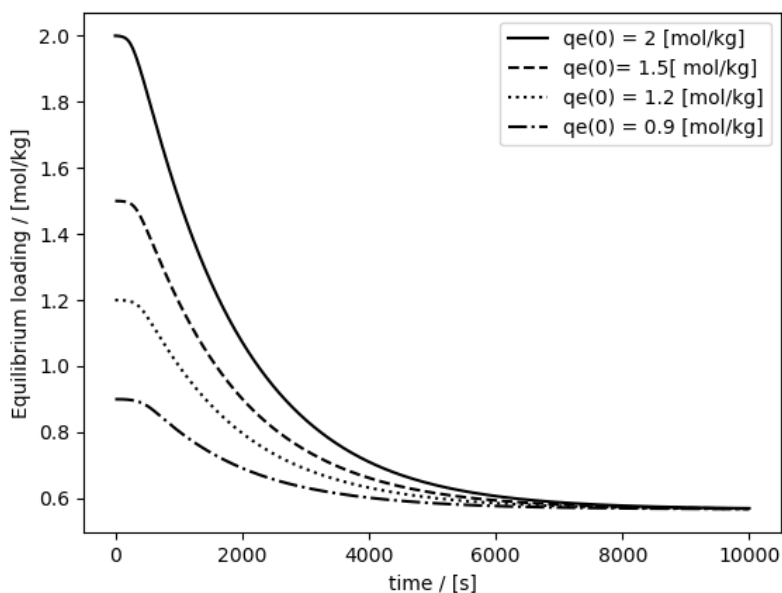


Figure 21: Course of sorbent unloading for different values for initial equilibrium loading of the sorbent as a function of time.

Though larger amounts of  $CO_2$  get desorbed, the time before  $t_{50}$  and  $t_{90}$  are reached stay the same, when the initial loading is increased. This means that the molar flow rate increases when initial loading is increased because more unloading occurs in the same amount of time. Thus the productivity becomes larger if only the initial loading is increased while the other variables are kept the same.

### 15.1.3 Temperature

Changing the heating temperature for this system changes the maximum achievable temperature of the reactor and the components inside. Looking at the isotherm, it can be seen that for the higher operating temperatures, lower values for the equilibrium loading can be achieved and thus more unloading can occur during desorption. This is exactly what happens to the system when the temperature is increased in the model. The total amount of unloaded  $CO_2$  increases when higher reactor temperatures are reached. These elevated temperatures lead to higher molar flow rates and the time it takes for all the  $N_2$  to exit the system decreases. This suggests that it is desirable to heat the reactor to higher temperatures to increase the desorption reaction kinetics.

The heating temperature of the desorption reaction should be considered carefully as the temperature of the system and the equilibrium loading are closely related, as is shown with the isotherm. The starting temperature for this model is 25°C and this will always be considered to be the starting point for the desorption. At different initial loading values, unloading starts at different temperatures. This means that for low loading values, high temperatures are needed to start the desorption process. For any given temperature, there is a maximum capacity when keeping the pressure constant, this limit is the value for the equilibrium loading that determines the maximum achievable desorption. At higher initial loading, more unloading can be achieved because there is more CO<sub>2</sub> on the sorbent, but when the temperature is kept constant there will always be the same amount of CO<sub>2</sub> left behind on the sorbent.

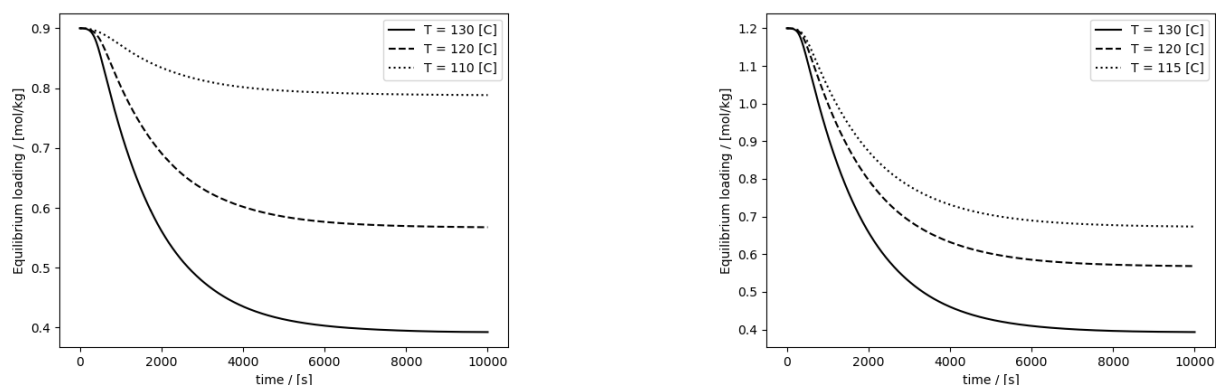


Figure 22: Sorbent unloading shown as a function of time for different values of the maximum temperature in the reactor for two different initial loading values. Unloading is shown systems with an initial sorbent loading of 0.9 and 1.2 mol/kg.

Keeping all the values constant and increasing the heating temperature, causes the minimum value of the  $q_e$  to decrease. At lower values for equilibrium loading, the driving force increases for the unloading reaction. When the loading of the reactor is 0.9 mol/kg and the heating temperature has a maximum of 100 °C then the line is constant for the entire reaction. For this situation, the temperature is not high enough to create a driving force between the minimum achievable value of the equilibrium loading. Repeating the exact process but for a reactor where initially there is a loading of 1.2 mol/kg shows that more desorption can be achieved for the same  $T$ , this becomes clear from Figure 22.

Another important observation is that lower temperatures are achieved faster than higher maximum reactor temperatures for this system where uniform heating has been assumed. In this case, more energy is needed for the system to achieve higher temperatures, first of all due to the fact that higher temperatures require more energy consumption but also because higher temperatures take longer to achieve. These energy requirements make it crucial to make a good trade-off between the highest reactor temperature and the duration of the regeneration, depending on the highest loading value that can be achieved by the adsorption reaction.

The last observations that can be made is that for the varying temperature limits, higher temperatures achieve higher molar flow rates than at lower temperatures. This is to be expected because more unloading occurs at higher temperatures, while it happens within the same time frame. Also the maximum amount of moles in the gas-phase increases slightly at lower temperatures, though it takes longer for all the N<sub>2</sub> to be pushed out of the reactor.

#### 15.1.4 Kinetic rate constant

The kinetic constant is a tricky variable because it is a simplification of a complicated set of equations that determine the rate of the reaction. However for simplicity this set of equations can be written as a constant that can be used in the model to describe the desorption system. Diving deep into the exact meaning of this parameter is beyond the scope of this thesis but the constant can be analysed in the model as it changes the behaviour for different values. The kinetic constant is a simplification of the rate of the reaction mechanism between the CO<sub>2</sub>

in adsorbed and gaseous phase, so it is expected that a higher value for  $k$  leads to a faster reaction of the system.

Changing the value for this simplified  $k$  does not affect the cyclic capacity or loading values. This is logical because  $k$  is a rate constant which influences the speed of the reaction rather than its capacity. The amount of unloading does not change for lower or higher values of  $k$ , however the time it takes to achieve  $t_{50}$  or  $t_{90}$  increases significantly when  $k$  is decreased. The same amount of unloading occurs in a shorter time period which means that the molar flow rate is higher and the productivity of the system for higher values of  $k$ .

Looking at Figure 23, the different slopes for the loading and actual loading for different values of the kinetic rate constant can be observed and this shows that both slopes differ considerably for the varying value of  $k$ . For lower values of the simplified constant  $k$ , a larger difference between the equilibrium and actual loading occurs and a slower reaction takes place. Larger values of  $k$  lead to steeper curves with faster kinetics, though the amount of unloading stays the same. Higher values for  $k$  are desirable, however it is important to use a realistic value for  $k$  because unlike other variables, this cannot be simply be changed by adding machinery like a pumps, heaters, building a bigger reactor, etc. The  $k$  is dependent on the chemical reaction between the sorbent and the adsorbable particles and this must be determined experimentally and should be investigated more in depth.

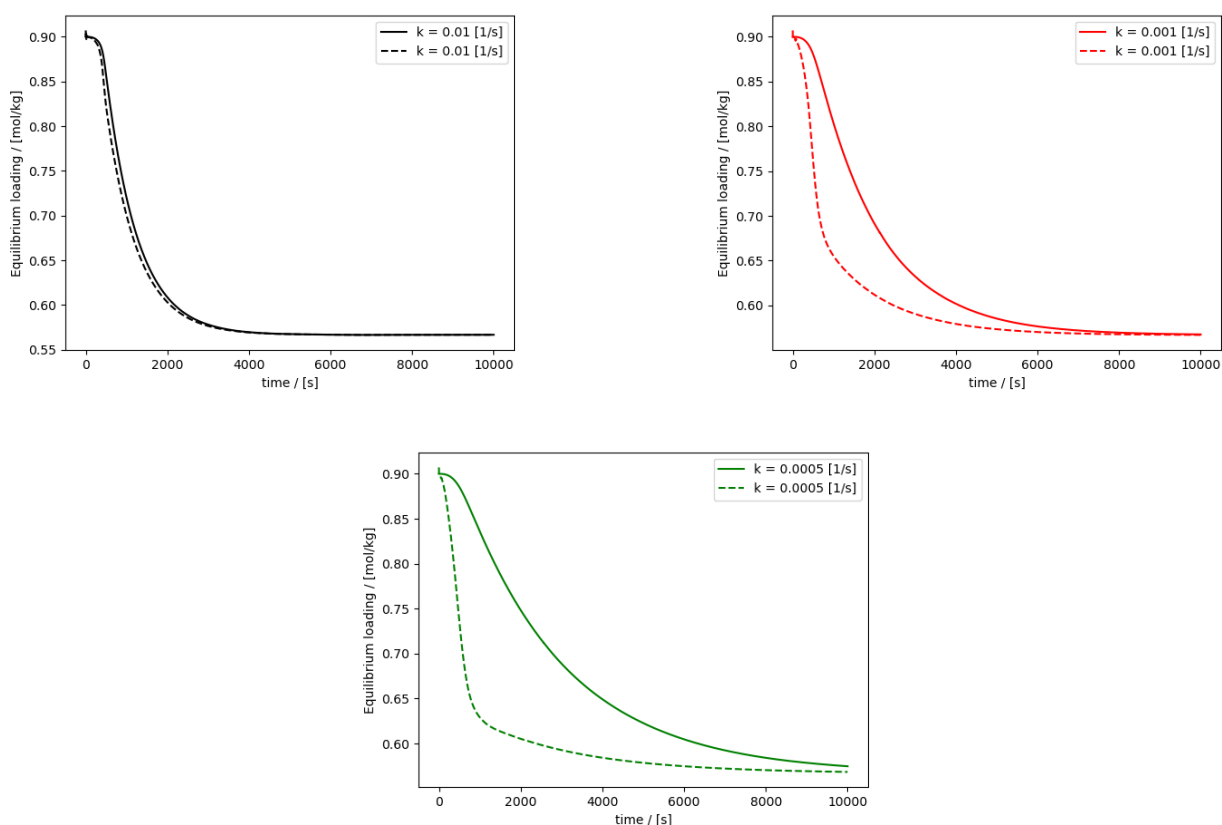


Figure 23: Slopes of the equilibrium loading and actual loading for different values of the kinetic rate constant ( $k$ ) as a function of time. The different figures show the course of these slopes for the values of  $k = 0.01$ ,  $k = 0.001$  and  $k = 0.0005$  respectively.

### 15.1.5 Area of heating

Another important variable is the heating area, which should also be estimated for a realistic value. In this model, the assumption is made that there is no heat loss from the system to the environment and all the components in the reactor are heated uniformly. Also the assumption is made that the reactor is heated by heating tubes that run through the reactor. These heating tubes can heat the system from the inside of the reactor. The reactor is modelled with a short length and a wide diameter, so there would realistically be room for the heating tubes running through the reactor. The tubes are assumed to have the same length as the reactor and the heating area can be determined by the number of tubes and an estimated value for the amount of volume

that they occupy. From these values, the radius and the heating area of a single tube are determined and thus the total area of heating.

To determine the total volume of the heating tubes, the assumption has been made that they take up 10% of the total reactor volume; however this value could be changed to fit the system. Consequently the heating area is changed by increasing or decreasing the number of heating tubes. This is the easiest way to increase the heating area while keeping the total volume constant. In the following table, the values are given for the reactor and heating tube dimensions when the number of heating tubes is changed. It should be mentioned that all the reactor dimensions stay the same as for the total volume of the heating tubes. While the heating tube volume stays the same at 10% of the total reactor volume and the length of the heating tubes, but the number of heating tubes changes, the tube dimensions change and the total heating area varies.

Table 3: Geometry of the reactor and the dimensions of the heating tubes inside the reactor as a function of the number of heating tubes for the system.

$n_{\text{tubes}}$	2	10	16	-	Source
$L_R$	0.082	0.082	0.082	m	[2]
$D_R$	0.5	0.5	0.5	m	Assumption
$V_R$	0.0545	0.0545	0.0545	$m^3$	$\frac{L_R \cdot \pi \cdot D_R^2}{4}$
$L_{\text{tube}}$	$L_R$	$L_R$	$L_R$	m	Assumption
$X_{\text{tubes}}$	10	10	10	%	Assumption
$V_{\text{tubes}}$	0.01675	0.01675	0.01675	$m^3$	$V_R \cdot X_{\text{tubes}}$
$V_{\text{tube}}$	0.00081	0.00016	0.00010	$m^3$	$V_{\text{tubes}} / X_{\text{tubes}}$
$R_{\text{tube}}$	0.056	0.025	0.0198	m	$V_{\text{tube}} / (\pi \cdot R_{\text{tube}}^2)$
$A_{\text{tube}}$	0.0288	0.0128	0.0102	$m^2$	$2 \cdot \pi \cdot R_{\text{tube}} \cdot L_{\text{tube}}$
$A_{\text{tubes}}$	0.0576	0.1287	0.1628	$m^2$	$R \cdot V_{\text{tubes}} \cdot n_{\text{tubes}}$

Increasing the number of heating tubes, while keeping the total tube volume constant, increases the heating contact area. This has no influence on the capacity of the system, so the amount of unloading stays the same. The biggest impact of the contact area is that the reactor is heated faster. The molar flow increases and this would improve the overall productivity. Also it stands to reason that when the dimensions of the reactor change, the heating area changes appropriately.

### 15.1.6 Heat transfer coefficient

The heat transfer coefficient determines the rate at which the system is heated, taking into account the conductive and convective heating rates. Generally this heat transfer coefficient is related to all the thermal resistances and depends on the geometry of the system. For this system, however, it has been assumed that the reactor heats uniformly and a generally used heating coefficient for tube and shell heat transfer systems has been implemented. The values chosen for the increased and decreased heat transfer coefficient are chosen to be in the realistic shell and heat transfer coefficient range.



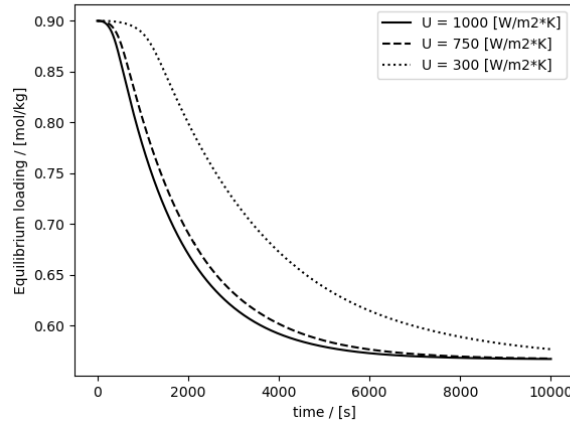


Figure 24: Unloading of the sorbent as a function of time for different values of the heat transfer coefficient.

The heat transfer coefficient has almost no influence on the capacity of the system as the total amount of unloading stays the same. Increasing the heat transfer coefficient results in faster heating of the reactor and thus 50% and 90% unloading is achieved more rapidly. For increased heat transfer the molar flow rate increases and its peak is higher. The time it takes for the nitrogen to flow out of the system is shorter, which also follows from both the mass and the energy balance when  $U$  is increased. From this it logically follows that the productivity of the system decreases or increases when the heat transfer coefficient is lower or higher respectively.

## 15.2 Testing the model

To determine the validity of the model, it is desirable to try to reproduce the results of other literature to compare the results. The paper of Young et al. [21] is one of the few papers describing DAC technology that models the desorption reaction of Lewatit based DAC system. It focuses on the water-CO<sub>2</sub> isotherm models but considers a pure CO<sub>2</sub> isotherm also. Their reactor is modeled as a short reactor with a wide diameter, with dimensions of  $L=1$  cm and  $D=10$  cm and this reactor is used to analyse what happens for the different isotherms. The four different co-adsorption isotherm models that were considered in this paper are pure a CO<sub>2</sub> isotherm model, the Mechanistic model, the WADST model and of another paper presented by Stampi-Bombelli et al. [22]. The parameters that have been analysed with these different isotherms are the CO<sub>2</sub> loading, H<sub>2</sub>O loading, CO<sub>2</sub> mole fraction in the gas phase, relative humidity, temperature, and pressure.

When the values of Young are used in our model, to try to reproduce their results for the no co-adsorption isotherm, the model shows that the system is unsolvable for these values. The reason for this error is that in this thesis, the model assumes a dry system where no water has adsorbed on to the sorbent while the paper by Young water has been co-adsorbed onto the sorbent. For a system where no water co-adsorption has taken place and the sorbent is exclusively loaded with CO<sub>2</sub>, the Toth isotherm expects no desorption at a temperature of 373 K and  $q_{eA} = 1.0$  (mol/kg) considering Figure 26. At this value for the equilibrium loading, the lowest temperature that leads to a stable unloading is at 378 K. As can be seen unloading does occur, though it is an incredibly small amount as the lowest value for the  $q_e$  that can be achieved for this temperature is approximately 0.915.

The graphs presented by Young et al. show what happens to the loading for multiple isotherms including the pure CO<sub>2</sub>-isotherm for a situation that is not completely free of water as is assumed in this thesis' model. The paper by Young presents two water co-adsorption isotherms and one dry Toth isotherm, The dry isotherm is used to make a comparison to the model developed in this thesis. Using the values from Young's paper to simulate their results with the H<sub>2</sub>O-free model that is designed in this thesis, does not give accurate results. The values used in the paper by Young fail do not provide a good comparison because these values create no driving force for the desorption reaction for a H<sub>2</sub>O-free Toth isotherm model.

When implementing the values as proposed by Young for a H<sub>2</sub>O-free model, with a temperature range of [70 - 100]°C, a pressure of 0.25 bars and an equilibrium loading of 1.0 (mol · kg<sup>-1</sup>), no unloading occurs. The reason for this is that the Toth isotherm proposed by Bos, shows that the combination of these values for pressure and

temperature, do not coincide with an isotherm that creates a driving force at an equilibrium loading of 1.0. For this reason, there is no accurate way to apply this model to analyse the results as provided by Young unless humidity and water loading can be accounted for with the model.

The paper of Young shows us that water adsorption during the DAC process has a significant influence on the desorption process and this effect should be investigated further. During adsorption, much of the sorbent will be filled with H<sub>2</sub>O molecules and this will, in turn, influence the entire system. The amount of H<sub>2</sub>O that is adsorbed depends on the relative humidity of the air that enters the system and will affect the productivity and final design of a realistic DAC system.

### 15.3 Case Study

In the attempt to design an optimal desorption system with the developed model, a case study can be devised to compare the optimised values for different desorption situations realistically. Though some assumptions and simplifications have been used during the development of this model, it can still produce results that are viable and scientifically relevant for the overall desorption analysis. During the model verification, multiple reactor variables were analysed to determine how these reactor characteristics individually influence the entire system. Combining this information with what is known from literature about existing desorption systems, the model can be used to design an optimal desorption reactor. In Table 4, the default values that are used for the desorption model are presented.

Table 4: Desorption systems default values

Variables			
Parameter	Default value	Unit	Equation
$L_R$	0.081954	m	Reactor length [2]
$D_R$	0.5	m	Diameter
$A_R$	0.1963	m	Reactor cross-sectional area
$V_R$	0.0161	m <sup>3</sup>	Volume reactor
$V_g$	$6.115 \cdot 10^{-3}$	m <sup>3</sup>	Volume gaseous part of reactor
$V_s$	0.01	m <sup>3</sup>	Volume sorbent bed reactor
$m_s$	8.78	kg	Mass of sorbent
$n_{A,0}$	$6 \cdot 10^{-5}$	mol	Initial amount of gaseous moles CO <sub>2</sub>
$n_{t,0}$	0.0617	mol	Initial total amount of gaseous moles
$q_{A,0}$	0.9	mol · kg <sup>-1</sup>	Initial sorbent loading
$qe_0$	0.9	mol · kg <sup>-1</sup>	Initial equilibrium loading
$T_{des}$	393	L	Max heating temperature
$P_{vac}$	0.25	bar	Desorption vacuum pressure
$k$	0.001	s <sup>-1</sup>	Kinetic rate constant
$A_{tube}$	0.0129	m <sup>2</sup>	Total contact area of single heating tube
$A$	0.129	m <sup>2</sup>	Total contact area
$V_{tube}$	$0.161 \cdot 10^{-3}$	m <sup>3</sup>	Total volume of a single heating tube
$L_{tube}$	0.081954	m	Length of heating tubes
$R_{tube}$	0.025	m	Radius of heating tubes
$n_{tube}$	10	-	Number of heating tubes
$X_{tubes}$	10	%	Percent volume of heating tubes
$U$	750	W · m <sup>-2</sup> · K <sup>-1</sup>	Overall heat transfer coefficient

During this case study some parameters are constant and others are the variables that should be changed to achieve the optimal design. For instance, the desorption reaction always starts at room temperature but the maximum heating temperature can be varied to find the limit for the reaction. The desorption reaction is always dependent on the capacity of the adsorption process, which means that the adsorption reaction determines the initial sorbent loading, around which the desorption should be designed. The reaction starts at room temperature as is assumed for adsorption, but the starting pressure is not at atmospheric conditions because the system is depressurised before desorption. The default conditions that are used during the model verification can be represented by Figure 25.

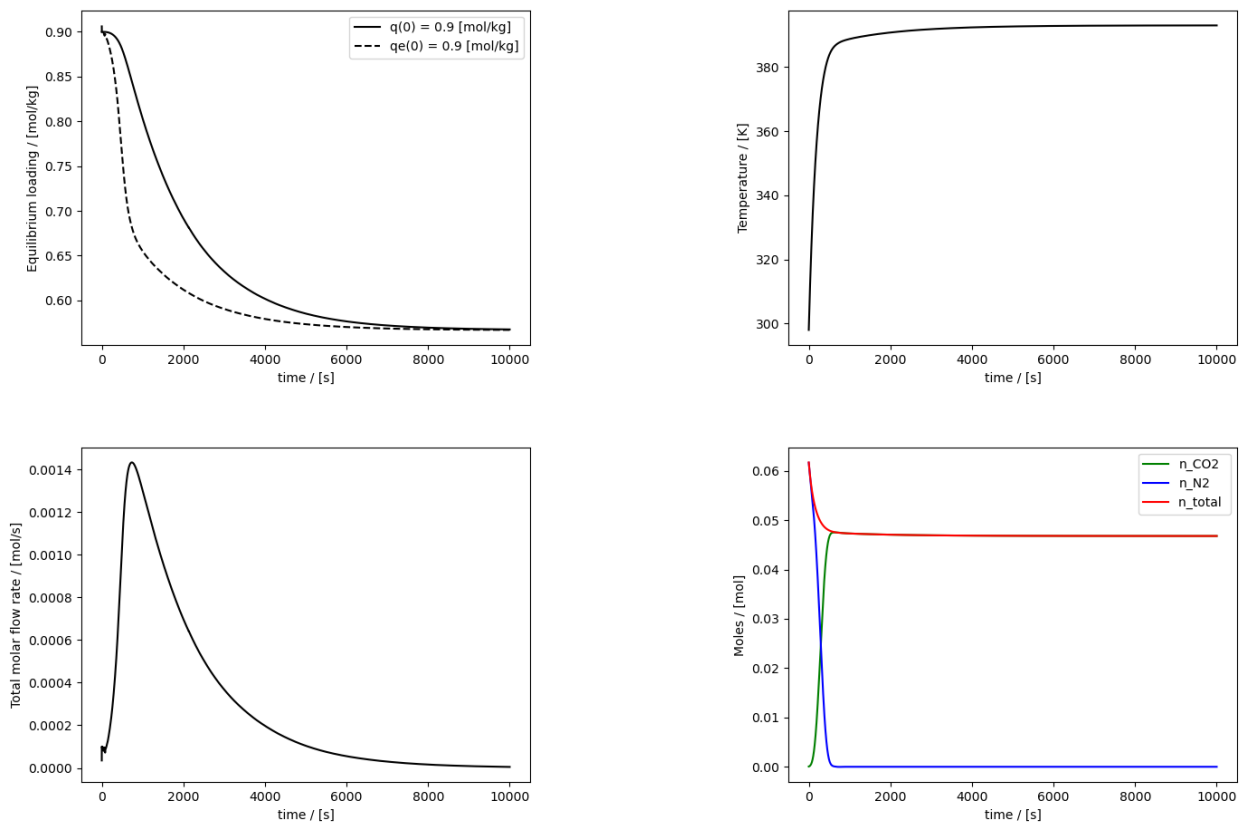


Figure 25: The case study figures showing the course of the different parameters as a function of time for the default conditions equilibrium loading, temperature, molar flow rate and number of moles respectively.

To make the best possible assumptions for the variables of the system it is important to know the dimensions of the reactor. The size of the reactor determines the efficiency of heating as well as the amount of heating surface area. For larger reactors, more CO<sub>2</sub> can be extracted per cycle, but it becomes more energy intensive to heat the entire reactor sufficiently. Designing a DAC reactor for the sorbent Lewatit, which is a dense sorbent, it is desirable to have a short reactor length. Designing a reactor with a longer length will not influence the model as the pressure drop is negligible, however it is known that for such systems the pressure drop becomes significant for longer reactors. The reactor will be modeled as a flat 'disc' reactor, with a short length and a relatively wide diameter. The reactor length that is used is the reactor length used in the experiments of Surati [2] and a diameter of 50 cm. With these variables set to these values, it will be easier to determine the optimal values for the other parameters.

As mentioned, the initial loading for the desorption is determined by the effectiveness of the adsorption reaction. A system that operates with air containing 400 ppm CO<sub>2</sub> is assumed to achieve an adsorption loading of  $q_{eA,(ads)} = 0.9$  (mol/kg). It was shown in the work by Surati [2] that if the experiment was repeated for a situation with air containing 2000 ppm CO<sub>2</sub>, a loading of  $q_{eA,(ads)} = 1.4$  (mol/kg) was achieved. Comparing the two different cases could provide interesting insights for the optimisation design.

During the verification process, it was found that lower vacuum pressure improves the desorption reaction and more unloading can be achieved. The pressure inside this DAC system is at 1 bar before the system is depressurised for desorption. Assuming that the maximum vacuum capability of a vacuum pump is a factor of 4, the minimum pressure that can be achieved with one vacuum pump is 0.25 bar. For the system to achieve lower vacuum pressure, before the desorption reaction starts, more vacuum pumps need to be implemented for this case study, it will be assumed that only one vacuum pump will be used for this system and the minimum pressure inside the system is 0.25 bar, the lowest value that can be achieved by a single gas pump for an initial pressure of 1 bar.

Lewatit is an amine based sorbent that chemically binds with the CO<sub>2</sub> in air. To extract the CO<sub>2</sub> molecules

from the sorbent, the reactor needs to be heated sufficiently to be able to collect these molecules. At elevated temperatures more desorption is possible, however the model does not take into account the amine degradation that would occur in an actual DAC system. Elevated temperatures increase the cyclic capacity of the desorption process, however the sorbent will degrade at a certain temperature. Therefore the maximum heating temperature is set to be  $T_{\text{des}} = 393 \text{ K}$  with the assumption that higher temperatures are not possible for a Lewatit based DAC system.

Another important variable is the heating area, which should also be given a realistic value. In this model, the assumption is made that there is no heat loss from the system and all the components in the reactor are heated uniformly. Higher heating contact area leads to faster heating and the productivity of the system increases. For this system, the heating area could be thought of as heating tubes inside the reactor that can heat the system from the inside. This is a realistic reactor heating system and modelling the reactor as a flat disc, it can be assumed that there is room inside the reactor for heating tubes to exist. Assuming that these tubes have the same length as the reactor, the number of tubes and the amount of volume that they occupy can be set. From these values, the radius and the heating area of the tubes can be calculated from the corresponding geometry chosen for the model. The heating area can be expanded by increasing the number of heating tubes and by increasing the percentage of volume that the heating tubes occupy.

The kinetic rate constant  $k$  is a term that determines the rate of the reaction, where higher values for  $k$  lead to a faster reaction. This means that higher values for  $k$  are desirable, however this value is based on the reaction kinetics and is determined experimentally. This means that a realistic value for  $k$  must be determined for the reaction and this will be assumed to be the correct kinetic rate constant for this type of desorption reaction at  $k = 0.001 \text{ s}^{-1}$ .

As with the kinetic rate constant, the overall heat transfer reaction only influences the rate of the reaction and higher values increase the speed of the overall desorption system. The overall heat transfer reaction depends on the heating method and the efficiency of the heating system. For the desorption, heating is done by heating tubes that run through the reactor and have been assumed to achieve heating values similar to that of shell and tube heating systems. These type of systems are widely used and can achieve heat transfer coefficients of approximately  $U = 1000 \text{ W}/(\text{m}^2\text{K})$ .

## 16 Results desorption

The desorption model is created as a CSTR to simulate a VTSA desorption reaction of a chemical amine based DAC system. Though there is little information available for such systems, the produced model provides reasonable results. The models parameters and its equations that describe the system are based on the literature and have been carefully derived based on rational assumptions and available data.

### 16.1 Model justification

#### 16.1.1 System

During the design of the model, the assumption was made to consider the system as a CSTR that describes a desorption reactor using VTSA instead of a purge gas for unloading the CO<sub>2</sub>. The equations that describe this system are independent of the spatial domain and there is no inflow into the system, informing the decision to model the system as a CSTR viable. The reactor system desorbs mainly due to heating and the outflow is caused by the varying partial pressure as the unloading of the sorbent occurs. A system that is described by a PFR is dependent on the spatial propagation of its bulk, which is important in the adsorption system, but this is not the case for a VTSA desorption system. If a purge gas had been used to unload the sorbent, then the spatial domain might have played a role as the gas must be inserted into the system at one end and would flow out at a different point. In the case where the system could be sensitive to the systems geometry and the flow propagation, then a PFR could be considered for the desorption, however this is not the case for this VTSA desorption system.

Another important characteristic of the CSTR is that it assumes ideal mixing between the gaseous components. For this case, the mixing is between the carbon dioxide and nitrogen which does not pose a problem. The actual situation would present a reactor initially filled with carbon-poor air, and for this situation, a CSTR would still be appropriate as air is considered an ideal gas. A major difficulty occurs when water co-adsorption is taken into account for the DAC system. Though Young [21] predict that a system where water co-adsorption occurs has larger productivity, the system become more complex and the appropriate addition must be added to the system to model such a system properly.

#### 16.1.2 Python script

The desorption model has been modelled in Python and is programmed to find the solutions for the differential equations with a reliable ODE solver called *scipy.integrate.solve\_ivp*. During the first attempt to create the desorption model, the 'SciPy' solver was used with the 'RK45' method. This method is a built-in solver that uses the traditional Runge-Kutta 4<sup>th</sup>-order method, however this showed large instabilities in the resulting figures. Subsequently this method was changed to the 'LSODA' method to solve the instabilities, which provides better results with greatly reduced instabilities. The 'LSODA' method is a solver for ODEs that automatically switches between stiff and non-stiff methods. This means that the solver method determines when the problem is stiff or not and it automatically chooses the appropriate method. The solver always starts with the non-stiff method, where a stiff equation is a differential equation for which certain numerical methods for solving the equation are numerically unstable, unless the step size is taken to be extremely small. The main idea is that the equation includes some terms that can lead to rapid variation in the solution. This method proved to be considerably better, but not all instabilities are prevented as can be seen when considering the number of gaseous moles in the system. During desorption the reactor should become completely filled with CO<sub>2(g)</sub> once all the nitrogen has left the system. This should mean that the total number of moles in the system should become equal to the moles of CO<sub>2(g)</sub> in the system. Unfortunately the value  $n_A$  and  $n_t$  are not equal and therefore the value for  $n_B$  in the system, that should be zero from the moment that all the nitrogen has left the system, is close to zero but not exactly zero. These remaining instabilities can be a result of the inaccuracy of the solver and the fact that no boundary conditions can be set for these solvers.

### 16.2 Case study results

The model is used to determine the consequences of changing the different parameter values that are important for the reactor design of a desorption system. Though some results might appear to be straightforward, it is useful to have a model that can predict what happens for a complete system. The overall speed of the reaction is desired to be high so the operation time of equipment decreases for better efficiency and to achieve a less energy and cost intensive system. The total time before enough unloading has occurred partly determines the productivity of the reactor. The kinetic rate constant determines the overall speed of the reaction and it

is desirable to design a system where the  $k$  is large. Other variables that influence the reaction time of the reactor are the overall heat transfer coefficient and the area of heating; for instance, they can accelerate the heating speed of the system and consequently the overall time needed for the desorption to take place. The volume of the reactor also has a big influence on the productivity of the reactor since the time taken to heat the system increases significantly as the volume increases, which in turn influences the productivity. The other most important term to determine the efficiency and productivity of the system is the capacity that can be achieved, where the pressure and temperature are the most important values determining the amount of unloading possible for a desorption system. Together, these parameters determine the isotherm of a given system and the total potential of desorption. Increasing the temperature and decreasing the temperature both contribute to a system that can achieve lower equilibrium capacity and thus higher total unloading of the system, depending on the amount of initial actual loading when the desorption process starts.

### 16.2.1 Productivity

Productivity is an interesting term that can be used to describe the overall efficiency of a system. For the desorption case, 'productivity' for a given capacity is a term that describes the amount of CO<sub>2</sub> that has been desorbed from the sorbent, depending on the geometry and speed of reactor system. The units of productivity is mass per hour per volume of reactor ( $\text{kg}_{\text{CO}_2} \cdot \text{hr}^{-1} \cdot \text{m}_R^{-3}$ ):

$$Prod = \frac{m}{hr \cdot V}$$

The productivity term is used to show the overall effectiveness of the process, taking into account the amount CO<sub>2</sub> that gets desorbed, the time it takes to do this in and the overall size of the reactor. Higher productivity suggests that the system is better and can achieve better values. Generally the productivity is taken to be either 50% or 90% of the total reaction in determining the best system design:

$$Prod_{50} = \frac{m_{\text{CO}_2, \text{des}, 50}}{hr_{t_{50}} \cdot V_R} \quad (\text{at } 50\% \text{ unloading})$$

$$Prod_{90} = \frac{m_{\text{CO}_2, \text{des}, 90}}{hr_{t_{90}} \cdot V_R} \quad (\text{at } 90\% \text{ unloading})$$

Typically the productivity is higher at 50% unloading than for higher unloading percentages. This is due to the fact that the reaction starts fast and slows down for higher unloading percentages. It becomes increasingly hard to fully desorb the system for the last few percent and the graph flattens out at the end. The productivity can be used to compare different desorption systems easily as the desorption term is a function of the important characteristics that determine how good the desorption design works. In Table 5 all the results are shown for the case study, which shows a system with 400 ppm CO<sub>2</sub> in air which has an initial loading of 0.9 and another system with 2000 ppm CO<sub>2</sub> in air which has an initial loading of 1.4 ( $\text{mol} \cdot \text{kg}^{-1}$ ). All the different variables shown in the table result from the default reactor design and these results determine the overall productivity of the two different systems. As mentioned, both systems show a higher productivity for the system at  $t_{50}$  than  $t_{90}$  as is expected.

Another important result that is not considered during the calculation of the system productivity is the time it takes until all the N<sub>2</sub> has exited the reactor ( $t_{B=0}$ ). This term cannot be neglected during the design of a desorption system, because this term determines when the actual extraction of pure CO<sub>2</sub> can commence. The pure stream of CO<sub>2</sub> can't be extracted until, in this case, enough N<sub>2</sub> has flowed out of the system. So until this has occurred, none of the extracted CO<sub>2</sub> has actually been captured from the air.

The model has been constructed as a flexible code that can easily be changed or expanded with extra information or for other similar desorption type systems. This model could easily be changed to fit a system that can simulate another type of amine adsorbent, given that enough information is available.

Table 5: Resulting values from the two different situations as described for the case study, where 400 ppm CO<sub>2</sub> is assumed a loading of 0.9 mol/kg and 2000 ppm CO<sub>2</sub> is assumed a loading of 1.4 mol/kg

Results				
Parameter	Value	Value	Unit	Equation
	400	2000	ppm	PPM of CO <sub>2</sub> in processed air
$q_{A,max}$	0.9	1.4	mol · kg <sup>-1</sup>	Maximum actual loading
$m_{des,50}$	0.064	0.161	kg	Total unloaded CO <sub>2</sub> at 50%
$m_{des,90}$	0.116	0.289	kg	Total unloaded CO <sub>2</sub> at 90%
$M_{t,max}$	$1.433 \cdot 10^{-3}$	$3.585 \cdot 10^{-3}$	mol · s <sup>-1</sup>	Maximum molar flow rate
$n_{A,cap,50}$	1.461	3.654	mol	Number of moles CO <sub>2</sub> unloaded at 50%
$n_{A,cap,90}$	2.630	6.576	mol	Number of moles CO <sub>2</sub> unloaded at 90%
$n_{A,max}$	0.0475	0.0493	mol	Maximum number of gaseous moles CO <sub>2</sub> in the reactor
$n_{t,0}$	0.0617	0.0617	mol	Initial amount of gaseous moles in the reactor
$n_{t,M}$	0.0468	0.0468	mol	Final amount of gaseous moles in the reactor
$q_{A,min}$	0.568	0.569	mol · kg <sup>-1</sup>	Minimum actual loading
$q_{cyc,50}$	0.166	0.416	mol · kg <sup>-1</sup>	Cyclic capacity at 50% unloading
$q_{cyc,90}$	0.3	0.749	mol · kg <sup>-1</sup>	Cyclic capacity at 90% unloading
$q_{e,max}$	0.9	1.399	mol · kg <sup>-1</sup>	Maximum equilibrium loading
$q_{e,min}$	0.567	0.568	mol · kg <sup>-1</sup>	Minimum equilibrium loading
$t_{50}$	0.43	0.41	hrs	Time until 50% unloading
$t_{90}$	1.13	1.11	hrs	Time until 90% unloading
$t_{A>B}$	294.4	209.3	s	Time until more CO <sub>2(g)</sub> exists in reactor than N <sub>2(g)</sub>
$t_{B=0}$	679.6	526.3	s	Time until more no N <sub>2(g)</sub> exists in reactor than
$t(T_{max-5})$	807.7	2097.8	s	Seconds until (T <sub>max</sub> -5) is reached [388K]
$X_{des,50}$	18.49	29.72	%	Percentage of unloaded CO <sub>2</sub> at 50%
$X_{des,90}$	33.29	53.5	%	Percentage of unloaded CO <sub>2</sub> at 90%
$prod_{des,50}$	9.28	24.25	kg · hrs <sup>-1</sup> · m <sup>-3</sup>	Productivity of desorption reactor at 50% unloading
$prod_{des,90}$	6.366	16.16	kg · hrs <sup>-1</sup> · m <sup>-3</sup>	Productivity of desorption reactor at 90% unloading

## 17 Conclusion

The objective of the desorption model was to produce a model that can both describe the reaction process and simulate the process for varying parameters. The simulations created by this model give results that are instinctively correct, verification showed that the extremes of the system follow the expected results. The results help give insight into the overall process and can be used to help in the design of a desorption reactor. The model is a good first step towards the design of a complete desorption reactor design. Expanding this model with additional knowledge and more complete data will lead to an even better and more accurate model.

The goal of producing a good model that works well based on the assumptions and limited data that was available has been achieved. This model is a good first attempt at predicting the general desorption kinetics for a Lewatit based DAC system. Expanding the model further with additional experimental data and more in-depth literature will help specify this model to produce even more accurate data and better understanding of values that have been considered here as simplified constants e.g. the kinetic rate constant. Furthermore it will be interesting to be able to add in factors such as humidity and water co-adsorption in this model in the future. However, this model still gives a good understanding of a general desorption system and can successfully be used to predict the effect of various system parameters for the reactor's design.

Furthermore, the model has been used to analyse the different important design parameters of a desorption system and to predict what should be considered as for optimal design criteria. During the consideration of the design criteria, optimum values have been chosen using the model simulations combined with viable limits for similar systems.

## 18 Recommendations

- To improve the model, it would be desirable to be able to calculate or estimate the total energy demands of the system. Increasing the temperature is desirable but costs more energy, especially for bigger reactor systems. It would therefore be interesting to model the energy demands in order to make a trade-off between the reactor characteristics and the energy that the system would require
- Taking into account the energy consumption, an estimation should be made as to the best possible point in the desorption process at which to stop unloading while achieving the maximum possible CO<sub>2</sub> extraction. As the unloading becomes harder in the last part of the desorption reaction, it should be determined at what point the best balance can be found between CO<sub>2</sub> unloading and energy consumption, in order to achieve the highest potential productivity and the most CO<sub>2</sub> extraction with the system.
- Heat losses for a non-adiabatic system and a non-uniform heating could be considered. The reactor will lose heat to its environment while heated and this will lead to an increased energy demand and a slower overall heating of the system. Also it has been assumed that the reactor heats uniformly for all the components in the reactor, whilst in reality the different components will heat non-uniformly.
- The desorption reaction of the sorbent is an endothermic reaction and so will extract some heat from the system in order for the unloading reaction to take place. A calculation should be done to determine if this heat consumption will have an effect on the overall process or that it can be neglected, as has been done for this system.
- It will prove helpful to determine the electricity demand for the compressors before desorption starts. Taking into account the amount of desorption and electricity demand for different pressure values, a better trade-off could be made.
- The value for the kinetic rate constant should be determined experimentally for the desorption process. Furthermore it would be interesting to be able to derive a more in-depth value for this constant. Determining the set of equations, which are simplified by the value  $k$ , could provide the information about what happens inside the (un)loading process. This could help get a better overall understanding of the desorption and how the kinetics change as a result of the systems parameters.
- For this model it has been assumed that relative humidity of the entire system has been zero. The relative humidity will influence the adsorption reaction due to water co-adsorption and the water will be inside the bulk of the reactor during the desorption reaction.
- Water co-adsorption has been ignored during the design of the models; in practise, however this will significantly influence the entire DAC system significantly in an actual DAC system. Water co-adsorption isotherms have been determined by some papers as proposed by Young [21] and this information can help determine the amount of water adsorption. Water will influence the amount of CO<sub>2</sub> that can be adsorbed and desorbed per DAC cycle. Furthermore, the presence of water will increase the complexity of the desorption process as it must be separated from the CO<sub>2</sub> before the gas is extracted as a pure stream of CO<sub>2</sub>.
- The desorption has been modelled as a reactor containing only nitrogen and carbon dioxide. For the actual system, all components of the air inside the reactor should be considered before desorption takes place. All these components need to be removed from the reactor before pure CO<sub>2</sub> can be extracted from the system.
- The model showed some instabilities for both molar flow rate and equilibrium capacity parameters at its first time-step ( $t_0 - t_1$ ) for both molar flow rate and equilibrium capacity parameters. This has been corrected with a "quick-fix" inside the code, but for further model expansion the cause of this instability should be determined and solved. The instability could be a consequence of the steep isotherm curve at the start of the isotherm. The model's solver could have trouble with accurately predicting the first step, leading to this instability.
- Both the LSODA and RK45 method are not completely stable ODE solver methods. Other solving methods could provide better results and more stable solutions for the system.



## 19 Nomenclature desorption

Table 6: Parameters used for the desorption model

Symbol	Value	Unit	Meaning	Source
$A$	-	$[\text{m}^2]$	Total contact area	[-]
$A_R$	-	$[\text{m}]$	Reactor cross-sectional area	[-]
$A_{\text{tube}}$	-	$[\text{m}^2]$	Total contact area of single heating tube	[-]
$b_0$	93	$[\text{bar}^{-1}]$	Toth isotherm parameter	[3]
$c_{p,A,g}$	696.7	$[\text{J} \cdot \text{kg}^{-1} \cdot \text{K}^{-1}]$	Heat capacity coefficient of $\text{CO}_2$ at constant P	[3]
$c_{p,B,g}$	744.3	$[\text{J} \cdot \text{kg}^{-1} \cdot \text{K}^{-1}]$	Heat capacity coefficient of $\text{N}_2$ at constant P	[3]
$c_{v,A,g}$	892.5	$[\text{J} \cdot \text{kg}^{-1} \cdot \text{K}^{-1}]$	Heat capacity coefficient of $\text{CO}_2$ at constant V	[3]
$c_{v,B,g}$	1042	$[\text{J} \cdot \text{kg}^{-1} \cdot \text{K}^{-1}]$	Heat capacity coefficient of $\text{N}_2$ at constant V	[3]
$c_{p,s}$	1580	$[\text{J} \cdot \text{kg}^{-1} \cdot \text{K}^{-1}]$	Heat capacity coefficient of the sorbent at constant P	[19] [3]
$D_R$	-	$[\text{m}]$	Diameter of the reactor	[-]
$\Delta H_{\text{rxn}}$	95300	$[\text{J} \cdot \text{mol}^{-1}]$	Toth isotherm heat of reaction	[3]
$k$	0.001	$[\text{s}^{-1}]$	Kinetic rate constant	[-]
$L_R$	0.081954	$[\text{m}]$	Reactor length	[2]
$L_{\text{tube}}$	-	$[\text{m}]$	Length of heating tubes	[-]
$m_s$	-	$[\text{kg}]$	Mass of sorbent	[-]
$M_{\text{CO}_2}$	0.044009	$[\text{kg} \cdot \text{mol}^{-1}]$	Molar mass $\text{CO}_2$	
$M_{\text{N}_2}$	0.028014	$[\text{kg} \cdot \text{mol}^{-1}]$	Molar mass $\text{N}_2$	
$M_t$	-	$[\text{mol}_g \cdot \text{s}^{-1}]$	Total molar flow rate	[-]
$n_{A,0}$	-	$[\text{mol}]$	Initial amount of gaseous moles $\text{CO}_2$ in reactor	[-]
$n_{B,0}$	-	$[\text{mol}]$	Initial amount of gaseous moles $\text{N}_2$ in reactor	[-]
$n_{t,0}$	-	$[\text{mol}]$	Initial total amount of gaseous moles	[-]
$n_{\text{tube}}$	-	[-]	Number of heating tubes	[-]
$P_{\text{amb}}$	1	$[\text{bar}]$	Ambient pressure	
$P_{\text{vac}}$	-	$[\text{bar}]$	Desorption vacuum pressure	[-]
$prod_{\text{des},50}$	-	$[\text{kg} \cdot \text{hrs}^{-1} \cdot \text{m}^{-3}]$	Productivity of desorption reactor at 50% unloading	[-]
$prod_{\text{des},90}$	-	$[\text{kg} \cdot \text{hrs}^{-1} \cdot \text{m}^{-3}]$	Productivity of desorption reactor at 90% unloading	[-]
$q_{s0}$	3.4	$[\text{mol} \cdot \text{kg}^{-1}]$	Toth isotherm parameter	[3]
$q_{A,0}$	0.9	$[\text{mol} \cdot \text{kg}^{-1}]$	Initial sorbent loading	[-]
$q_{e0}$	0.9	$[\text{mol} \cdot \text{kg}^{-1}]$	Initial equilibrium loading	[-]
$\dot{Q}$	-	$[\text{J} \cdot \text{s}^{-1}]$	Heat transfer rate to or from surroundings	[-]
$R$	8.314	$[\text{J} \cdot \text{mol}^{-1} \cdot \text{K}^{-1}]$	Universal gas constant	
$R_{\text{tube}}$	-	$[\text{m}]$	Radius of heating tubes	[-]
$T_0$	298	$[\text{K}]$	Initial temperature of reactor	[-]
$T_H$	-	$[\text{K}]$	Heating temperature of reactor	[-]
$T_{0,\text{Toth}}$	353.15	$[\text{bar}^{-1}]$		[-]
$t_{h0}$	0.37	[-]	Toth isotherm parameter	[-]
$T$	-	$[\text{K}]$	Temperature of reactor	[-]
$U$	-	$[\text{W} \cdot \text{m}^{-2} \cdot \text{K}^{-1}]$	Overall heat transfer coefficient	[-]
$V_g$	-	$[\text{m}^3]$	Volume gaseous part of reactor	[-]
$V_R$	-	$[\text{m}^3]$	Volume reactor	[-]
$V_s$	-	$[\text{m}^3]$	Volume sorbent bed reactor	[-]
$V_{\text{tube}}$	-	$[\text{m}^3]$	Total volume of a single heating tube	[-]
$\dot{W}$	-	$[\text{J} \cdot \text{s}^{-1}]$	External heating or cooling done on the system	[-]
$X_{\text{tubes}}$	-	$[\%]$	Percent volume of heating tubes	[-]
Greek				
$\alpha$	0.14	[-]	Toth parameter	[3]
$\chi$	0	$[\text{mol}_j \cdot \text{mol}_{\text{tot}}^{-1}]$	Ratio of amount of species j in gas mixture	[3]
$\epsilon_b$	0.38	$[\text{m}_{\text{gas}}^3 \cdot \text{m}_{\text{reac}}^{-3}]$	Bed voidage	[19]
$\epsilon_p$	0.23	$[\text{m}_{\text{gas}}^3 \cdot \text{m}_{\text{bed}}^{-3}]$	Particle voidage	[3]
$\rho_s$	880	$[\text{kg} \cdot \text{m}^{-3}]$	Sorbent density	

# Appendices

## Appendix A. [Equations]

### Toth isotherm

$$q_e = \frac{q_s b P_{CO_2}}{(1 + (b P_{CO_2})^{t_h})^{\frac{1}{t_h}}} \quad (17)$$

$$q_s = q_{s0} \cdot \exp(\chi(1 - \frac{T}{T_0})) \quad (18)$$

$$b = b_0 \cdot \exp(\frac{\Delta H_0}{RT_0}(\frac{T_0}{T} - 1)) \quad (19)$$

$$t_h = t_{h0} + \alpha(1 - \frac{T}{T_0}) \quad (20)$$

$$P_A = \frac{n_A \cdot R \cdot T}{V}$$

$$= C_A \cdot R \cdot T$$

$$n_{A,0} = \frac{100000 \cdot q_{e_{A,0}} \cdot V_g \cdot \exp(\frac{\ln(-(-1 + \exp(\ln(\frac{q_{e_{A,0}}}{q_{s,0}}) \cdot t_h))^{-1})}{t_h})}{(q_{s,0} \cdot b \cdot R \cdot T_0)}$$

## Appendix B. [Tables]

Table 8: Toth isotherm parameters

Symbol	Veneman et al. [17] Parameter set A	Bos[3] Parameter set B	Unit
$q_{s0}$	3.40	3.40	$[mol \cdot kg^{-1}]$
$\chi$	0	0	$[-]$
$T_0$	353.15	353.15	$[bar^{-1}]$
$b_0$	408.84	93.0	$[bar^{-1}]$
$\Delta H_0$	86.7	95.3	$[kJ \cdot mol^{-1}]$
$t_{h0}$	0.30	0.37	$[-]$
$\alpha$	0.14	0.33	$[-]$

Table 9: Adsorption verification table

Symbol	Value	Unit	Description
General			
$\epsilon_p$	0.23	$m_g^3 \cdot m_s^{-3}$	Sorbent particle voidage inside the sorbent material
$\epsilon_b$	0.38	$m_g^3 \cdot m_R^{-3}$	Sorbent bed voidage within the entire reactor
$\rho_{CO_2}$	1.795	$kg \cdot m^{-3}$	Density of $CO_2$ at room temperature
$\rho_{p,lit}$	880	$kg \cdot m^{-3}$	General density of Lewatit from literature
$M_{CO_2}$	0.04401	$kg \cdot mol^{-1}$	Molar mass of $CO_2$
$C_{2000}$	2000	ppm	Concentration of treated air with $CO_2$ of 2000 ppm
$C_{in}$	0.08157	$mol \cdot m^{-3}$	Concentration of $CO_2$ at experimental conditions
Experimental			
	[2]		
$L_R$	0.08195	m	Height of the reactor bed
$D_R$	0.03	m	Diameter of the reactor bed
$A_R$	$0.71 \cdot 10^{-3}$	$m^2$	Cross-sectional area of the reactor
$A_g$	$0.27 \cdot 10^{-3}$	$m^2$	Cross-sectional bed voidage area of the reactor
$V_R$	$5.79 \cdot 10^{-5}$	$m^3$	Volume of the reactor
$\dot{V}$	4000	ml · min	Flow rate through the reactor in ml per minute
$u_{superficial}$	0.09431	ml · min	Flow rate through the reactor if solid bed were neglected
$u_{actual}$	0.24819	ml · min	Flow rate through the reactor including solid bed
$m_{s,wet}$	39.07	g	Mass of wet Lewatit before pre-treatment
$m_s$	20.2	g	Mass of dry Lewatit after pre-treatment
$\rho_p$	562.41	$kg \cdot m^{-3}$	Density of dry Lewatit after pre-treatment
$qe_{exp}$	1.494	$mol \cdot kg^{-1}$	Total sorbent loading for the experimental set-up at 2000 ppm
$qe_{exp,90}$	1.406	$mol \cdot kg^{-1}$	90% sorbent loading for the experimental set-up at 2000 ppm
$t_{90}$	1.68	hrs	Hours for the reactor to achieve 90% capacity
$prod_{90}$	24.9	$kg \cdot hrs^{-1} \cdot m^{-3}$	Productivity of the reactor to at 90% of its capacity
	11.56	$kg \cdot hrs^{-1} \cdot m^{-3}$	Productivity of the reactor to at 90% of its capacity
$t_{90}$	1.68	hrs	Hours for the reactor to achieve 90% capacity
Model			
$k$	0.01	$s^{-1}$	Kinetic rate constant of the reaction
$T_{ads}$	298	K	Operating temperature of the adsorption reaction
$T$	9000	s	Total amount of time of the reaction in seconds
$\Delta t$	0.001	–	Size of the time-steps
$T_{STEPS}$	9,000,000	–	Number of time points that are calculated
$L_R$	0.08195	m	Length of the reactor bed
$\Delta z$	0.008195	–	Size of the length-steps
$Z_{STEPS}$	10	–	Number of length points that are calculated
Iterations	20	–	Number of iterations for every implicit step calculation
$H$	17.24	$m^3 \cdot kg^{-1}$	Henry's constant calculated from the experimental data
Results			
$c_{max}$	0.08338	$mol \cdot m^{-3}$	Max concentration in the reactor
$q_{max}$	1.437	$mol \cdot kg^{-1}$	Max loading on to the sorbent
$t_{c,max}$	8604.92	s	Time until maximum concentration in the reactor is achieved
$t_{q,max}$	8713.1	s	Time until maximum loading of the sorbent is achieved
$t_{q,50}$	1.585	hrs	Time until 50% of the loading capacity is achieved
$t_{q,90}$	2.023	hrs	Time until 90% of the loading capacity is achieved
$prod_{50}$	6.954	$kg \cdot hrs^{-1} \cdot m^{-3}$	Productivity of the adsorption reactor at 50% capacity
$prod_{90}$	9.806	$kg \cdot hrs^{-1} \cdot m^{-3}$	Productivity of the adsorption reactor at 90% capacity
Check			
$A_{under}$	286.42	$mol \cdot m^{-3} \cdot s^{-1}$	Area under graph of concentration and time
$A_{square}$	717.468	$mol \cdot m^{-3} \cdot s^{-1}$	Total square area above and below graph
$A_{above}$	431.048	$mol \cdot m^{-3} \cdot s^{-1}$	Total square area above and below graph
$\dot{V}$	$6.667 \cdot 10^{-5}$	$m^3 \cdot s^{-1}$	
$qe_{check}$	1.4226	$mol \cdot kg^{-1}$	Total sorbent loading for the experimental set-up at 2000 ppm
$qe_{exp,actual}$	1.209	$mol \cdot kg^{-1}$	Total sorbent loading for the experimental set-up at 2000 ppm
$qe_{exp,fitted}$	1.326	$mol \cdot kg^{-1}$	Total sorbent loading fitted for the experimental set-up at 2000 ppm

Table 10: Experimental data Surati

Symbol	Value	Unit	Description
$C_{400}$	400	ppm	Concentration of CO <sub>2</sub> of treated air in ppm
$\phi_{400}$	4000	$ml \cdot min^{-1}$	Flow rate
$qe_{400}$	0.958	kg	Amount of CO <sub>2</sub> adsorbed
$m_{sorb}$	39.07	kg	Weight of sorbent pre-treatment
$m_{sorb}$	20.2	kg	Weight of sorbent post-treatment
$L_R$	8.2	cm	Bed height
$V_{sorb}$	$5.792 \cdot 10^{-5}$	$m^3$	Volume of sorbent bed
$t_{90}$	5.91	hrs	Number of hours taken to reach t-90
$prod_{400}$	4.8	$kg \cdot hrs^{-1} \cdot m^{-3}$	Productivity
$C_{2000}$	2000	ppm	Concentration of CO <sub>2</sub> of treated air in ppm
$\phi_{2000}$	4000	$ml \cdot min^{-1}$	Flow rate
$qe_{2000}$	1.406	kg	Amount of CO <sub>2</sub> adsorbed
$m_{sorb}$	39.07	kg	Weight of sorbent pre-treatment
$m_{sorb}$	20.2	kg	Weight of sorbent post-treatment
$L_R$	8.2	cm	Bed height
$V_{sorb}$	$5.792 \cdot 10^{-5}$	$m^3$	Volume of sorbent bed
$t_{90}$	1.68	hrs	Number of hours taken to reach t-90
$prod_{400}$	24.9	$kg \cdot hrs^{-1} \cdot m^{-3}$	Productivity

Table 11: Desorption case study results

Results				
Parameter	Value 400 ppm	Value 2000 ppm	Unit	Equation
$m_{des,50}$	0.064	0.161	kg	Total unloaded CO <sub>2</sub> at 50%
$m_{des,90}$	0.116	0.289	kg	Total unloaded CO <sub>2</sub> at 90%
$M_{t,max}$	1.433 E-3	$3.585 \cdot 10^{-3}$	$mol \cdot s^{-1}$	Maximum molar flow rate
$n_{A,cap,50}$	1.461	3.6536	mol	Number of moles CO <sub>2</sub> unloaded at 50%
$n_{A,cap,90}$	2.6304	6.5764	mol	Number of moles CO <sub>2</sub> unloaded at 90%
$n_{A,max}$	0.0475	0.0493	mol	Maximum number of gaseous moles CO <sub>2</sub> in the reactor
$n_{t,0}$	0.0617	0.0617	mol	Initial amount of gaseous moles in the reactor
$n_{t,M}$	0.0468	0.0468	mol	Final amount of gaseous moles in the reactor
$prod_{des,50}$	9.279	24.254	$kg \cdot hrs^{-1} \cdot m^{-3}$	Productivity of desorption reactor at 50% unloading
$prod_{des,90}$	6.365	16.158	$kg \cdot hrs^{-1} \cdot m^{-3}$	Productivity of desorption reactor at 90% unloading
$q_{A,max}$	0.9	1.4	$mol \cdot kg^{-1}$	Maximum actual loading
$q_{A,min}$	0.5677	0.5688	$mol \cdot kg^{-1}$	Minimum actual loading
$q_{cyc,50}$	0.166	0.416	$mol \cdot kg^{-1}$	Cyclic capacity at 50% unloading
$q_{cyc,90}$	0.3	0.749	$mol \cdot kg^{-1}$	Cyclic capacity at 90% unloading
$qe_{max}$	0.9	1.399	$mol \cdot kg^{-1}$	Maximum equilibrium loading
$qe_{min}$	0.5671	0.5677	$mol \cdot kg^{-1}$	Minimum equilibrium loading
$t_{50}$	0.43	0.41	hrs	Time until 50% unloading
$t_{90}$	1.13	1.11	hrs	Time until 90% unloading
$t_{A>B}$	294.4	209.3	s	Time until more CO <sub>2(g)</sub> exists in reactor then N <sub>2(g)</sub>
$t_{B=0}$	679.6	526.3	s	Time until more no N <sub>2(g)</sub> exists in reactor then
$t_{(T_{max-5})}$	807.7	2097.8	s	Seconds until T <sub>max-5</sub> is reached [388K]
$X_{des,50}$	18.49	29.72	%	Percentage of unloaded CO <sub>2</sub> at 50%
$X_{des,90}$	33.29	53.5	%	Percentage of unloaded CO <sub>2</sub> at 90%

## 20 Appendix C. [Derivations]

### C.1 Adsorption derivations

#### 20.1 Ordering of equations

Table 12: Sequencing of adsorption equations

Initial conditions	z for i= 0	z for 0 < i < N	z for i = N
t for j = 0	$q_{0,0} = D$ $c_{0,0} = c_{in}$ $\frac{\partial q_{0,0}}{\partial t} = 0$ $\frac{\partial c_{0,0}}{\partial t} = 0$	$q_{i,0} = D$ $c_{i,0} = 0$ $\frac{\partial q_{i,0}}{\partial t} = 0$ $\frac{\partial c_{i,0}}{\partial t} = 0$	$q_{N,0} = D$ $c_{N,0} = 0$ $\frac{\partial q_{N,0}}{\partial t} = 0$ $\frac{\partial c_{N,0}}{\partial t} = 0$
	$qe_{0,0} = H \cdot c_{0,0}$	$qe_{i,0} = H \cdot c_{i,0}$	$qe_{i,0} = H \cdot c_{N,0}$
Explicit t = 1	$\frac{\partial q_{0,0}}{\partial t} = k(qe_{0,0} - q_{0,0})$ $\frac{\partial c_{0,0}}{\partial t} = B \frac{\partial q_{0,0}}{\partial t}$ $q_{0,1}^{exp} = q_{0,0} + \Delta t \cdot \frac{\partial q_{0,0}}{\partial t}$ $c_{0,1}^{exp} = c_{0,0} + \Delta t \cdot \frac{\partial c_{0,0}}{\partial t}$	$\frac{\partial q_{i,0}}{\partial t} = k(qe_{i,0} - q_{i,0})$ $\frac{\partial c_{i,0}}{\partial t} = A \frac{c_{i,0} - c_{i-1,0}}{2\Delta z} + B \frac{\partial q_{i,0}}{\partial t}$ $q_{i,1}^{exp} = q_{i,0} + \Delta t \frac{\partial q_{i,0}}{\partial t}$ $c_{i,1}^{exp} = c_{i,0} + \Delta t \frac{\partial c_{i,0}}{\partial t}$	$\frac{\partial q_{N,0}}{\partial t} = k(qe_{N,0} - q_{N,0})$ $\frac{\partial c_{N,0}}{\partial t} = A \frac{c_{N,0} - c_{N-1,0}}{2\Delta z} + B \frac{\partial q_{N,0}}{\partial t}$ $q_{N,1}^{exp} = q_{N,0} + \Delta t \frac{\partial q_{N,0}}{\partial t}$ $c_{N,1}^{exp} = c_{N,0} + \Delta t \frac{\partial c_{N,0}}{\partial t}$
	$qe_{0,1} = H \cdot c_{0,1}^{exp}$	$qe_{i,1} = H \cdot c_{i,1}^{exp}$	$qe_{N,1} = H \cdot c_{N,1}^{exp}$
Implicit #1 t = 1	$\frac{\partial q_{0,1}}{\partial t} = k(qe_{0,1} - q_{0,1}^{exp})$ $\frac{\partial c_{0,1}}{\partial t} = B \frac{\partial q_{0,1}}{\partial t}$ $q_{0,1}^{imp} = q_{0,0} + \Delta t \cdot \frac{\partial q_{0,1}}{\partial t}$ $c_{0,1}^{imp} = c_{0,0} + \Delta t \cdot \frac{\partial c_{0,1}}{\partial t}$	$\frac{\partial q_{i,1}}{\partial t} = k(qe_{i,1} - q_{i,1}^{exp})$ $\frac{\partial c_{i,1}}{\partial t} = A \frac{c_{i,1}^{exp} - c_{i-1,1}^{exp}}{2\Delta z} + B \frac{\partial q_{i,1}}{\partial t}$ $q_{i,1}^{imp} = q_{i,0} + \Delta t \frac{\partial q_{i,1}}{\partial t}$ $c_{i,1}^{imp} = c_{i,0} + \Delta t \frac{\partial c_{i,1}}{\partial t}$	$\frac{\partial q_{N,1}}{\partial t} = k(qe_{N,1} - q_{N,1}^{exp})$ $\frac{\partial c_{N,1}}{\partial t} = A \frac{c_{N,1}^{exp} - c_{N-1,1}^{exp}}{2\Delta z} + B \frac{\partial q_{N,1}}{\partial t}$ $q_{N,1}^{imp} = q_{N,0} + \Delta t \frac{\partial q_{N,1}}{\partial t}$ $c_{N,1}^{imp} = c_{N,0} + \Delta t \frac{\partial c_{N,1}}{\partial t}$
	$qe_{0,1} = H \cdot c_{0,1}^{imp}$	$qe_{i,1} = H \cdot c_{i,1}^{imp}$	$qe_{N,1} = H \cdot c_{N,1}^{imp}$
Implicit #2 t = 1	$\frac{\partial q_{0,1}}{\partial t} = k(qe_{0,1} - q_{0,1}^{imp})$ $\frac{\partial c_{0,1}}{\partial t} = B \frac{\partial q_{0,1}}{\partial t}$ $q_{0,1}^{imp} = q_{0,0} + \Delta t \cdot \frac{\partial q_{0,1}}{\partial t}$ $c_{0,1}^{imp} = c_{0,0} + \Delta t \cdot \frac{\partial c_{0,1}}{\partial t}$	$\frac{\partial q_{i,1}}{\partial t} = k(qe_{i,1} - q_{i,1}^{imp})$ $\frac{\partial c_{i,1}}{\partial t} = A \frac{c_{i,1}^{imp} - c_{i-1,1}^{imp}}{2\Delta z} + B \frac{\partial q_{i,1}}{\partial t}$ $q_{i,1}^{imp} = q_{i,0} + \Delta t \frac{\partial q_{i,1}}{\partial t}$ $c_{i,1}^{imp} = c_{i,0} + \Delta t \frac{\partial c_{i,1}}{\partial t}$	$\frac{\partial q_{N,1}}{\partial t} = k(qe_{N,1} - q_{N,1}^{imp})$ $\frac{\partial c_{N,1}}{\partial t} = A \frac{c_{N,1}^{imp} - c_{N-1,1}^{imp}}{2\Delta z} + B \frac{\partial q_{N,1}}{\partial t}$ $q_{N,1}^{imp} = q_{N,0} + \Delta t \frac{\partial q_{N,1}}{\partial t}$ $c_{N,1}^{imp} = c_{N,0} + \Delta t \frac{\partial c_{N,1}}{\partial t}$
Iterations	$q_{0,1}$ $c_{0,1}$ $qe_{0,1} = H \cdot c_{0,1}$	$q_{i,1}$ $c_{i,1}$ $qe_{i,1} = H \cdot c_{i,1}$	$q_{N,1}$ $c_{N,1}$ $qe_{i,1} = H \cdot c_{N,1}$
Explicit t = 2	$\frac{\partial q_{0,1}}{\partial t} = k(qe_{0,1} - q_{0,1})$ $\frac{\partial c_{0,1}}{\partial t} = B \frac{\partial q_{0,1}}{\partial t}$ $q_{0,2}^{exp} = q_{0,1} + \Delta t \cdot \frac{\partial q_{0,1}}{\partial t}$ $c_{0,2}^{exp} = c_{0,1} + \Delta t \cdot \frac{\partial c_{0,1}}{\partial t}$	$\frac{\partial q_{i,1}}{\partial t} = k(qe_{i,1} - q_{i,1})$ $\frac{\partial c_{i,1}}{\partial t} = A \frac{c_{i,1} - c_{i-1,1}}{2\Delta z} + B \frac{\partial q_{i,1}}{\partial t}$ $q_{i,2}^{exp} = q_{i,1} + \Delta t \frac{\partial q_{i,1}}{\partial t}$ $c_{i,2}^{exp} = c_{i,1} + \Delta t \frac{\partial c_{i,1}}{\partial t}$	$\frac{\partial q_{N,1}}{\partial t} = k(qe_{N,1} - q_{N,1})$ $\frac{\partial c_{N,1}}{\partial t} = A \frac{c_{N,1} - c_{N-1,1}}{2\Delta z} + B \frac{\partial q_{N,1}}{\partial t}$ $q_{N,2}^{exp} = q_{N,1} + \Delta t \frac{\partial q_{N,1}}{\partial t}$ $c_{N,2}^{exp} = c_{N,1} + \Delta t \frac{\partial c_{N,1}}{\partial t}$
	$qe_{0,2} = H \cdot c_{0,2}^{exp}$	$qe_{i,2} = H \cdot c_{i,2}^{exp}$	$qe_{N,2} = H \cdot c_{N,2}^{exp}$
Implicit #1 t = 2	$\frac{\partial q_{0,2}}{\partial t} = k(qe_{0,2} - q_{0,2}^{exp})$ $\frac{\partial c_{0,2}}{\partial t} = B \frac{\partial q_{0,2}}{\partial t}$ $q_{0,2}^{imp} = q_{0,1} + \Delta t \cdot \frac{\partial q_{0,2}}{\partial t}$ $c_{0,2}^{imp} = c_{0,1} + \Delta t \cdot \frac{\partial c_{0,2}}{\partial t}$	$\frac{\partial q_{i,2}}{\partial t} = k(qe_{i,2} - q_{i,2}^{exp})$ $\frac{\partial c_{i,2}}{\partial t} = A \frac{c_{i,2}^{exp} - c_{i-1,2}^{exp}}{2\Delta z} + B \frac{\partial q_{i,2}}{\partial t}$ $q_{i,2}^{imp} = q_{i,1} + \Delta t \frac{\partial q_{i,2}}{\partial t}$ $c_{i,2}^{imp} = c_{i,1} + \Delta t \frac{\partial c_{i,2}}{\partial t}$	$\frac{\partial q_{N,2}}{\partial t} = k(qe_{N,2} - q_{N,2}^{exp})$ $\frac{\partial c_{N,2}}{\partial t} = A \frac{c_{N,2}^{exp} - c_{N-1,2}^{exp}}{2\Delta z} + B \frac{\partial q_{N,2}}{\partial t}$ $q_{N,2}^{imp} = q_{N,1} + \Delta t \frac{\partial q_{N,2}}{\partial t}$ $c_{N,2}^{imp} = c_{N,1} + \Delta t \frac{\partial c_{N,2}}{\partial t}$
	$qe_{0,2} = H \cdot c_{0,2}^{imp}$	$qe_{i,2} = H \cdot c_{i,2}^{imp}$	$qe_{N,2} = H \cdot c_{N,2}^{imp}$
Implicit #2 t = 1	$\frac{\partial q_{0,2}}{\partial t} = k(qe_{0,2} - q_{0,2}^{imp})$ $\frac{\partial c_{0,2}}{\partial t} = B \frac{\partial q_{0,2}}{\partial t}$ $q_{0,2}^{imp} = q_{0,1} + \Delta t \cdot \frac{\partial q_{0,2}}{\partial t}$ $c_{0,2}^{imp} = c_{0,1} + \Delta t \cdot \frac{\partial c_{0,2}}{\partial t}$	$\frac{\partial q_{i,2}}{\partial t} = k(qe_{i,2} - q_{i,2}^{imp})$ $\frac{\partial c_{i,2}}{\partial t} = A \frac{c_{i,2}^{imp} - c_{i-1,2}^{imp}}{2\Delta z} + B \frac{\partial q_{i,2}}{\partial t}$ $q_{i,2}^{imp} = q_{i,1} + \Delta t \frac{\partial q_{i,2}}{\partial t}$ $c_{i,2}^{imp} = c_{i,1} + \Delta t \frac{\partial c_{i,2}}{\partial t}$	$\frac{\partial q_{N,2}}{\partial t} = k(qe_{N,2} - q_{N,2}^{imp})$ $\frac{\partial c_{N,2}}{\partial t} = A \frac{c_{N,2}^{imp} - c_{N-1,2}^{imp}}{2\Delta z} + B \frac{\partial q_{N,2}}{\partial t}$ $q_{N,2}^{imp} = q_{N,1} + \Delta t \frac{\partial q_{N,2}}{\partial t}$ $c_{N,2}^{imp} = c_{N,1} + \Delta t \frac{\partial c_{N,2}}{\partial t}$
Iterations	$q_{0,2}$ $c_{0,2}$ $qe_{0,2} = H \cdot c_{0,2}$	$q_{i,2}$ $c_{i,2}$ $qe_{i,2} = H \cdot c_{i,2}$	$q_{N,2}$ $c_{N,2}$ $qe_{N,2} = H \cdot c_{N,2}$

## C.II Desorption derivations

### 20.2 Derivation of the energy balance

- A = CO<sub>2</sub>
- B = N<sub>2</sub>
- $n_{A,g} = n_A$
- $n_{B,g} = n_B$
- $n_{A,ads} = q_A \cdot m_s$
- $\frac{dn_{A,ads}}{dt} = \frac{dq_A}{dt} \cdot m_s$
- $n_t = n_A + n_B$
- $M_t = \text{Total molar flow rate (mol/s)}$
- $\frac{dV}{dt} = 0$
- $\frac{dP}{dt} = 0$
- $\frac{dn_t}{dt} \neq 0$
- $\frac{dT}{dt} \neq 0$
- $c_{v,A,ads} = c_{v,A,g}$

$$\frac{dq_A}{dt} = k(q_e - q_A) \quad (\text{MB 1})$$

$$\frac{dn_A}{dt} = m_s \cdot k(q_A - q_e) - M_t \frac{n_A}{n_t} \quad (\text{MB 2})$$

$$\frac{dn_t}{dt} = m_s \cdot k(q_A - q_e) - M_t \quad (\text{MB 3})$$

**Starting point for the energy balance of the system**

$$E_{cv} = n_{A,ads} \cdot c_{v,A,ads} \cdot T + n_{A,g} \cdot c_{v,A,g} \cdot T + n_{B,g} \cdot c_{v,B,g} \cdot T + m_s \cdot c_s \cdot T$$

$$\frac{dE_{cv}}{dt} = c_{v,A,ads} \left( \frac{dn_{A,ads}}{dt} \cdot T + \frac{dT}{dt} \cdot n_{A,ads} \right) + c_{v,A,g} \left( \frac{dn_A}{dt} \cdot T + \frac{dT}{dt} \cdot n_A \right) + c_{v,B,g} \left( \frac{dn_B}{dt} \cdot T + \frac{dT}{dt} \cdot n_B \right) + c_s \cdot m_s \cdot \frac{dT}{dt}$$

**General terms of the energy balance**

$$\frac{dE}{dt} = -\dot{m}_{out} h_{out} + \dot{Q} + \dot{W}$$

**General terms for the differentials inside the energy balance**

$$\frac{dn_{A,ads}}{dt} = \frac{d(q_A \cdot m_s)}{dt} = \frac{dq_A}{dt} \cdot m_s$$

$$\frac{dn_A}{dt} = m_s \cdot k(q_A - q_e) - M_t \frac{n_A}{n_t}$$

$$\frac{dn_B}{dt} = m_s \cdot k(q_A - q_e) - M_t \frac{n_B}{n_t}$$

**General equation for the molar flow rate**

$$M_t = m_s \cdot k(q_A - q_e) - \frac{dn_t}{dt}$$

$$\begin{aligned} \frac{dq_A}{dt} &= k(q_e - q_A) \\ &= -k(q_A - q_e) \end{aligned}$$

**General filled in for its molar differentials**

$$c_{v,A,g}\left(\frac{dq_A}{dt} \cdot m_s \cdot T + \frac{dT}{dt} \cdot n_{A,ads}\right) + c_{v,A,g}\left((m_s \cdot k(q_A - qe) - M_t \frac{n_A}{n_t}) \cdot T + \frac{dT}{dt} \cdot n_A\right) +$$

$$c_{v,B,g}\left((m_s \cdot k(q_A - qe) - M_t \frac{n_B}{n_t}) \cdot T + \frac{dT}{dt} \cdot n_B\right) + c_s \cdot m_s \cdot \frac{dT}{dt}$$

**General filled in for its molar flow rate**

$$c_{v,A,g}\left(k(qe - q_A) \cdot m_s \cdot T + \frac{dT}{dt} \cdot n_{A,ads}\right) + c_{v,A,g}\left((m_s \cdot k(q_A - qe) - (m_s \cdot k(q_A - qe) - \frac{dn_t}{dt}) \frac{n_A}{n_t}) \cdot T + \frac{dT}{dt} \cdot n_A\right) +$$

$$c_{v,B,g}\left((m_s \cdot k(q_A - qe) - (m_s \cdot k(q_A - qe) - \frac{dn_t}{dt}) \frac{n_B}{n_t}) \cdot T + \frac{dT}{dt} \cdot n_B\right) + c_s \cdot m_s \cdot \frac{dT}{dt}$$

**General relation between temperature and total moles**

$$P = \frac{n \cdot T \cdot R}{V}$$

$$\frac{dP}{dt} = 0$$

$$\frac{dP}{dt} = \frac{d(n_t \cdot T)}{dt} \cdot \frac{R}{V}$$

$$= \frac{dn_t}{dt} \cdot \left(\frac{T \cdot R}{V}\right) + \frac{dT}{dt} \cdot \left(\frac{n_A \cdot R}{V}\right)$$

$$= \frac{dn_t}{dt} \cdot \left(\frac{T \cdot R}{V}\right) + \frac{dT}{dt} \cdot \left(\frac{n_t \cdot R}{V}\right) = 0$$

$$\frac{dn_t}{dt} = -\frac{dT}{dt} \cdot \frac{n_t}{T}$$

**General equation filled in for total molar flow rate differential**

$$c_{v,A,g}\left(k(qe - q_A) \cdot m_s \cdot T + \frac{dT}{dt} \cdot n_{A,ads}\right) + c_{v,A,g}\left((m_s \cdot k(q_A - qe) - (m_s \cdot k(q_A - qe) - (-\frac{dT}{dt} \cdot \frac{n_t}{T})) \frac{n_A}{n_t}) \cdot T + \frac{dT}{dt} \cdot n_A\right) +$$

$$c_{v,B,g}\left((m_s \cdot k(q_A - qe) - (m_s \cdot k(q_A - qe) - (-\frac{dT}{dt} \cdot \frac{n_t}{T})) \frac{n_B}{n_t}) \cdot T + \frac{dT}{dt} \cdot n_B\right) + c_s \cdot m_s \cdot \frac{dT}{dt}$$

**Rewriting in terms of mass balance variables**

$$n_B = n_t - n_A$$

$$\frac{n_B}{n_t} = \frac{n_t - n_A}{n_t} = 1 - \frac{n_A}{n_t}$$

$$c_{v,A,g}\left(k(qe - q_A) \cdot m_s \cdot T + \frac{dT}{dt} \cdot n_{A,ads}\right) + c_{v,A,g}\left((m_s \cdot k(q_A - qe) - (m_s \cdot k(q_A - qe) - (-\frac{dT}{dt} \cdot \frac{n_t}{T})) \frac{n_A}{n_t}) \cdot T + \frac{dT}{dt} \cdot n_A\right) +$$

$$c_{v,B,g}\left((m_s \cdot k(q_A - qe) - (m_s \cdot k(q_A - qe) - (-\frac{dT}{dt} \cdot \frac{n_t}{T}))(1 - \frac{n_A}{n_t})) \cdot T + \frac{dT}{dt} \cdot (n_t - n_A)\right) + c_s \cdot m_s \cdot \frac{dT}{dt}$$

**Rewriting energy balance to solve for T**

$$\frac{dT}{dt} = \frac{1}{c_{p,A} \cdot n_A + c_{p,B} \cdot (n_t - n_A) + c_{v,A,g} \cdot q_A \cdot m_s + c_s \cdot m_s}$$

$$\left[ T \cdot m_s \cdot k(q_A - qe) \cdot \left(\frac{n_A}{n_t} (c_{v,A,g} - c_{v,B,g} - c_{p,A} + c_{p,B}) - c_{p,B}\right) \right.$$

$$\left. + UA(T_H - T) + \Delta H \cdot m_s \cdot k(q_A - qe) \right] \quad (\text{EB})$$



### 20.3 Molar flow rate equations

$$M_t = m_s \cdot k(q_A - q_e) - \frac{dn_t}{dt}$$

$$\frac{dn_t}{dt} = -\frac{dT}{dt} \cdot \frac{n_t}{T}$$

Rewrite the equation for the molar flow rate as a function of the temperature differential

$$M_t = m_s \cdot k(q_A - q_e) - \left(-\frac{dT}{dt} \cdot \frac{n_t}{T}\right)$$

$$\frac{dT}{dt} = \frac{1}{c_{p,A} \cdot n_A + c_{p,B} \cdot (n_t - n_A) + c_{v,A,g} \cdot q_A \cdot m_s + c_s \cdot m_s} \cdot \left[ T \cdot m_s \cdot k(q_A - q_e) \cdot \left(\frac{n_A}{n_t} (c_{v,A,g} - c_{v,B,g} - c_{p,A} + c_{p,B}) - c_{p,B}\right) + UA(T_H - T) + \Delta H \cdot m_s \cdot k(q_A - q_e) \right]$$

Implementing the temperature differential to solve for  $M_t$

$$M_t = m_s \cdot k(q_A - q_e) + \frac{n_t}{T} \cdot \frac{1}{c_{p,A} \cdot n_A + c_{p,B} \cdot (n_t - n_A) + c_{v,A,g} \cdot q_A \cdot m_s + c_s \cdot m_s} \cdot \left[ T \cdot m_s \cdot k(q_A - q_e) \cdot \left(\frac{n_A}{n_t} (c_{v,A,g} - c_{v,B,g} - c_{p,A} + c_{p,B}) - c_{p,B}\right) + UA(T_H - T) + \Delta H \cdot m_s \cdot k(q_A - q_e) \right] \quad (M_t)$$

## 21 Appendix D. [Figures]

### Toth isotherm vs. Henry's coefficient

Toth isotherm

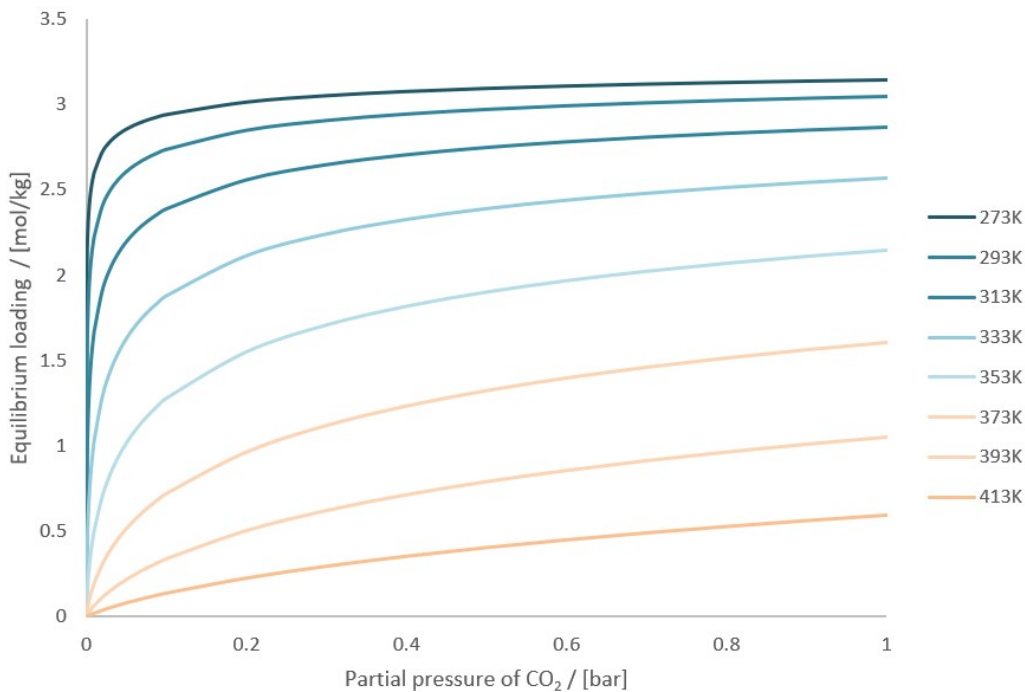


Figure 26: Reproduced representation of the experimental Toth isotherm equation as determined by Bos [3] that shows the effect of temperature and the partial pressure of CO<sub>2</sub> on the capacity of the sorbent from 0 to 1 bar

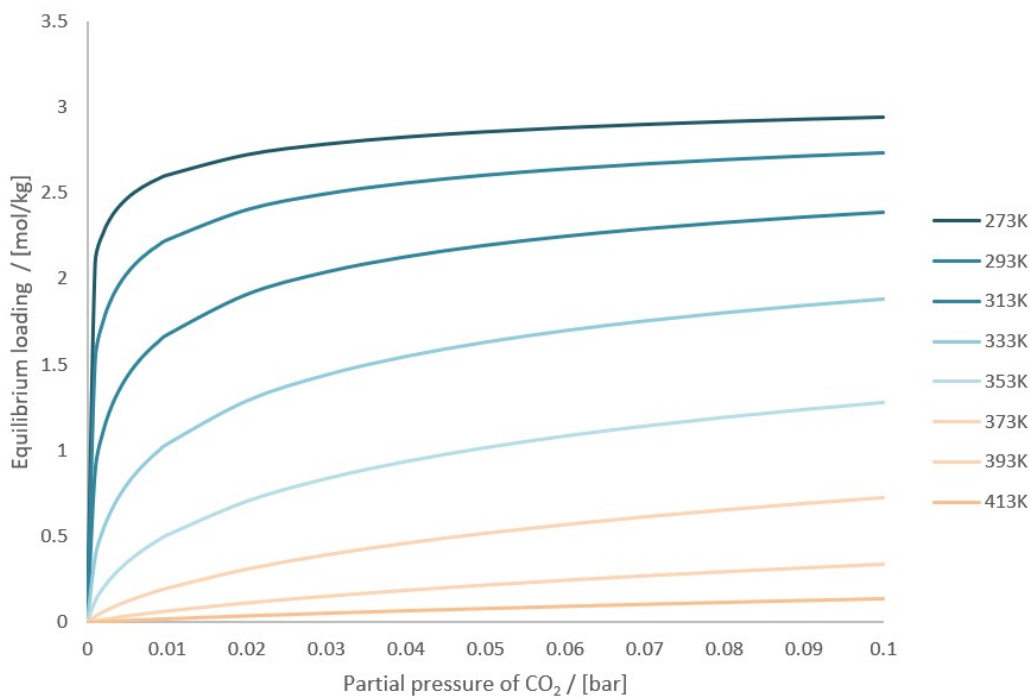


Figure 27: Reproduced representation of the experimental Toth isotherm equation as determined by Bos [3] that shows the effect of temperature and the partial pressure of CO<sub>2</sub> on the capacity of the sorbent from 0 to 0.1 bar

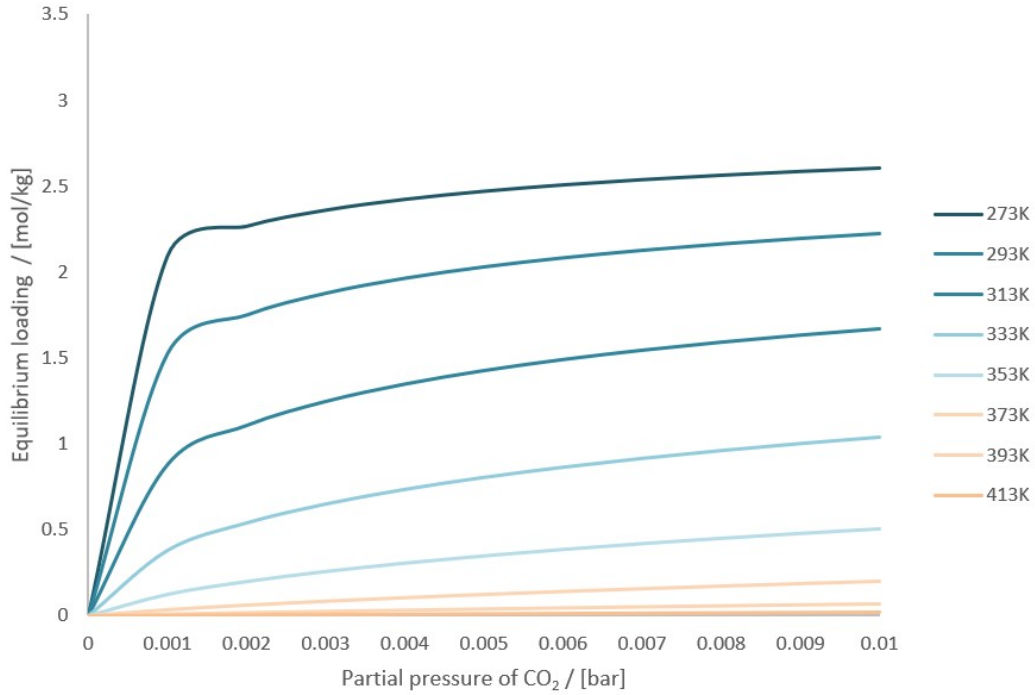


Figure 28: Reproduced representation of the experimental Toth isotherm equation as determined by Bos [3] that shows the effect of temperature and the partial pressure of  $\text{CO}_2$  on the capacity of the sorbent from 0 to 0.01 bar

### Crank Nicolson results

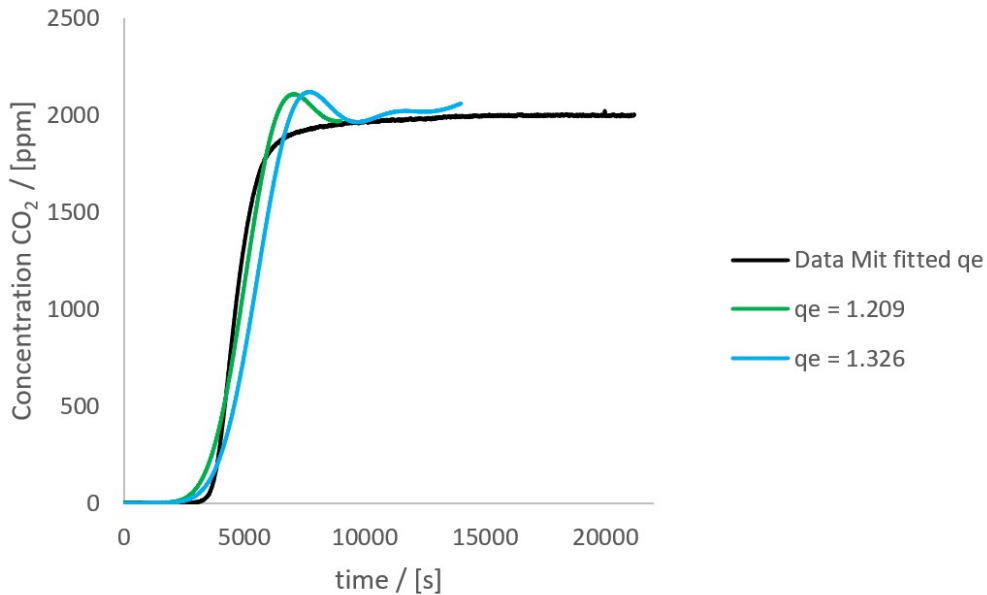


Figure 29: Comparing the fitted experimental results of a 2000 ppm system at the outlet of the reactor by Surati [2] to the simulation done by the model for  $k = 0.02 \text{ s}^{-1}$  and different equilibrium loading values for 1,400 seconds, solved with the Crank-Nicolson method.

## 22 Appendix E. [Python code]

### Adsorption code

*Listing 1: Adsorption model script*

```
from pprint import pprint
from typing import Dict

import pandas as pd
import matplotlib.pyplot as plt
import numpy as np
import decimal
import time
from numpy import trapz

    ##Overall mass balance parameters##
epsilon_p = 0.23 #m3_g/m3_s
epsilon_b = 0.38 #m3_g/m3_reac
# rho_p = 1.829 #kg/m3
# rho_p = 880 # kg_s/m3
rho_p = 562.414 #Dry actual density of mit's lewatit

T_ads = 273+25 #K (25C)
R = 8.314 #Universal gas constant (J/K*mol)
ppm = 0.000001 #0.0001%
M_CO2 = 0.04401 #kg/mol (44.01 g/mol)
rho_CO2_25 = 1.795 #kg/m3
# rho_CO2_20 = 1.815 #kg/m3
air_ppm = 2000
C_ppm_25 = ppm*air_ppm*rho_CO2_25/M_CO2

#Volumetric flow rate
flow_rate = 4000 #ml/min Mit
Cubic_flow = flow_rate/(60*1000**2) #m3/s
D_R = 0.03 #m Mit diameter
A_R = 0.25*np.pi*D_R**2
A_g = A_R*epsilon_b
u_superficial = Cubic_flow/A_R
u_actual = Cubic_flow/A_g

u_air = u_actual

# C_in = 0.0163 #0.016314474 #mol_CO2/m3 = 400 ppm @ 25 C
# C_in = 0.0816 #0.08157237 #mol_CO2/m3 = 2000 ppm @ 25 C
# C_in = 0.0165 #0.016496251 #mol_CO2/m3 = 400 ppm @ 20 C
# C_in = 0.0825 #0.082481254 #mol_CO2/m3 = 2000 ppm @ 20 C

C_in = C_ppm_25
C_i_0 = 0 #mol_CO2/m3
D0 = 0 #mol_CO2/kg_s

A = u_air
B = ((1-epsilon_b)/epsilon_b)*rho_p

qe_Mit_2000 = 1.326 #mol/kg_s Nieuwe qe
H = qe_Mit_2000/C_in
```

```

##Loop functions##
k = 0.04 #m3_g/(molCO2*s)

#####
T = 14000 #s (Total time)
# T_STEPS = 100000 #Number of steps per T
Dt = 0.0014 #Magnitude of time steps
T_STEPS = int(T/Dt)

t = 0.0
#####
# L = 0.4 #m (Total length of reactor, constant)
L = 0.081954185 #m (Total length of reactor, constant)
# L = 0.01
Z_STEPS = 12 #Number of z-gridpoints
Dz = L/Z_STEPS
#####
ITERATIONS = 12
#op een gegeven moment iteraties naar oneindig maar iteratie stoppen als niet meer
convergeert voor 6 decimalen bv.

print(T/T_STEPS)
print(Dz)

#####Main Code#####
-----
##Dictionaries##
t = time.time()

C_imp_outlet = []
q_imp_outlet = []
# C_imp_outlet = {}
# q_imp_outlet = {}
C_imp_jmin1 = {}
q_imp_jmin1 = {}

check_difference_switch = 0 # 1 is on, 0 is off (Iteration error-check switch)
if check_difference_switch == 1:
    C_imp_difference = {}
    q_imp_difference = {}

for j in range(T_STEPS):

    C = {}
    q = {}
    qe = None

    q_exp = {}
    C_exp = {}

    if j != 0:
        C_imp_jmin1 = C_imp
        q_imp_jmin1 = q_imp
    C_imp = {}
    q_imp = {}
    # q_imp[j] = {}
    # C_imp[j] = {}

```

```

dqdt_exp = None
dCdt_exp = None

qe_exp = None
qe_imp = None
dqdt_imp = None
dCdt_imp = None

if check_difference_switch == 1:
    C_imp_previous = None
    C_imp_difference[j] = {}
    q_imp_previous = None
    q_imp_difference[j] = {}

if j == 0:

    for i in range (0, Z_STEPS + 1): #uitkijken hier is Z_steps van 0 t/m 7

        ## Setting BC & IC's ##
        print(i, j, Z_STEPS)

        if (i == 0):
            C[i] = C_in
            C[i+1] = C_i_0
            q[i] = D0

        elif (i != 0):
            C[i] = C_i_0
            q[i] = D0

            if i != Z_STEPS: #uitkijken hier is Z_STEPS wel weer 8
                C[i+1] = C_i_0
            else:
                pass

        ### Explicit for t = 0 ###
        qe = H*C[i]

        dqdt_exp = k*(qe - q[i])

        if (i == 0):
            dCdt_exp = 0
        #Upwind
        elif (i != 0):
            dCdt_exp =  $(-(A*(C[i] - C[i-1])/(Dz)) - (B*dqdt\_exp))$ 
        #
        #
        #
        elif (i != 0) & (i != Z_STEPS):
            dCdt_exp =  $(-(A*(C[i+1] - C[i-1])/(2*Dz)) - (B*dqdt\_exp))$ 
        #
        elif (i == Z_STEPS):
            dCdt_exp =  $(-(A*(C[i] - C[i-1])/(2*Dz)) - (B*dqdt\_exp))$ 

        q_exp[i] = D0 + (Dt*dqdt_exp)

        if i == 0:
            C_exp[i] = C_in + (Dt*dCdt_exp)
        elif i != 0:
            C_exp[i] = C_i_0 + (Dt*dCdt_exp)

        #
        qe_exp = H*C_exp[i]

```

```

C = C_exp
q = q_exp

### Implicit loop for = 0 ###
for implicit_loop in range (0, ITERATIONS):

    ## After loop is complete, save all values to list ->
    if (implicit_loop == 0):

        for i in range (0, Z_STEPS + 1): #uitkijken hier is Z_steps van 0 t/m 7

            qe = H*C[i]

            dqdt_imp = k*(qe - q[i])

            #                print(i, j)

            if (i == 0):
                dCdt_imp = 0
            #Upwind
            elif (i != 0):
                dCdt_imp = (-(A*(C[i] - C[i-1])/(Dz))-(B*dqdt_imp))
            #                elif (i != 0) & (i != Z_STEPS):
            #                    dCdt_imp = (-(A*(C[i+1] - C[i-1])/(2*Dz))-(B*dqdt_imp))
            #                elif (i == Z_STEPS):
            #                    dCdt_imp = (-(A*(C[i] - C[i-1])/(2*Dz))-(B*dqdt_imp))

            q_imp[i] = D0 + (Dt*dqdt_imp)

            if i == 0:
                C_imp[i] = C_in + (Dt*dCdt_imp)
            elif i != 0:
                C_imp[i] = C_i_0 + (Dt*dCdt_imp)

        elif (implicit_loop != 0):

            for i in range (0, Z_STEPS + 1):

                qe_imp = H*C_imp[i]
                dqdt_imp = k*(qe_imp - q_imp[i])

                if check_difference_switch == 1:
                    ###Iterations Error check###
                    C_imp_previous = C_imp[i]
                    q_imp_previous = q_imp[i]

                if (i == 0):
                    dCdt_imp = 0
                #Upwind
                elif (i != 0):
                    dCdt_imp = (-(A*(C_imp[i] - C_imp[i-1])/(Dz))-(B*dqdt_imp))
            #                elif (i != 0) & (i != Z_STEPS):
            #                    dCdt_imp = (-(A*(C_imp[i+1] - C_imp[i-1])/(2*Dz))-(B*dqdt_imp))
            #                elif (i == Z_STEPS):
            #                    dCdt_imp = (-(A*(C_imp[i] - C_imp[i-1])/(2*Dz))-(B*dqdt_imp))

```

```

q_imp[i] = D0 + (Dt*dqdt_imp)

if i == 0:
    C_imp[i] = C_in + (Dt*dCdt_imp)
elif i != 0:
    C_imp[i] = C_i_0 + (Dt*dCdt_imp)

if check_difference_switch == 1:
    ###Iterations Error check###
    C_imp_difference[j][i] = C_imp[i] - C_imp_previous
    q_imp_difference[j][i] = q_imp[i] - q_imp_previous

elif j != 0:
    #####

### Explicit for t > 0 ###
for i in range (0, Z_STEPS + 1):

    q_imp[i] = q_imp_jmin1[i]
    C_imp[i] = C_imp_jmin1[i]

    if (i == 0):
        #boundaries
        C_imp[i] = C_in
        C_imp[i+1] = C_imp_jmin1[i+1]

        #equations
        qe_imp = H*C_imp[i]
        dqdt_exp = k*(qe_imp - q_imp_jmin1[i])
        dCdt_exp = 0

        #Upwind
    elif (i != 0):
        C_imp[i] = C_imp_jmin1[i]

        qe_imp = H*C_imp[i]
        dqdt_exp = k*(qe_imp - q_imp_jmin1[i])
        dCdt_exp = (-(A*(C_imp[i] - C_imp[i-1]))/(Dz))-(B*dqdt_exp))

    q_exp[i] = q_imp_jmin1[i] + (Dt*dqdt_exp)

    if i == 0:
        C_exp[i] = C_in + (Dt*dCdt_exp)
    elif i != 0:
        C_exp[i] = C_imp_jmin1[i] + (Dt*dCdt_exp)

C = C_exp
q = q_exp

### Implicit for t > 0 ###
for implicit_loop in range (0, ITERATIONS):

    ## Loop iterations for iterations -> all values don't change for all values
    at 10(-6) decimal points ##

```



```

if (implicit_loop == 0):
    for i in range (0, Z_STEPS + 1): #uitkijken hier is Z_steps van 0 t/m 7
        qe = H*C[i]
        dqdt_imp = k*(qe - q[i])
        #
            print(i, j)
        if (i == 0):
            dCdt_imp = 0
        #Upwind
        elif (i != 0):
            dCdt_imp = (-(A*(C[i] - C[i-1])/(Dz))-(B*dqdt_imp))

        q_imp[i] = q_imp_jmin1[i] + (Dt*dqdt_imp)

        if i == 0:
            C_imp[i] = C_in + (Dt*dCdt_imp)
        elif i != 0:
            C_imp[i] = C_imp_jmin1[i] + (Dt*dCdt_imp)

elif (implicit_loop != 0):

    for i in range (0, Z_STEPS + 1):

        qe_imp = H*C_imp[i]
        dqdt_imp = k*(qe_imp - q_imp[i])

        ###Iterations Error check###
        if check_difference_switch == 1:
            C_imp_previous = C_imp[i]
            q_imp_previous = q_imp[i]

        if (i == 0):
            dCdt_imp = 0
        #Upwind
        elif (i != 0):
            dCdt_imp = (-(A*(C_imp[i] - C_imp[i-1])/(Dz))-(B*dqdt_imp))

        q_imp[i] = q_imp_jmin1[i] + (Dt*dqdt_imp)

        if i == 0:
            C_imp[i] = C_in + (Dt*dCdt_imp)
        elif i != 0:
            C_imp[i] = C_imp_jmin1[i] + (Dt*dCdt_imp)

        if check_difference_switch == 1: #Determines the difference
        between successive iterations
        ###Iterations Error check###
            C_imp_difference[j][i] = C_imp[i] - C_imp_previous
            q_imp_difference[j][i] = q_imp[i] - q_imp_previous

C_imp_outlet.append(C_imp[Z_STEPS])
q_imp_outlet.append(q_imp[Z_STEPS])

```

```

#      C_imp_outlet[j] = C_imp[Z_STEPS]
#      q_imp_outlet[j] = q_imp[Z_STEPS]
if (j%(T_STEPS/20))==0:
    print(f' {j} time_steps_complete ({round(j/T_STEPS*100,1)}%), time_elapsed:
    .....{round((time.time()-t)/60,1)} min ')

#####PLOT C_imp at outlet#####

x = np.arange(0,T,Dt)
y = C_imp_outlet

plt.xlabel("Time/[s]")
plt.ylabel("Concentration/[mol/m3]")
# plt.title("Outlet CO2 concentration")

plt.plot(x,y)

area_under_graph = trapz(C_imp_outlet, dx=Dt)
print("area_under_graph=", area_under_graph)

#####PLOT q_imp at outlet#####

x = np.arange(0,T,Dt)
y = q_imp_outlet

plt.xlabel("Time/[s]")
plt.ylabel("q_CO2/[mol/kg]")
# plt.title("Outlet sorbent loading")

area = trapz(q_imp_outlet, dx=Dt)
print("area=", area)

plt.plot(x,y)

#####Taking fewer data point so exporting to Excel possible#####
C_imp_outlet_cropped_fit = C_imp_outlet[1::1000]

#####Python data to Excel#####

#Save as a dataframe
df_C_fit = pd.DataFrame(C_imp_outlet_cropped_fit)

#Excel file name (example of file destination)
# C:\Users\jamie\OneDrive\Documents\Thesis\JJ - Thesis\Excel\Henry_Toht.xlsx
df_C_fit.to_excel(r'C:\Users\jamie\OneDrive\Documents\Thesis\JJ--Thesis\Excel
\Adsorption_python_data.xlsx', sheet_name='Data_model', index=False)

#####Productivity#####
V_R = A_R*L
V_s = V_R*(1-epsilon_b) #Sorbent volume (m3)
V_g = V_R*epsilon_b #Gas volume (m3)
V_ads = V_s*epsilon_p #Adsorbed gas in bed volume (m3)

m_p = rho_p*V_s
max_C = np.max(C_imp_outlet)

```

```

max_q = np.max(q_imp_outlet)

def find_nearest_C(C_imp_outlet, value):
    C_imp_outlet= np.asarray(C_imp_outlet)
    idx = (np.abs(C_imp_outlet - value)).argmin()
    return C_imp_outlet[idx]

def find_nearest_q(q_imp_outlet, value):
    q_imp_outlet = np.asarray(q_imp_outlet)
    idx = (np.abs(q_imp_outlet - value)).argmin()
    return q_imp_outlet[idx]

C_cap90 = max_C*0.9 - C_i_0 #Amount unloaded CO2 at 90% of de total loading
C_cap50 = max_C*0.5 - C_i_0 #Amount unloaded CO2 at 50% of de total loading
q_cap90 = max_q*0.9 - D0 #Amount unloaded CO2 at 90% of de total loading
q_cap50 = max_q*0.5 - D0 #Amount unloaded CO2 at 50% of de total loading

t_steps_C_max = np.where(C_imp_outlet == max_C)
t_steps_q_max = np.where(q_imp_outlet == max_q)

t_steps_C_cap50 = np.where(C_imp_outlet == find_nearest_C(C_imp_outlet, value=C_cap50))
t_steps_C_cap90 = np.where(C_imp_outlet == find_nearest_C(C_imp_outlet, value=C_cap90))
t_steps_q_cap50 = np.where(q_imp_outlet == find_nearest_q(q_imp_outlet, value=q_cap50))
t_steps_q_cap90 = np.where(q_imp_outlet == find_nearest_q(q_imp_outlet, value=q_cap90))

t_C_max = float(Dt*t_steps_C_max[0])
t_q_max = float(Dt*t_steps_q_max[0])

t_C_50 = float(Dt*t_steps_C_cap50[0])
t_C_90 = float(Dt*t_steps_C_cap90[0])
t_q_50 = float(Dt*t_steps_q_cap50[0])
t_q_90 = float(Dt*t_steps_q_cap90[0])

square = max_C*(t_C_max/1000)

hr_C_50 = t_C_50/3600
hr_C_90 = t_C_90/3600
hr_q_50 = t_q_50/3600
hr_q_90 = t_q_90/3600

m_max_q= max_q*m_p*M_CO2
m_q_ads_50 = q_cap50*m_p*M_CO2
m_q_ads_90 = q_cap90*m_p*M_CO2 #m_CO2 = mol_CO2/kg_s *kg_s * M_CO2 = kg_CO2

# prod_max = m_max_q/(hr_q_100*V_R)
prod_50 = m_q_ads_50/(hr_q_50*V_R)
prod_90 = m_q_ads_90/(hr_q_90*V_R)

print('max_C=%%', max_C, '_[mol/m3]')
print('max_q=%%', max_q, '_[mol/kg]')

print('Concentration_capacity_at_50%%_C_50=%%', C_cap50, '_[mol/m3]')
print('Concentration_capacity_at_90%%_C_90=%%', C_cap90, '_[mol/m3]')
print('Loading_capacity_at_50%%_C_50=%%', q_cap50, '_[mol/kg]')
print('Loading_capacity_at_90%%_C_90=%%', q_cap90, '_[mol/kg]')

```

```

print('seconds_until_maximum_concentration=', t_C_max, '[s]')
print('seconds_until_maximum_concentration=', t_q_max, '[s]')

print('seconds_until_C50=', hr_C_50, '[hrs]')
print('seconds_until_C90=', hr_C_90, '[hrs]')
print('seconds_until_q50=', hr_q_50, '[hrs]')
print('seconds_until_q90=', hr_q_90, '[hrs]')

# print('Productivity = ', prod_max)
print('Productivity_at_50%=', prod_50)
print('Productivity_at_90%=', prod_90)

#Actual sorbent loading check with the area above the concentration graph
M_CO2 = 0.044009 #Molecular weight CO2 (kg/mol)

square = max_C*T
C_load = square - area_under_graph #area above the graph
loading = (C_load*Cubic_flow)/m_p # mol/m3/s m3/s * 1/kg *

print('square=', square, 'mol_CO2*s*m3_g-1')
print('area_under_graph=', area_under_graph, 'mol_CO2*s*m3_g-1')
print('C_load=', C_load, 'mol_CO2*s*m3_g-1')
print('flow_rate=', Cubic_flow, 'm3*s-1')
print('loading=', loading, 'mol_CO2*kg_s-1')

###qe list###
qe_imp_list = []

for j in range(0, T_STEPS):
    qe_imp_list.append(C_imp_outlet[j]*H)

###LDF list###

# qe_imp_list = []
LDF_list = []

# for j in range(0, T_STEPS):
#     qe_imp_list.append(C_imp_outlet[j]*H)

for j in range(0, T_STEPS):
    LDF_list.append(k*(qe_imp_list[j]-q_imp_outlet[j]))

###PLOT LDF###

x = np.arange(0,T,Dt)
y = LDF_list

plt.xlabel("Time/[s]")
plt.ylabel("LDF/[mol/kg_s]")
# plt.title("Outlet CO2 concentration")

plt.plot(x,y)

# area_under_graph = trapz(C_imp_outlet, dx=Dt)

```

```

# print("area under graph =", area_under_graph)

####List of max error per time-step####
C_max_list = []

for jj in range(0, T_STEPS):
    current_C_max = 0

    for ii in range(1, Z_STEPS):
#         print(abs(C_imp_difference[jj][ii]))

        if abs(C_imp_difference[jj][ii]) > current_C_max:
            current_C_max = abs(C_imp_difference[jj][ii])

#         print(current_max)

    C_max_list.append(current_C_max)

####List of max error per time-step####
q_max_list = []

for jj in range(0, T_STEPS):
    current_q_max = 0

    for ii in range(1, Z_STEPS):
#         print(abs(q_imp_difference[jj][ii]))

        if abs(q_imp_difference[jj][ii]) > current_q_max:
            current_q_max = abs(q_imp_difference[jj][ii])

#         print(current_max)

    q_max_list.append(current_q_max)

####PLOT C_imp error last 2 iterations ####

x = np.arange(0,T,Dt)
y = C_max_list

plt.plot(x,y)

plt.yscale("log")
plt.xlabel("timesteps_(s)")
plt.ylabel("C_error_(mol/m3)")
plt.title("C_imp_error")

####PLOT q_imp error last 2 iterations ####

x = np.arange(0,T,Dt)
y = q_max_list

plt.yscale("log")
plt.plot(x,y)

plt.xlabel("timesteps_(s)")

```

```
plt.ylabel("q_error_(mol/m3)")  
plt.title("q_imp_error")
```

## Desorption code

*Listing 2: Desorption model script*

```
import numpy as np
import matplotlib.pyplot as plt
import scipy.optimize as opt

#ODE int from scipy integrate module
from scipy.integrate import solve_ivp
import math

from numpy import trapz

#####Ractor Parameters#####
R = 8.314 #Universal gas constant (J/K*mol)
epsilon_b = 0.38 #Bed voidage (m3_g/m3_reac)
epsilon_p = 0.23 #Particle voidage (m3_g/m3_bed)
P_amb = 100000 #Pressure of reactor at ambient conditions (Pa)
T0 = 273+25 #Initial temperature (K)
rho_s = 880 #kg/m3

P_vac = 25000 #Pressure of reactor at vacuum condition in (Pa) = 0.25 bar default
T_H = 273+120 # Heating temperature 120C default
U = 750 #Shell and tube heating (W/m2*K)

###Reactor dimensions
L_R = 0.081954 #m Mit 0.081954
D_R = 0.5 #m Flat pancake assumption T

A_R = 0.25*np.pi*D_R**2 #m2 crossectional area reactor
# A_s = A_R*(1-epsilon_b) #m2 crossectional area sorbent space
# A_g = A_R*epsilon_b #m2 crossectional area gas flow space
# A_ads = A_s*epsilon_p #m2 crossectional adsorption area

V_R = L_R*A_R #Reactor volume (m3)
V_s = V_R*(1-epsilon_b) #Sorbent volume (m3)
V_g = V_R*epsilon_b #Gas volume (m3)
V_ads = V_s*epsilon_p #Adsorbed gas in bed volume (m3)

### Heating tubes system estimation
L_tube = L_R #Heating tubes have same length as reactor
n_tubes = 10 #number of tubes
V_n_tubes = 0.10 *V_R #Percentage of reactor volume that is occupied by heating tubes 10%
V_tube = V_n_tubes/n_tubes #Volume of a single tube

R_tube = (V_tube/(np.pi*L_tube))**0.5 #Diameter of a single tube
# A_cs_tube = np.pi*R_tube**2
# A_cs_n_tubes = A_cs_tube*n_tubes
A_H_tube = L_tube*2*np.pi*R_tube #Heating area of a single heating tube
A_H_n_tubes = A_H_tube*n_tubes #Total heating area of all heating tubes

A = A_H_n_tubes #Contact heating area

#Molar masses
M_CO2 = 0.044009 #Molecular weight CO2 (kg/mol)
M_N2 = 0.028014 #Molecular weight N2 (kg/mol)
```

```

M_O2 = 0.031998 #Molecular weight O2 (kg/mol)
M_Ar = 0.039948 #Molecular weight Ar (kg/mol)

m_s = rho_s*V_s #Sorbent mass in the system

#Simplification
#A = CO2
#B = N2

#Averaged specific heats
cv_A_g = 696.7 #J/K*mol
cv_B_g = 744.3 #J/K*mol
cp_A = 892.5 #J/K*mol
cp_B = 1042 #J/K*mol
c_s = 1580 #J/K*mol

#Initial conditions
T = 273 + 25 #Initial temperature; room temperature
n_t0 = (P_vac*V_g)/(R*T0) #Total amount of gaseous moles initially in the reactor
q_A0 = 1.4 #Initial desorption loading, should be the same as final adsorption value
qe_A0 = q_A0 #Assumption is made that for initial equilibrium loading == q_A0

#Toth isotherm constants, values used from paper by M.Bos
T0_Toht = 353.15 #K
q_s0 = 3.4 #(mol/kg) Maximum CO2 capacity
b0 = 93 #(1/Pa) Toth isotherm equilibrium
alpha = 0.33 #(-)
t_h0 = 0.37 #(-) Toth isotherm parameter
DH = 95300 #(J/mol)

#Toth isotherm equations used only to calculate the initial value for n_A0:
t_h1 = t_h0 + alpha*(1-(T0_Toht/T0))
b1 = b0*np.exp((DH/(R*T0_Toht))*((T0_Toht/T0)-1))

#"Cheat code" Maple is used to calculate the initial values for q_A and M_t
to minimize initial instability ("goal_seeking")
n_A0 = round(100000*qe_A0*V_g*np.exp(np.log(-1/(-1 +
np.exp(np.log(qe_A0/q_s0)*t_h1)))/t_h1)/(q_s0*b1*R*T0), 5)

### Variable time parameters ###
T_SPAN = 10000 #Seconds of the system
Dt = 0.1 #Time-stepping value
# T_STEPS = 100000 #steps
T_STEPS = int(T_SPAN/Dt) #Number of time-intervals

#Kinetic constant
k = 0.001 # (1/s) kinetic rate constant

###ODE mass and energy balances with isotherm###

def f(t, y): #y is assumed to be a vector
    q_A = y[0]
    n_A = y[1]
    n_t = y[2]

```



T = y[3]

*#MB 1 - Sorbent unloading (LDF)*

dq\_Adt = k\*(qe(n\_A,T)-q\_A)

*#MB 2 - CO2 mass balance - (production and outflow)*

##### [dn\_Adt] = [-k\*m\_s\*(qe(n\_A)-q\_A)] - [M\_t\*n\_A/n\_t]

dn\_Adt = k\*m\_s\*(q\_A-qe(n\_A,T)) - ((m\_s\*k\*(q\_A-qe(n\_A,T)) + (n\_t/(T\*((cv\_A\_g\*q\_A\*m\_s)  
+(cp\_A\*n\_A)+(cp\_B\*(n\_t-n\_A))+(c\_s\*m\_s))))\*  
(T\*m\_s\*k\*(q\_A-qe(n\_A,T)))\*(n\_A/n\_t  
\*(cv\_A\_g-cv\_B\_g-cp\_A+cp\_B)-cp\_B) + U\*A\*(T\_H-T) +  
DH\*m\_s\*k\*(q\_A-qe(n\_A,T)))))\*n\_A/n\_t)

*#MB 3 Adsorbate unloading and total gaseous outflow*

##### [dn\_tdt] = [-k\*m\_s\*(qe(n\_A)-q\_A)] - [M\_t]

dn\_tdt = -k\*m\_s\*(qe(n\_A,T)-q\_A) - (m\_s\*k\*(q\_A-qe(n\_A,T))  
+ (n\_t/(T\*((cv\_A\_g\*q\_A\*m\_s)+(cp\_A\*n\_A)+(cp\_B\*(n\_t-n\_A))+(c\_s\*m\_s))))\*  
(T\*m\_s\*k\*(q\_A-qe(n\_A,T)))\*(n\_A/n\_t\*(cv\_A\_g-cv\_B\_g-cp\_A+cp\_B)-cp\_B) +  
U\*A\*(T\_H-T) + DH\*m\_s\*k\*(q\_A-qe(n\_A,T))))

*#EB 1 Energy balance of the system*

##### [Internal energy] = [-Ouflow] + [Heating] + [Production]

dTdt = 1/((cv\_A\_g\*q\_A\*m\_s)+(cp\_A\*n\_A)+(cp\_B\*(n\_t-n\_A))+(c\_s\*m\_s))\*  
(T\*m\_s\*k\*(q\_A-qe(n\_A,T)))\*(n\_A/n\_t\*(cv\_A\_g-cv\_B\_g-cp\_A+cp\_B)-cp\_B) +  
U\*A\*(T\_H-T) + DH\*m\_s\*k\*(q\_A-qe(n\_A,T)))

**return** np.array([dq\_Adt, dn\_Adt, dn\_tdt, dTdt])

*##The Toth isotherm##*

**def** qe(n\_A, T):

P\_A = (n\_A\*R\*T)/(V\_g\*100000)

q\_s = q\_s0

t\_h = t\_h0 + alpha\*(1-(T0\_Toht/T))

b = b0\*np.exp((DH/(R\*T0\_Toht))\*((T0\_Toht/T)-1))

qe\_A = (q\_s\*b\*P\_A)/((1+(b\*P\_A)\*\*t\_h)\*\*(1/t\_h))

**return** qe\_A

*###Solver conditions###*

*##Time units##*

*# -> !!Don't change in here!! <- #*

t\_span = np.array([0, T\_SPAN])

times = np.linspace(t\_span[0], t\_span[1], T\_STEPS)

*# t = np.linspace(0, T\_SPAN, T\_STEPS)*

*##Set initial conditions ##*

*# -> needs to be array even for 1 IC <- #*

y0 = np.array([q\_A0, n\_A0, n\_t0, T0])#, n\_B0])#, n\_B0])

*#respectively to the differential equations*

```

##Solve the problem##
# scipy.integrate.solve_ivp
# (fun, t_span, y0, method='RK45', t_eval=None, dense_output=False, events=None,
vectorized=False, args=None, **options)
soln = solve_ivp(f, t_span, y0, method = 'LSODA', t_eval=times)
t = soln.t
q_A = soln.y[0] #returns an array
n_A = soln.y[1]
n_t = soln.y[2]
T = soln.y[3]

#Algebraic equations
n_B = n_t - n_A # Mol_N2(g)

M_t = (m_s*k*(q_A-qe(n_A,T)) + (n_t/(T*((cv_A_g*q_A*m_s)+(cp_A*n_A)+
(cp_B*(n_t-n_A))+(c_s*m_s))))*(T*m_s*k*(q_A-qe(n_A,T))*
(n_A/n_t*(cv_A_g-cv_B_g-cp_A+cp_B)-cp_B) + U*A*(T_H-T) + DH*m_s*k*(q_A-qe(n_A,T))))

#Total molar flow rate filled in for dT/dt determined in Maple

P_A_bar = (n_A*R*T)/(V_g*100000) #Pressure of P_A in bar

#Loading plot#
x = np.arange(0, T_SPAN, Dt)
y = q_A

# plt.plot(x, n_A)

plt.plot(x, q_A, label = "q_A" ,color="black")
plt.plot(x, qe(n_A,T), label = "q_eq", color="black",
linestyle='--')

plt.xlabel("t/[s]")
plt.ylabel("qe/[mol/kg]")
# plt.title("Sorbent loading vs. equilibrium loading")
plt.legend()
# plt.savefig('D_R_0.4_loading.png')#, transparent=True)
plt.show()

max_q_A = np.max(q_A)
max_qe = np.max(qe(n_A,T))

min_q_A = np.min(q_A)
min_qe = np.min(qe(n_A,T))
print('minimum_values:', 'qe-', round(min_qe,4), 'mol/kg' )
print('maximum_values:', 'qe-', round(max_qe,4), 'mol/kg' )
print('minimum_values:', 'q_A-', round(min_q_A,4), 'mol/kg' )
print('maximum_values:', 'q_A-', round(max_q_A,4), 'mol/kg' )

#Cyclische capaciteit
qe_cyc_cap = q_A0 - min_qe #100% sorbent unloading, difference between

```

```

initial loading and end value
qe_cyc_cap90 = qe_cyc_cap*0.9 #Amount unloaded CO2 at 90% of de total unloading
qe_cyc_cap50 = qe_cyc_cap*0.5 #Amount unloaded CO2 at 50% of de total unloading

n_cap90 = qe_cyc_cap90*m_s
n_cap50 = qe_cyc_cap50*m_s

    #Temperature plot#
x = np.arange(0, T_SPAN, Dt)
y = T

fig,ax = plt.subplots()
plt.plot(x, T, color='black')#, label = "T_curve")

plt.xlabel("t/[s]")
plt.ylabel("T/[K]")
# plt.legend()
plt.show()

min_T = np.min(T)
max_T = np.max(T)

T_H_5 = T_H - 5
T_393 = np.where(T >= T_H_5)
t_T_393 = T_393[0][0]*Dt

print('minimum_value_', min_T, 'K' )
print('maximum_value_', round(max_T,3), 'K' )
print('time_for_T=', T_H_5, 'after_', round(t_T_393,3), 's')

    #Molar flowrate plot#
x = np.arange(0, T_SPAN, Dt)
y = M_t

fig,ax = plt.subplots()

plt.plot(x, M_t, color='black')#, label = "q_A")

plt.xlabel("t/[s]")
plt.ylabel("M_t/[mol/s]")
# plt.legend()
plt.show()

min_M_t = np.min(M_t)
max_M_t = np.max(M_t)
print('minimum_value_', min_M_t)
print('maximum_value_', max_M_t )

# Compute the area using the composite trapezoidal rule.

```

```

area = trapz(M_t, dx=Dt)
print("area_=", round(area,3))

#Check amount of moles, area under graph must be equal to the total amount
of desorbed CO2
n_cap = qe_cyc_cap*m_s #mol_CO2
print(n_cap)
n_area = area
print(n_area)

    #Amount of moles plot#
x = np.arange(0, T_SPAN, Dt)

# plt.plot(x, n_A)
fig,ax = plt.subplots()

plt.plot(x, n_A, label = "n_A", color='green')
plt.plot(x, n_B, label = "n_B", color='blue')#='black', linestyle='--')
plt.plot(x, n_t, label = "n_t", color='red')#='black',linestyle=':')

plt.xlabel("t/[s]")
plt.ylabel("n_tot/[mol]")
plt.legend()
plt.show()

max_n_A = np.max(n_A)
max_n_B = np.max(n_B)
max_n_t = np.max(n_t)

min_n_A = np.min(n_A)
min_n_B = np.min(n_B)
min_n_t = np.min(n_t)
print('minimum values:', 'n_A-', round(min_n_A,4), ' / ', 'n_t-',
round(min_n_t,4), ' / ', 'n_B-', round(min_n_B,4))
print('maximum values:', 'n_A-', round(max_n_A,4), ' / ', 'n_t-',
round(max_n_t,4), ' / ', 'n_B-', round(max_n_B,4))

### Results ###

#Capaciteit
q_90 = q_A0 - qe_cyc_cap90 #Amount of CO2 on sorbent at 90% of de total unloading
q_50 = q_A0 - qe_cyc_cap50 #Amount of CO2 on sorbent at 50% of de total unloading

print('total_cyclic_capacity_at_+/-_100%_desorption:', 'qe_cyc_cap_=',
round(qe_cyc_cap,3))
print('total_cyclic_capacity_at_+/-_90%_desorption:', 'qe_cyc_cap90_=',
round(qe_cyc_cap90,3))
print('total_cyclic_capacity_at_+/-_50%_desorption:', 'qe_cyc_cap50_=',
round(qe_cyc_cap50,3))

def find_nearest(qe, value):

```

```

qe = np.asarray(qe)
idx = (np.abs(qe - value)).argmin()
return qe[idx]

t_100 = np.where(q_A == find_nearest(q_A, value=min_qe))
t_90 = np.where(q_A == find_nearest(q_A, value=q_90))
t_50 = np.where(q_A == find_nearest(q_A, value=q_50))

hr_100 = float(Dt*t_100[0]/3600)
hr_90 = float(Dt*t_90[0]/3600)
hr_50 = float(Dt*t_50[0]/3600)

print('total_time_in_hours_until_t_90:', 't_hrs=', round(hr_90,2), 'hrs')
print('total_time_in_hours_until_t_50:', 't_hrs=', round(hr_50,2), 'hrs')

m_A_des100 = qe_cyc_cap*m_s*M_CO2
m_A_des90 = qe_cyc_cap90*m_s*M_CO2 #m_CO2 = mol_CO2/kg_s *kg_s * M_CO2 = kg_CO2
m_A_des50 = qe_cyc_cap50*m_s*M_CO2

# print('total kg CO2 desorbed at t_100:', 'm_A =', round(m_A_des100,3))
print('total_kg_CO2_desorbed_at_t_90:', 'm_A=', round(m_A_des90,3))
print('total_kg_CO2_desorbed_at_t_50:', 'm_A=', round(m_A_des50,3))

prod = m_A_des100/(hr_100*V_R)
prod_90 = m_A_des90/(hr_90*V_R)
prod_50 = m_A_des50/(hr_50*V_R)

# print('productivity of the reactor:', 'prod =', prod)
print('productivity_of_the_reactor_at_t90:', 'prod_90=', round(prod_90,3))
print('productivity_of_the_reactor_at_t50:', 'prod_50=', round(prod_50,3))

mol_CO2_adsorbed = q_A0 * m_s #mol/kg_s *k_s
m_CO2_adsorbed = mol_CO2_adsorbed*M_CO2

percent_CO2_desorption = 100*m_A_des100/m_CO2_adsorbed
percent_CO2_desorption90 = 100*m_A_des90/m_CO2_adsorbed
percent_CO2_desorption50 = 100*m_A_des50/m_CO2_adsorbed

# print('Percentage of desorbed CO2 at t_100 =', round(percent_CO2_desorption,2), '%')
print('Percentage_of_desorbed_CO2_at_t_90=', round(percent_CO2_desorption90,2), '%')
print('Percentage_of_desorbed_CO2_at_t_50=', round(percent_CO2_desorption50,2), '%')

###molar properties###
print('maximum_value_M_t-', max_M_t, 'mol/s')
print('time_for_T_des_minus_5=', T_H_5, 'after_', round(t_T_393,3), 's')
print('minimum_value:', 'q_A-', min_q_A, 'mol/kg')
print('maximum_value:', 'q_A-', max_q_A, 'mol/kg')
print('minimum_value:', 'qe-', min_qe, 'mol/kg')
print('maximum_value:', 'qe-', max_qe, 'mol/kg')
print('Number_of_moles_CO2_desorbed_at_t_90:', n_cap90, 'mol')
print('Number_of_moles_CO2_desorbed_at_t_50:', n_cap50, 'mol')
print('minimum_values:', 'n_A-', round(min_n_A,4), 'n_t-',
round(min_n_t,4), 'n_B-', round(min_n_B,4))
print('maximum_values:', 'n_A-', round(max_n_A,4), 'n_t-',
round(max_n_t,4), 'n_B-', round(max_n_B,4))

```

```

t_nA_nB = np.where(n_A >= n_B)
t_CO2_N2 = t_nA_nB[0][0]*Dt

t_nB_0 = np.where(n_B <= 0)
t_no_N2 = t_nB_0[0][0]*Dt

print('time_for_CO2_>=N2', 'after', round(t_CO2_N2,2), 's')
print('first_time_at_which_N2<=0', 'after', round(t_no_N2,2), 's')

q_no_B = q_A[round(t_nB_0[0][0])]
qe_no_B = qe(n_A,T)[round(t_nB_0[0][0])]

qe_cyc_100_no_B = q_no_B - min_qe
qe_cyc_90_no_B = q_no_B - q_90
qe_cyc_50_no_B = q_no_B - q_50

m_A_100_no_B = qe_cyc_100_no_B*m_s*M_CO2
m_A_90_no_B = qe_cyc_90_no_B*m_s*M_CO2
m_A_50_no_B = qe_cyc_50_no_B*m_s*M_CO2

print('total_kg_CO2_desorbed_at_t_90_after_no_more_N2_in_system:',
      'm_A_90_no_B=', round(m_A_90_no_B,3))
print('total_kg_CO2_desorbed_at_t_50_after_no_more_N2_in_system:',
      'm_A_50_no_B=', round(m_A_50_no_B,3))

# Temperature vs. Loading in one figure
x = np.arange(0, T_SPAN, Dt)
y1 = q_A
y2 = qe(n_A,T)
z = T

fig,ax = plt.subplots()
# make a plot
# plt.plot(x, q_A, label = "q_A")
# plt.plot(x, qe(n_A,T), label = "q_eq")

ax.plot(x,
        y1,
        color="r",
        label = "q_A")#, marker="o")
# set x-axis label
ax.set_xlabel("t/[s]", fontsize = 14)
# set y-axis label
ax.set_ylabel("Sorbent_loading",
              color="red",
              fontsize=14)
ax.plot(x,
        y2,
        color="red",
        label = "qe",
        linestyle='—')#, marker="o")
# set x-axis label

```

```

ax.set_xlabel("t/[s]", fontsize = 14)
# set y-axis label
ax.set_ylabel("qe/[mol/kg]",
              color="r",
              fontsize=14)
ax.legend(bbox_to_anchor=(1.2, 1.05))
# twin object for two different y-axis on the same plot
ax2=ax.twinx()
# make a plot with different y-axis using second axis object
ax2.plot(x,
        T,
        color="blue",
        label = "T",)#,marker="o")
ax2.set_ylabel("T/[K]", color="blue", fontsize=14)
# plt.legend()
# plt.savefig('case_study_default_T_q.png')#, transparent=True)
plt.show()
# save the plot as a file
# fig.savefig('case_study_default_T_q.png',
#            format='jpeg',
#            dpi=100,
#            bbox_inches='tight')

# plt.plot(x, T)#, label = "T_curve")
# # plt.scatter(t_heated, y = 393, color = 'g', label = "T = 393")

# plt.xlabel("Time (s)")
# plt.ylabel("Temperature (K)")
# plt.title("Temperature of reactor, sorbent and gasses")
# # plt.legend()
# plt.show()

```

## References

- R. Lindsey, "Climate change atmospheric carbon dioxide," <https://www.climate.gov/news-features/understanding-climate/climate-change-atmospheric-carbon-dioxide#:~:text=Based%20on%20preliminary%20analysis%2C%20the,to%20the%20COVID%2D19%20pandemic.>, 2022.
- M. R. SURATI, "Experimental characterization of a specific chemisorbent and a physisorbent for direct air capture application: Analyzing the effect of parameters such as desorption temperature, humidity and varying co2 partial pressure on the performance of the adsorbent material.(thesis work carried out at the netherlands organization for applied scientific research (tno), delft, the netherlands)," 2022.
- M. J. Bos, "Storage of renewable electricity in methanol: Technology development for co2 air capture and conversion to methanol," 2019.
- S. I. Zandalinas, F. B. Fritschi, and R. Mittler, "Global warming, climate change, and environmental pollution: recipe for a multifactorial stress combination disaster," *Trends in Plant Science*, vol. 26, no. 6, pp. 588–599, 2021.
- T. P. Agreement", "Key aspects of 'the paris agreement'," <https://unfccc.int/process-and-meetings/the-paris-agreement/the-paris-agreement/key-aspects-of-the-paris-agreement>, 2022.
- J. Lundahl, "Synthesis and testing of direct air capture adsorbents," 2021.
- Climeworks, "Climeworks sketch of dac plant 'orca'," <https://climeworks.com/>, May 2022.
- C. Beuttler, L. Charles, and J. Wurzbacher, "The role of direct air capture in mitigation of anthropogenic greenhouse gas emissions," *Frontiers in Climate*, vol. 1, 2019. [Online]. Available: <https://www.frontiersin.org/articles/10.3389/fclim.2019.00010>
- M. Erans, E. S. Sanz-Pérez, D. P. Hanak, Z. Clulow, D. M. Reiner, and G. A. Mutch, "Direct air capture: process technology, techno-economic and socio-political challenges," *Energy & Environmental Science*, 2022.
- O. S. Board, E. National Academies of Sciences, Medicine *et al.*, "Negative emissions technologies and reliable sequestration: A research agenda," 2019.
- I. G. G. R. P. ", "A brief history of ccs and current status," <https://ieaghg.org>, 2022.
- S. Budinis, S. Krevor, N. Mac Dowell, N. Brandon, and A. Hawkes, "An assessment of ccs costs, barriers and potential," *Energy strategy reviews*, vol. 22, pp. 61–81, 2018.
- G. status of CCS 2021 ", "Global ccs institute."
- E. E. Ünveren, B. Ö. Monkul, Ş. Sariođlan, N. Karademir, and E. Alper, "Solid amine sorbents for co2 capture by chemical adsorption: A review," *Petroleum*, vol. 3, no. 1, pp. 37–50, 2017.
- B. Singh, A. H. Strømman, and E. G. Hertwich, "Comparative life cycle environmental assessment of ccs technologies," *International Journal of Greenhouse Gas Control*, vol. 5, no. 4, pp. 911–921, 2011.
- N. McQueen, K. V. Gomes, C. McCormick, K. Blumenthal, M. Pisciotta, and J. Wilcox, "A review of direct air capture (dac): scaling up commercial technologies and innovating for the future," *Progress in Energy*, vol. 3, no. 3, p. 032001, 2021.
- R. Veneman, "Adsorptive systems for post-combustion co2 capture: design, experimental validation and evaluation of a supported amine based process," 2015.
- S. De Flart, "Capturing carbon dioxide directly from the air: A theoretical modeling approach," 2016.
- F. Sabatino, A. Grimm, F. Gallucci, M. van Sint Annaland, G. J. Kramer, and M. Gazzani, "A comparative energy and costs assessment and optimization for direct air capture technologies," *Joule*, vol. 5, no. 8, pp. 2047–2076, 2021.
- J. C. Knox, A. D. Ebner, M. D. LeVan, R. F. Coker, and J. A. Ritter, "Limitations of breakthrough curve analysis in fixed-bed adsorption," *Industrial & engineering chemistry research*, vol. 55, no. 16, pp. 4734–4748, 2016.



J. Young, E. García-Díez, S. Garcia, and M. Van Der Spek, “The impact of binary water–co<sub>2</sub> isotherm models on the optimal performance of sorbent-based direct air capture processes,” *Energy & Environmental Science*, vol. 14, no. 10, pp. 5377–5394, 2021.

V. Stampi-Bombelli, M. van der Spek, and M. Mazzotti, “Analysis of direct capture of co<sub>2</sub> from ambient air via steam-assisted temperature–vacuum swing adsorption,” *Adsorption*, vol. 26, no. 7, pp. 1183–1197, 2020.